R-05-42

Forsmark site investigation

Reflection seismic studies in the Forsmark area, 2004: Stage 2

Christopher Juhlin, Hans Palm
Uppsala University, Department of Earth Sciences

June 2005

Svensk Kärnbränslehantering AB
Swedish Nuclear Fuel
and Waste Management Co
Box 5864
SE-102 40 Stockholm Sweden
Tel 08-459 84 00
+46 8 459 84 00
Fax 08-661 57 19
+46 8 661 57 19

ISSN 1402-3091
SKB Rapport R-05-42

Forsmark site investigation

Reflection seismic studies in the Forsmark area, 2004: Stage 2

Christopher Juhlin, Hans Palm
Uppsala University, Department of Earth Sciences

June 2005

Keywords: Reflection seismics, Forsmark, AP PF 400-04-78.

Abstract

Reflection seismic data were acquired in the Fall of 2004 in the Forsmark area, located about 140 km north of Stockholm, Sweden. The Forsmark area has been targeted by SKB as a possible storage site for spent nuclear fuel. About 25 km of high resolution (nominal source and receiver spacing of maximum 10 m and a minimum of 160 active channels) seismic data were acquired along 10 profiles, varying in length from about 1 km to over 4 km. Three of these profiles are extensions of profiles that were acquired in 2002 (Stage 1). While the 2002 Stage 1 profiles were geared towards acquiring data from within the relatively undeformed lens, the current study focused on acquiring data from the boundaries of the lens. Data acquisition was also concentrated towards the western part of the candidate area.

Data were acquired using a combination of the same explosive source as in Stage 1 (15-75 g of explosives) and the VIBSIST mechanical source consisting of an industrial hammer mounted on a tractor. Earlier tests in Laxemar had shown that the VIBSIST source gives comparable data to the explosive source and is less expensive. It can also be used in areas where explosives are prohibited, such as close to the nuclear power plant. At present, the source cannot be used in the terrain, therefore an explosive component is still required. About 80% of the 2100 source points were activated using the VIBSIST system.

Stacked sections from the new profiles are generally consistent with the Stage 1 results. Reflections from the prominent south dipping A1 reflector can be observed on most profiles, however, it is not clear if it can be traced all the way to the surface. Neither is it clearly observed below the power plant, suggesting its lateral extent is limited to the west. Instead, a gently east dipping reflector (B8) is interpreted below the power plant. Reflections consistent with the A2 reflector are also found on two profiles, but cannot be traced very far to the south, suggesting that this structure is limited in this direction. The sub-horizontal C1 and C2 reflectors, at about 3 km depth, appear present on nearly all profiles. No pronounced set of reflections corresponding to the group A and B sets found in the south eastern part of the lens on the Stage 1 survey are observed. However, the upper 0.5 s of crust is very reflective north of the Singö zone. The reflectivity appears to be mainly south dipping.

Three new prominent reflectors have been identified in southern part of the survey area (J1, J2 and K1). These have different orientations from the A and B groups of the Stage 1 survey. None of them can be traced to the surface within the survey area. Reflections from the presumed steeply dipping Forsmark, Eckarfjärden and Singö deformation zones are not directly observed, consistent with these zones being near-vertical. The zones appear to disrupt reflectivity patterns on either side of them and some reflectors appear to terminate against them. However, the fact that profiles are not long enough, lack of 3D control and, on occasion, poorer data quality near the zones imply that this interpretation is very tentative.

Sammanfattning

Under hösten 2004 utfördes reflektionsseismiska undersökningar i Forsmark, ca 70 km norr om Uppsala. Området i Forsmark har av SKB valts som ett möjligt område för deponering av använt kärnbränsle. Totalt utfördes ca 25 km profil med hög upplösning (10 m geofonavstånd, 10 m skottavstånd, 160 kanaler) längs 10 profiler av varierande längd, från 1 km till mer än 4 km. Tre av dessa profiler utgör förlängningar av profiler från 2002 års mätkampanj (”Stage 1”). Medan mätningarna 2002 var fokuserade på att erhålla information om den s.k. tektoniska linsen i kandidatområdet, är innevarande undersökning fokuserat på randområdet runt linsen. Datainsamlingen koncentrerades också på den västliga delen av området.

Vid datainsamlingen användes en kombination av skott (15-75 g dynamit, som i ”Stage 1”) och VIBSIST, som är en mekanisk källa bestående av en hydraulisk hammare monterat på en traktorgrävare. Tidigare undersökningar i SKB:s undersökningsområde i Laxemar visade att VIBSIST-källan ger data som är jämförbara med data genererade med explosioner, men är billigare vid användning. Den kan också användas i områden där detonationer inte är lämpliga eller tillåtna, t.ex. nära kärnkraftverket. I skogsterräng är dock fortfarande detonationer med dynamit enklare i användning. Av totalt 2100 skottpunkter utfördes omkring 80 % med VIBSIST-systemet.

Stackade sektioner från de nya profilerna är i allmänhet konsistenta med resultaten från ”Stage 1”. Reflexer från den prominenta mot syd stupanda A1-reflektor kan observeras i de flesta sektioner. Det är däremot inte klart om reflektorn kan förlängas till markytan. Reflektorn syns inte heller klart i området runt kraftverket, vilket kan antyda att reflektorn är lateralt avgränsad mot väst. Däremot kan en mot öst svagt stupande reflektor (B8) observeras under kraftverket. Längs två profiler syns reflexer konsistenta med A2 reflektorn från ”Stage 1”. Dessa reflexer kan inte följas speciellt långt mot söder, vilket indikerar en avgränsning av A2 mot söder. De subhorisontella reflektorerna C1 och C2 vid ca 3 km djup syns i nästan samtliga profiler. Inga tydliga reflektorer som motsvarar A och B gruppen från ”Stage 1” har observerats under ”Stage 2” mätningarna. Däremot utvisar de översta 0.5 sek (ca 1500 m) från profilerna norr om Singö-zonen många mot söder flackt stupande reflexer.

Tre nya prominenta reflektorer (J1, J2 och K1) har identifierats den södra delen av området. Orienteringen av dessa skiljer sig från A och B-gruppen från ”Stage 1”. Inga av dem kan följes till markytan inom mätområdet. Inga direkta reflektioner från Forsmark-, Eckarfjärds- och Singö-deformationszonerna har observerats. Detta är konsistent med hypotesen, att dessa zoner är subvertikala. Zonerna utgör till synas en gräns mellan olika mönster i reflexerna, och vissa reflektorer är klart avgränsade av t.ex. Forsmark-zonen. För att åstadkomma en mer direkt tolkning av dessa zoner behövs längre profiler, eventuellt kombinerat med 3D-täckning.

Contents

1 Introduction

Seismic data were acquired in the Forsmark area in northeastern Uppland (Figure 1-1) during the autumn of 2004 by Uppsala University in agreement with the instructions and guidelines from SKB (activity plan AP PF 400-04-78 and method description SKB MD 241.004, SKB internal controlling documents) and under supervision of Johan Nissen, SKB. Approximately 25 km of high-resolution (maximum 10 m source and receiver spacing) reflection seismic data were acquired with the SERCEL 408UL system along 10 different profiles (Figure 1-2). Aside from the explosive source used in the 2002 survey (Juhlin et al., 2002a), a mechanical VIBSIST source was used at about 80% of the source points. Studies at Laxemar showed this source to be a good alternative to explosives (Juhlin et al., 2004).

The area covered by the data set reported on here is referred to as Stage 2 and is an extension of the area that was covered in 2002 (Stage 1) and reported on in Juhlin et al. (2002a).

The reflection seismic method used here imaged the bedrock from the near surface (upper 100 metres) down to depths of several km. Zones or changes in the elastic properties of the bedrock, i.e. lithological changes or possible fracture zones, greater than about a metre in thickness and dipping up to 75° can be imaged.

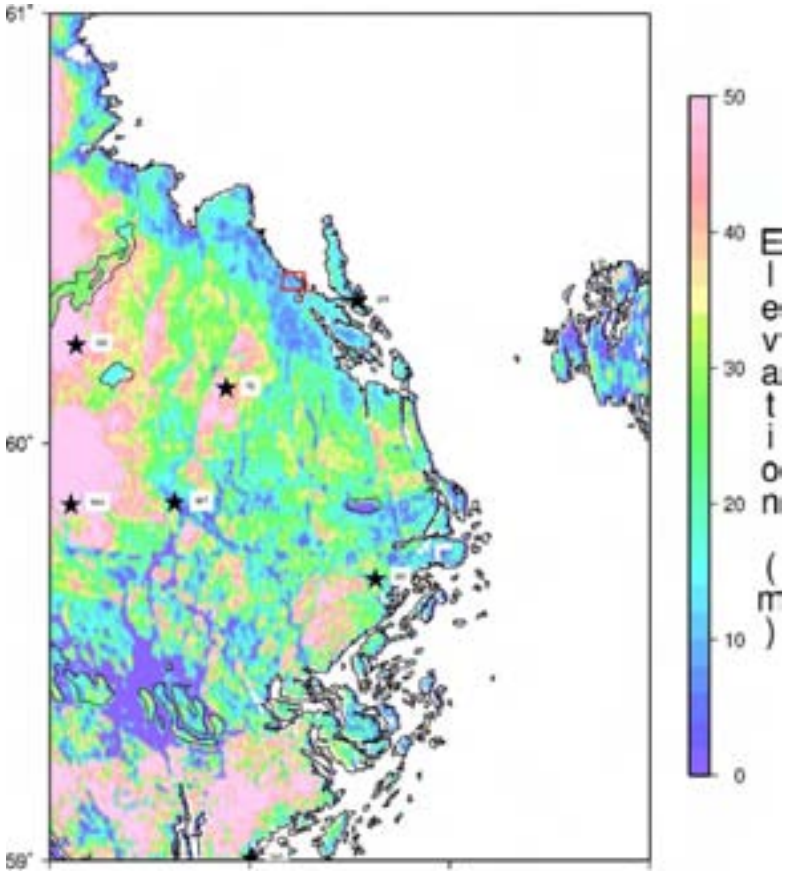

Figure 1-1. Location of study area (red box). Permanent seismological stations of the Swedish Seismological Network are marked by stars.

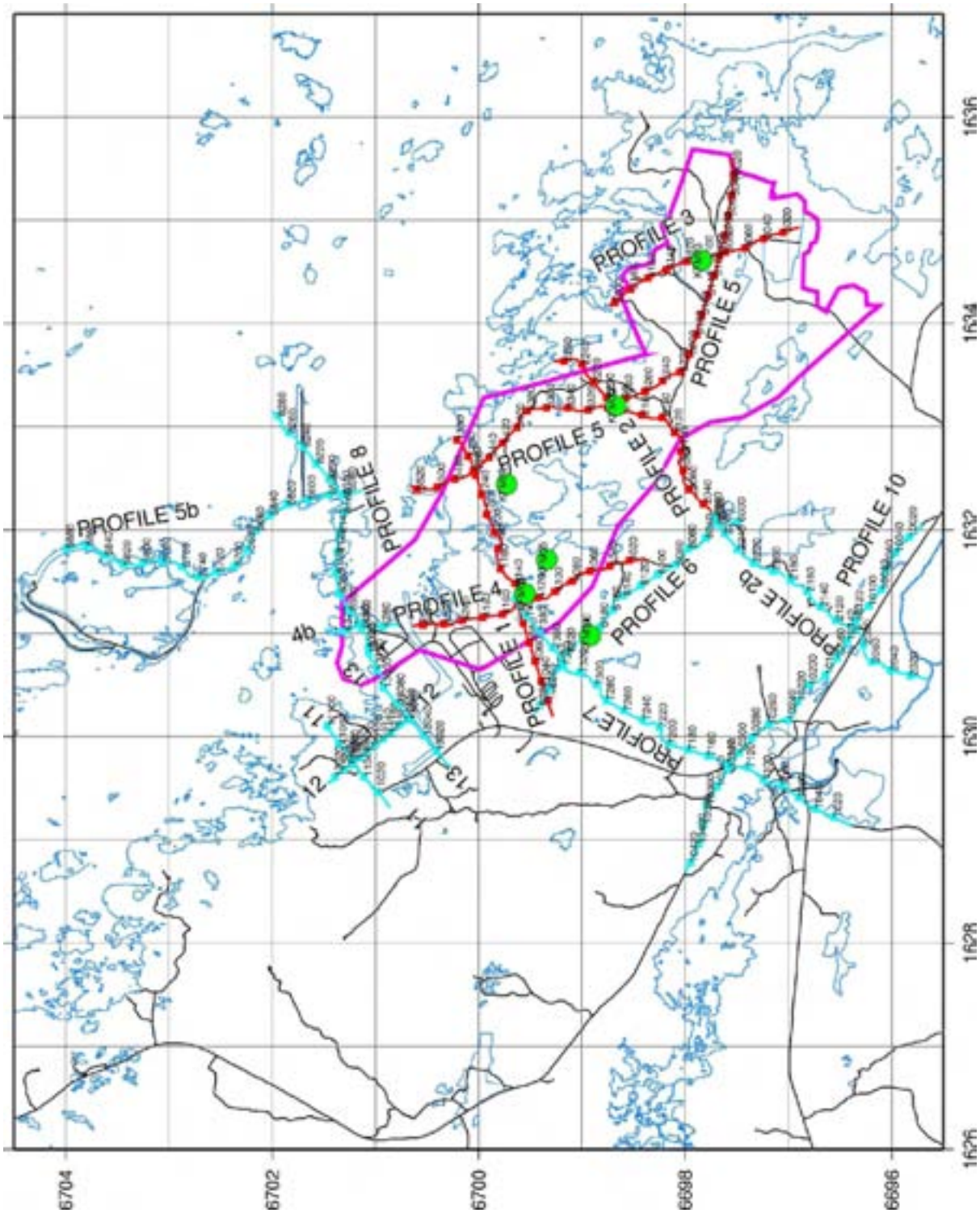

Figure 1-2. Stage 2 profiles acquired in 2004 are shown as light blue lines. Station locations for profiles acquired in 2002 (Stage 1) are shown with red lines. Green circles are deep boreholes. Candidate area is marked by purple line.

2 Data acquisition

The acquisition crew arrived in the field on October 4 and data acquisition began on October 9, 2004 along profile 2b using the acquisition parameters given in Table 2-1. Data acquisition finished on December 17, 2004 followed by 2 days of demobilization and clean-up. Breaks in the acquisition were held for a total of 10 days during the field work.

A major difference from previous site investigations was the use of the VIBSIST source in a production mode. Seismic signals were produced by a VIBSIST (Park et al., 1996; Cosma and Enescu, 2001; Juhlin et al., 2002b) mechanical source mounted on a tractor. The tractor with the hydraulic arm and rock-breaking head was rented from NCC by SKB. The computer-controlled flow regulator, command equipment and software were supplied by Vibrometric Oy. The geophone closest to the VIBSIST source was used as the pilot signal for later decoding of the data. In general, 3-5 sweeps were recorded at each source point and later input into decoding software. The hydraulic hammer hit the road for 28 seconds and data were recorded at a 1 ms sampling rate for 30 seconds.

When explosives were used as the source the same procedure was followed as in Stage 1 and is described in Juhlin et al. (2002a).

Geophones were placed in drilled bedrock holes wherever possible, otherwise they were placed directly in the soil cover.

All source points and geophone locations were surveyed with high precision GPS instruments in combination with a total station. Horizontal and vertical precision of better than 10 cm.

Noise conditions varied considerably along the profiles. In general, data from profiles close to the Forsmark power station and the coast were noisier (Figure 2-1).

Table 2-1. Acquisition parameters for the reflection seismic profiles.

Parameter	*Value*
Spread type	Asymmetric split (40-120)
Number of channels	Minimum 160 / Maximum 276
Near offset	0 m
Geophone spacing	10 m / 5 m on Profile 12
Geophone type	28 Hz single
Source spacing	10 m / 5 m on Profile 12
Charge size	15/75 gram
Nominal charge depth	0.9/1.5 m
VIBSIST	2000 kJoule/impact
Nominal fold	80
Recording instrument	SERCEL 408
Sample rate	0.5 ms explosive /1 ms VIBSIST
Field low cut	Out
Field high cut	500 Hz explosive / 250 Hz VIBSIST
Record length	3 seconds / 30 s VIBSIST
Profile length / source points	2n - 2780 m / 191 4n - 740 m / 79 5n - 3360 m / 305 6 - 2900 m / 255 7 - 4240 m / 287 8 – 2860 m / 196 10 – 4300 m / 235 11 – 1040 m / 68 12 – 1010 m / 150 13- 1390 m / 99

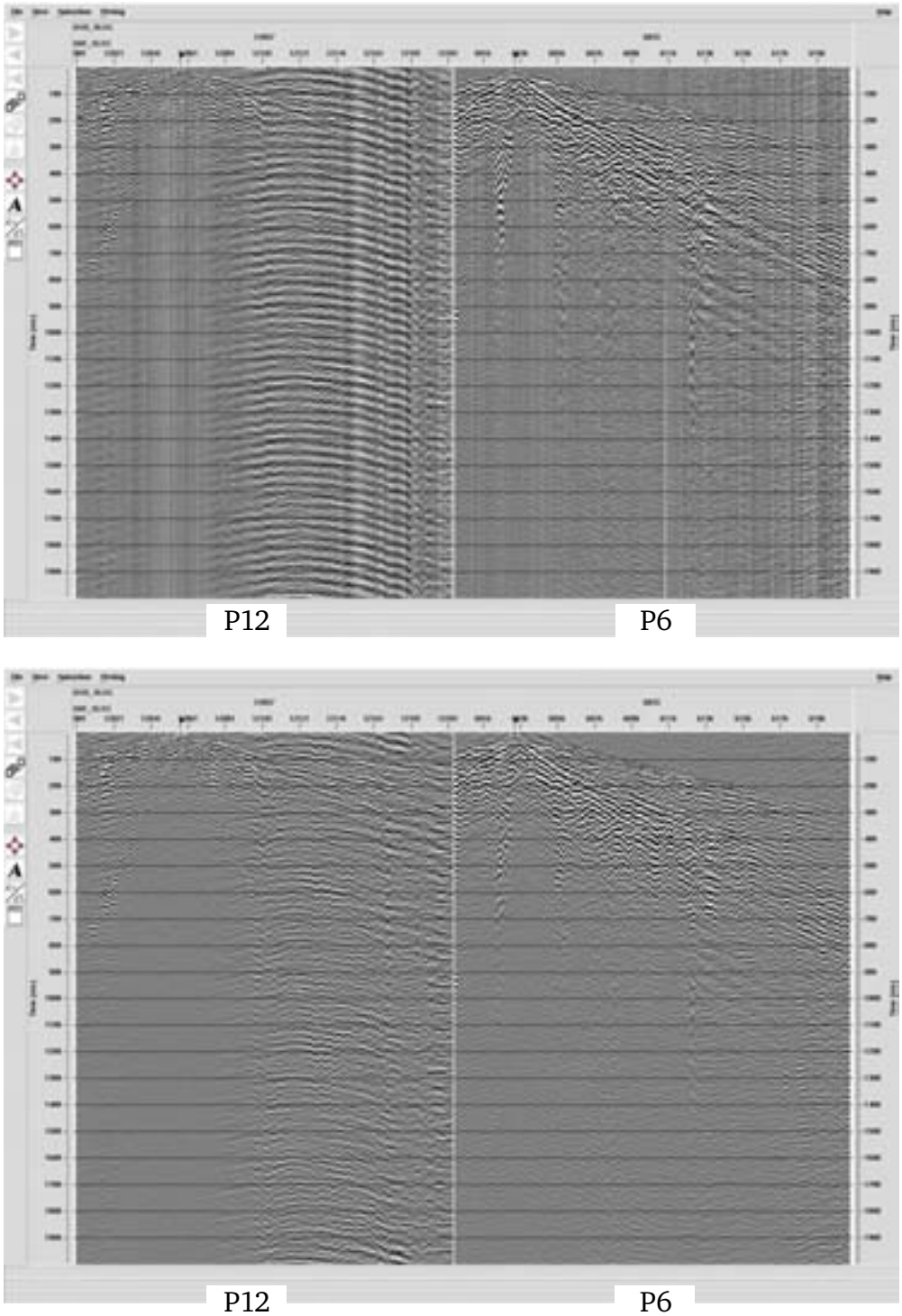

Figure 2-1. Comparison of typical source gathers from profile 12 and profile 6. Noise levels are much higher on profile 12 in both unfiltered (top) and filtered (bottom) gathers. Gather on the left is from profile 12 and gather on the right is from profile 6.

3 Data processing

The reflection seismic data were acquired along crooked lines. CDP stacking lines were chosen that were piece-wise straight. The data were projected on to these lines prior to stacking (Figure 3-1). The stacks shown in this report refer to the CDP numbers along these lines. Extensions of profiles 2, 4 and 5 from Stage 1 have been labelled as profiles 2b, 4b and 5b, respectively.

Required pre-processing of the VIBSIST records is described elsewhere (Cosma and Enescu, 2001; Juhlin et al., 2002b). After pre-processing, the VIBSIST and explosive source data were merged for each line and processed together as a single line. Lower frequencies were used in the processing for the profiles near the power plants and the coast (Table 3-1). Important processing parameters were refraction statics along with spectral whitening and filtering. In general data from profiles 2b, 6, 7 and 10 are of the highest quality and the same filtering parameters were applied to these profiles as those from stage 1. However, penetration depth and frequency content varies along all profiles.

Raw VIBSIST shot gathers generally show stronger surface waves and higher signal to noise ratios than the explosive data. However, after spectral whitening and filtering shot gathers from explosive and VIBSIST sources acquired from adjacent source points show nearly the same signature (Figures 3-2 to 3-5).

Table 3-1. Processing parameters for the seismic profiles.

Step	*Process*	*Profile*									
		2b	*6*	*7*	*10*	*4b*	*5b*	*8*	*11*	*12*	*13*
1	Read SEGD data - 3000 ms	x	x	x		x	x	x			
	Read VIBISIST SEG2 data – 2000 ms	x	x	x	x	x	x	x	x	x	x
2	Spike and noise edit	x	x	x	x	x	x	x	x	x	x
3	Pick first breaks	x	x	x	x	x	x	x	x	x	x
4	Scale by time	x	x	x	x	x	x	x	x	x	x
5	Spectral whitening 50-60-240-270 Hz	x	x	x	x						
	Spectral whitening 40-60-180-200 Hz					x	x	x	x	x	x
6	Bandpass filter 70-140-300-450 Hz 0-200 ms 60-120-300-450 Hz 100-400 ms 50-100-300-450 Hz 300-2000 ms	x	x	x	x						
	Bandpass filter 70-100-250-350 Hz 0-200 ms 60-90-230-300 Hz 100-400 ms 50-80-210-270 Hz 300-2000 ms					x	x	x	x	x	x
7	Refraction statics	x	x	x	x	x	x	x	x	x	x
8	Trace top mute: 10 +offset /5.5 ms	x	x	x	x	x	x	x	x	x	x
9	Sort to CDP domain	x	x	x	x	x	x	x	x	x	x
10	Velocity analyses	x	x	x	x	x	x	x	x	x	x
11	Residual statics	x	x	x	x	x	x		x	x	x
12	AGC - 50 ms window	x	x	x	x	x	x	x	x	x	x
13	NMO	x	x	x	x	x	x	x	x	x	x
14	T-X DMO	x	x	x	x	x	x	x			
15	AGC - 50 ms window	x	x	x	x	x	x	x			
16	Iterative DMO velocity analysis	x	x	x	x	x	x	x			
17	Stack (mean)	x	x	x	x	x	x	x	x	x	x
18	Trace equalization 0-800 ms	x	x	x	x	x	x	x	x	x	x
19	F-X Decon	x	x	x	x	x	x	x			

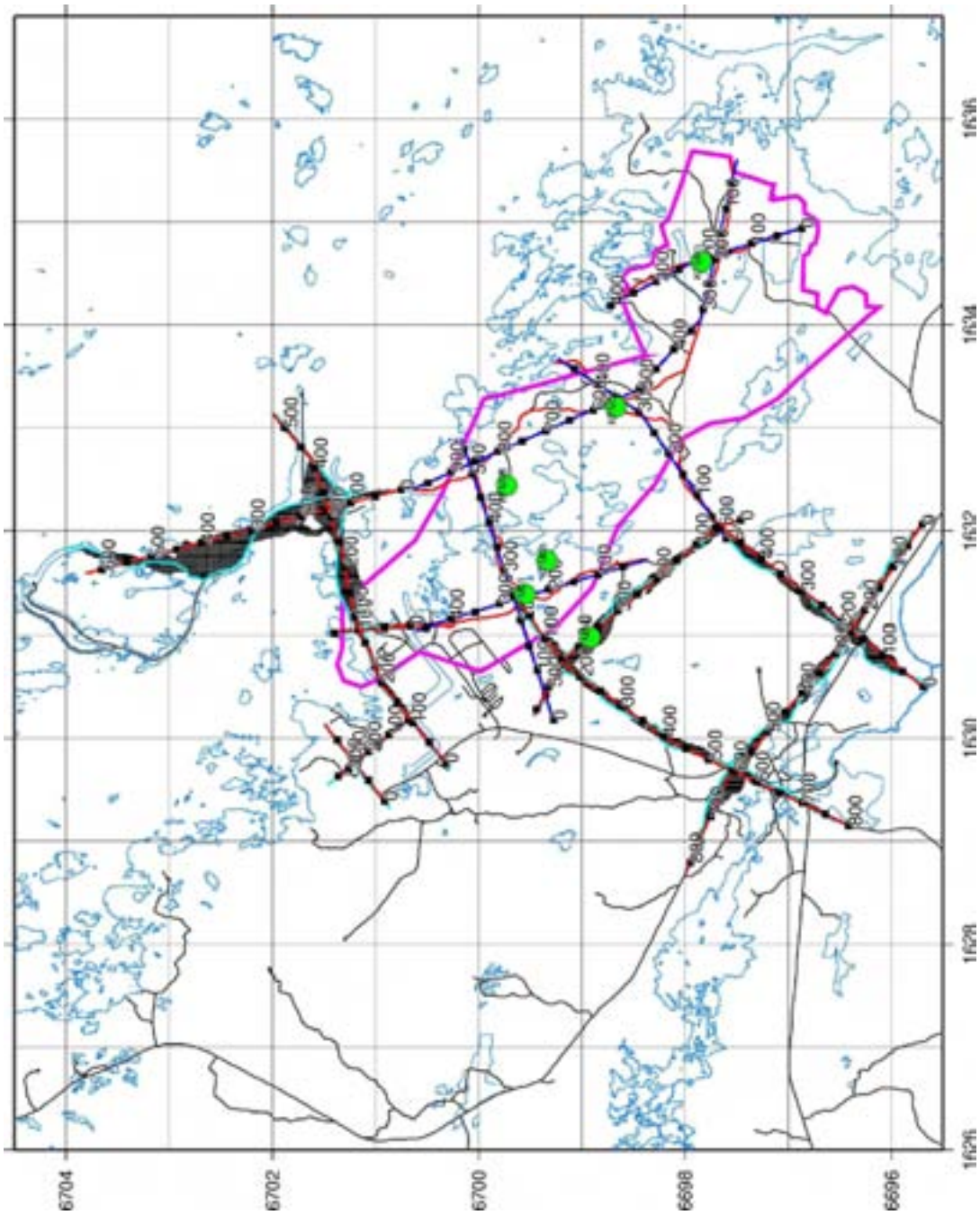

Figure 3-1*. Midpoints between shots and receivers (black dots) for the Stage 2 data. These midpoints were projected onto the CDP profiles (red lines) before stacking. Where the lines are straight the midpoints fall directly on the CDP profile. Stage 1 CDP profiles are shown in blue. Numbering refers to CDP position along the stacking line.*

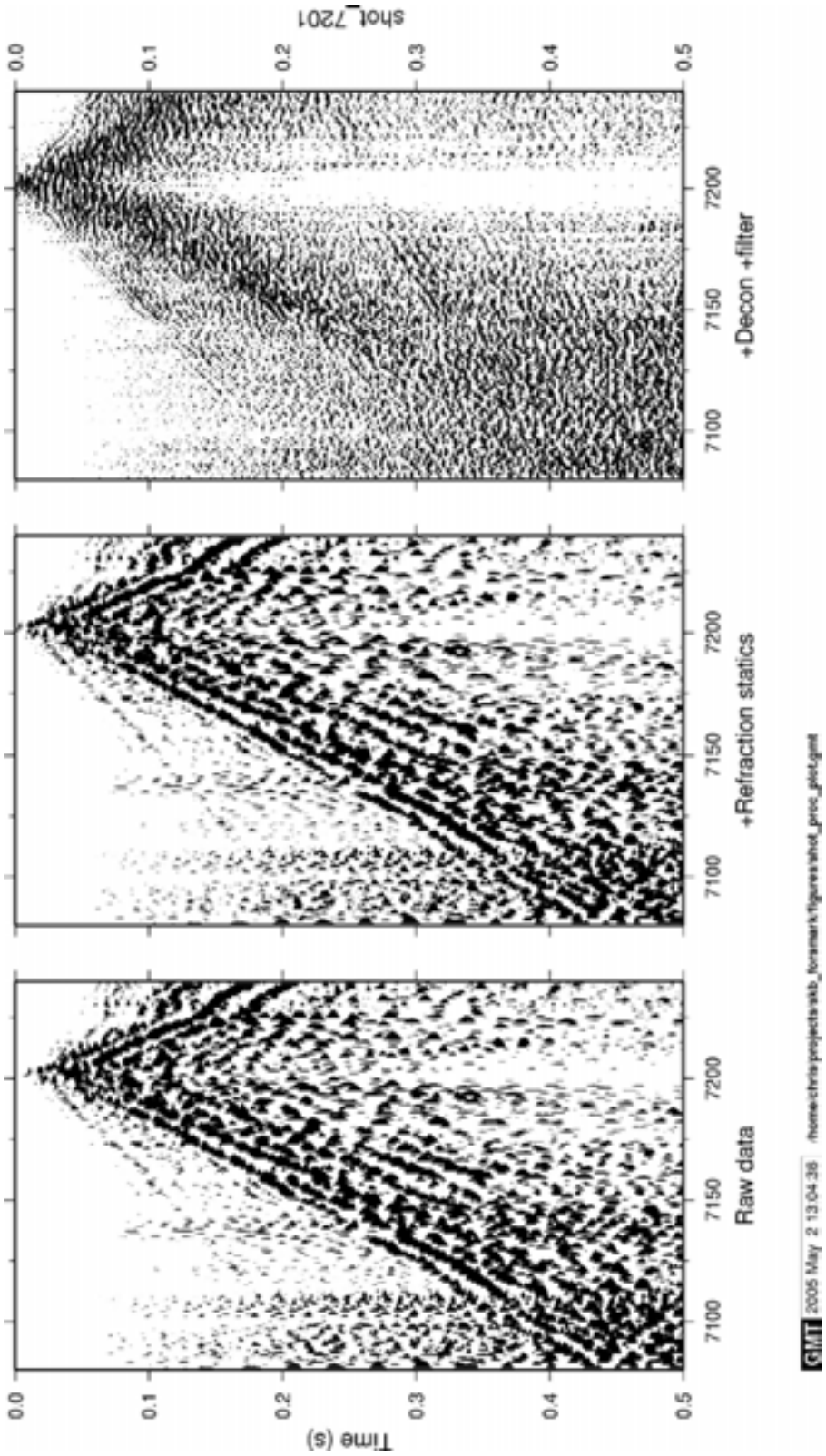

Figure 3-2*. Explosive shot gather from SP 7201 along profile 7 showing raw data scaled by time, with refraction statics added, and after spectral whitening and filtering.*

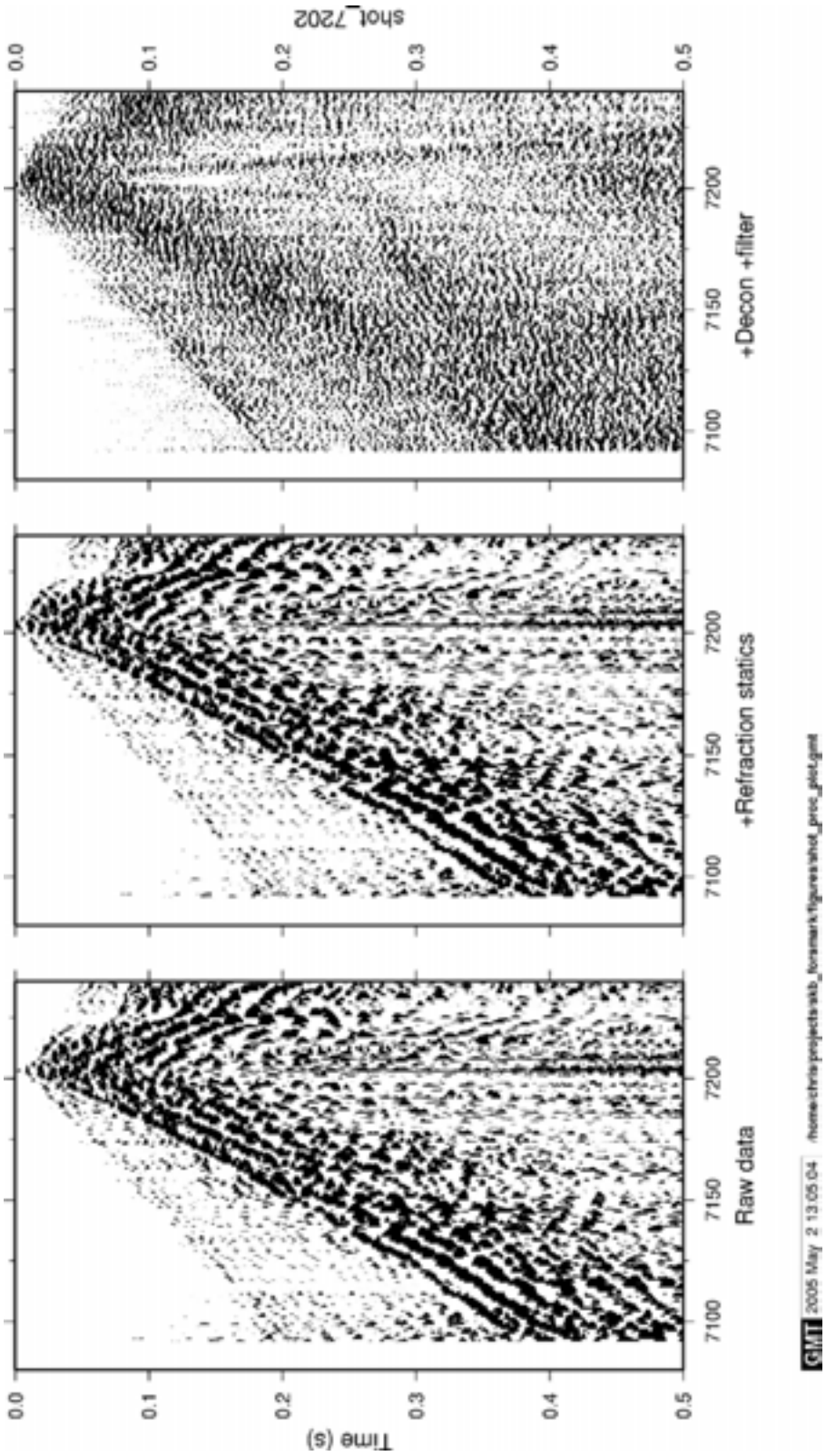

Figure 3-3*. VIBSIST shot gather from SP 7202 along profile 7 showing raw data scaled by time, with refraction statics added, and after spectral whitening and filtering.*

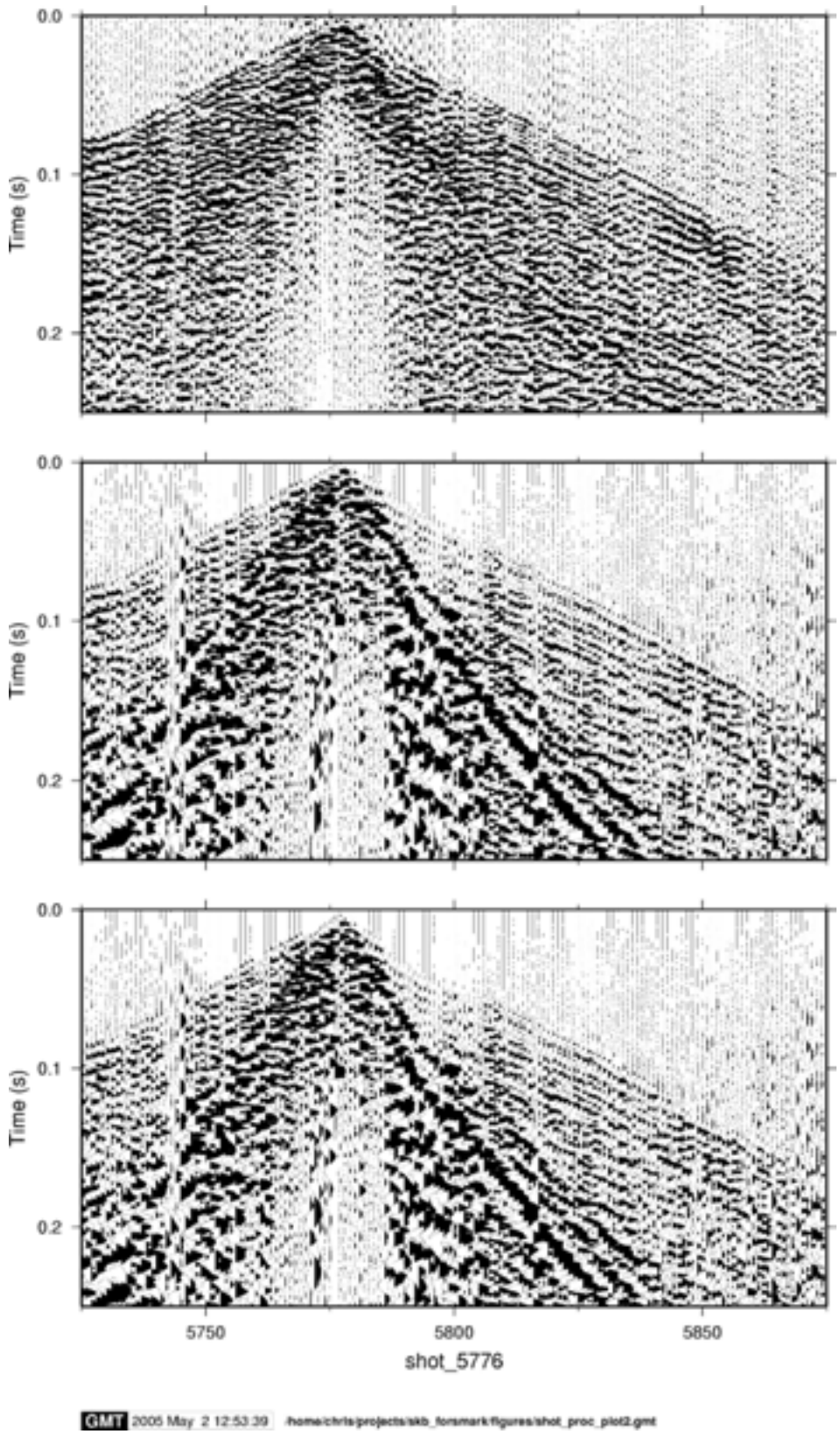

Figure 3-4*. Explosive shot gather from SP 5776 along profile 5 showing raw data scaled by time (bottom), with refraction statics added (middle), and after spectral whitening and filtering (top).*

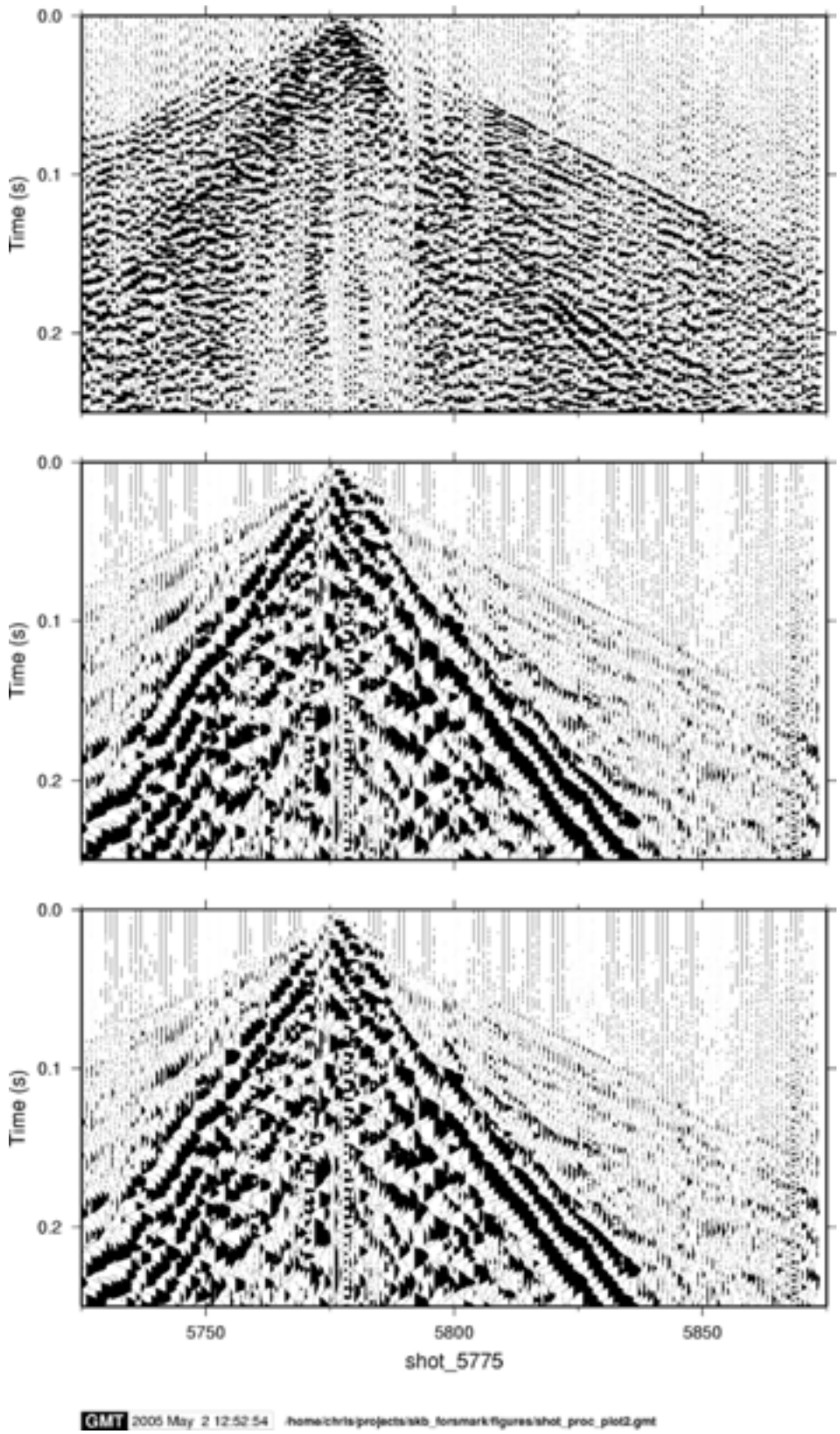

Figure 3-5*. VIBSIST shot gather from SP 5775 along profile 5 showing raw data scaled by time (bottom), with refraction statics added (middle), and after spectral whitening and filtering (top).*

4 Stacked sections

In the figures that follow (Figures 4-1 to 4-16) stacked sections are shown down to 0.6 seconds for all profiles. On those profiles where deeper reflections are observed, sections down to 2.0 seconds are presented. In these figures the data have been processed to step 19 in Table 3-1. On the sections down to 2.0 seconds the fold (the number traces stacked at that CDP location) is shown in the elevation panel as a grey shading with maximum fold at 100. Fold decreases to the edges of the profiles and on sections along the profiles where it was not possible to activate a source. Where fold is low, image quality is sometimes, but no always, poorer.

Aside from profiles 11, 12, and 13, acquired close to the power plant, data quality is poorer along much of profile 8 and on the southern part (south of CDP 200) of profile 5b. The poorer data quality is apparent in stacked sections, making interpretation more difficult along these profiles.

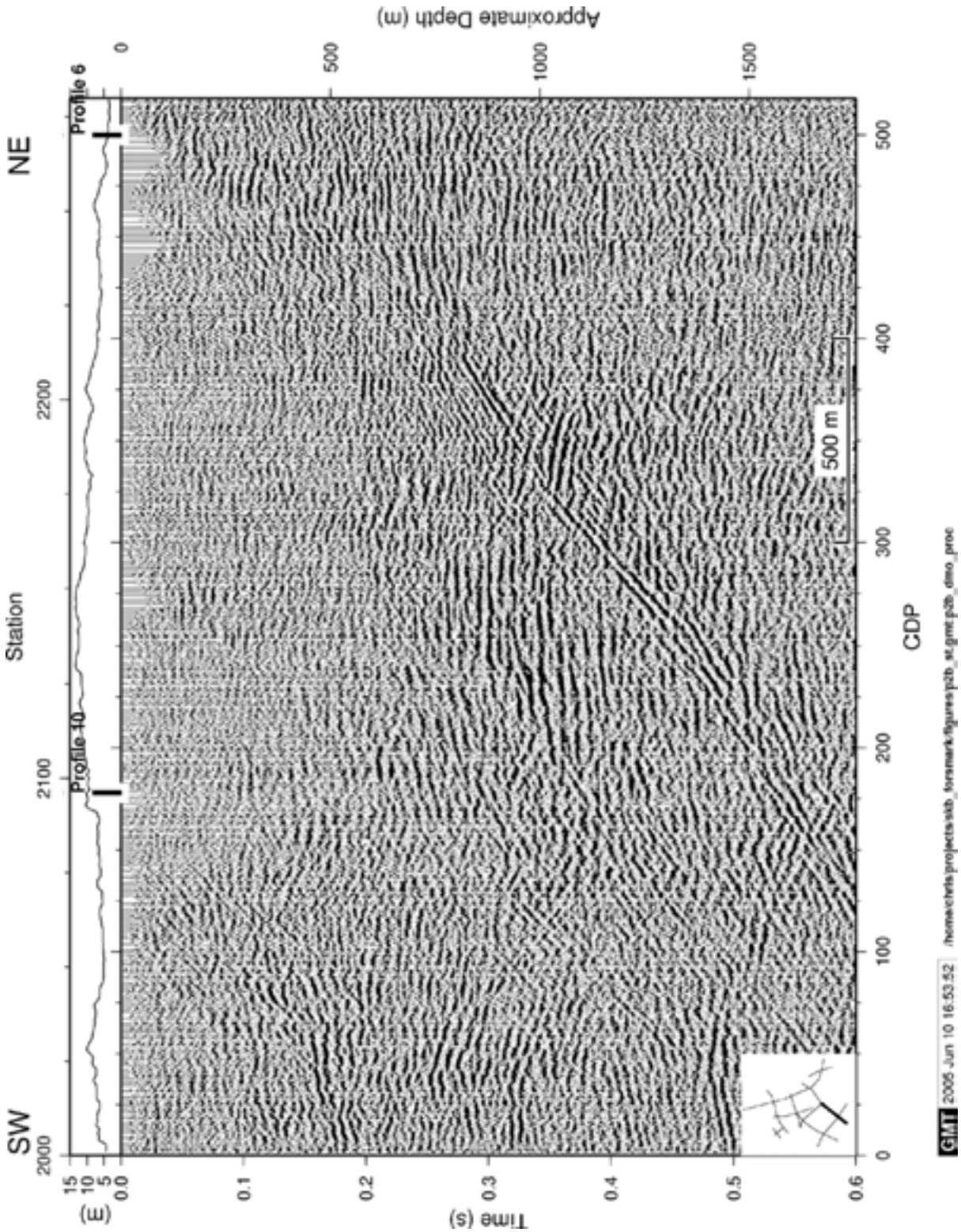

Figure 4-1. Stacked section of profile 2b down to 0.6 seconds. Location of section indicated in lower left corner. Depth scale only valid for true sub-horizontal reflections.

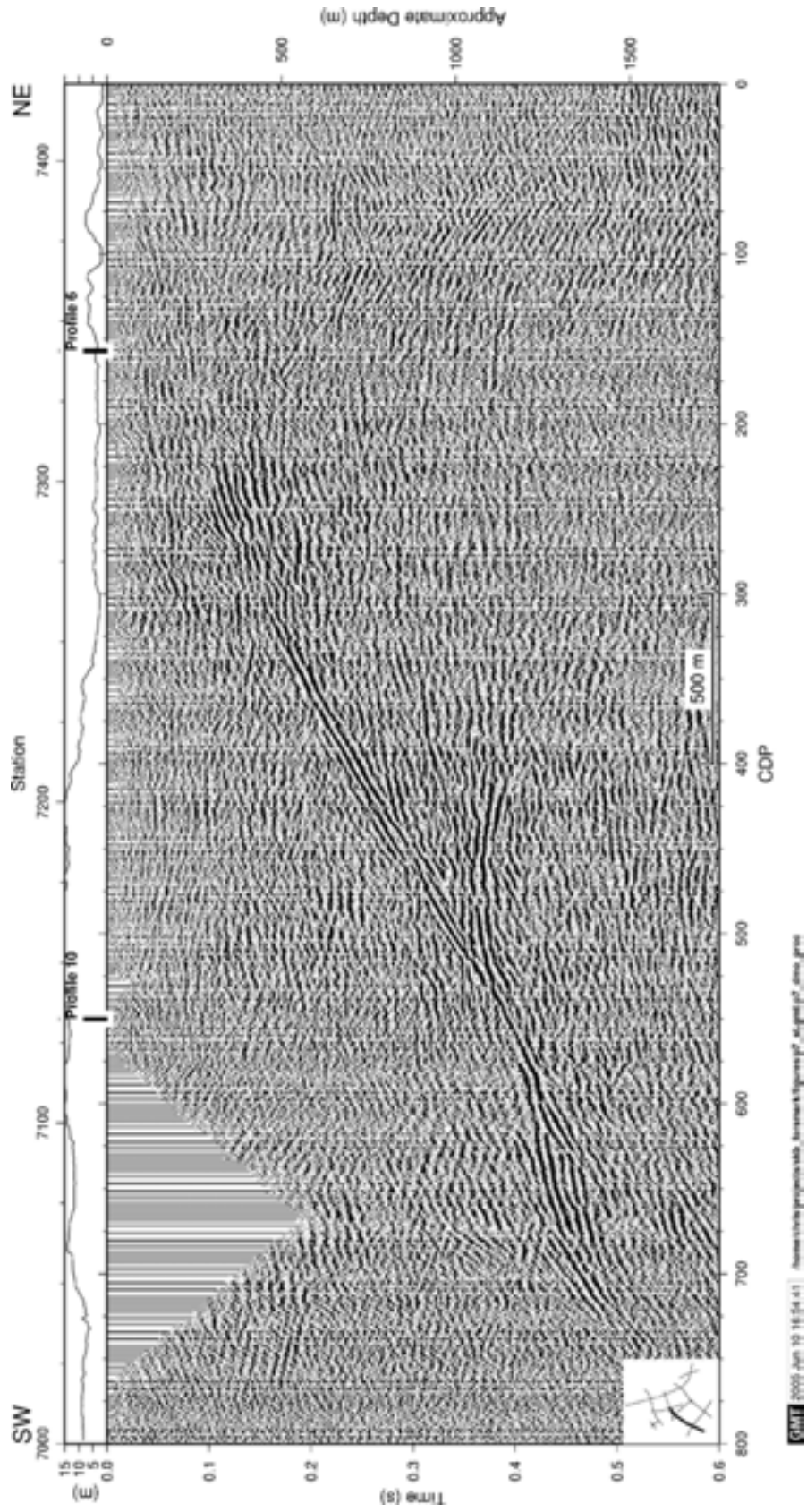

Figure 4-2. Stacked section of profile 7 down to 0.6 seconds. Location of section indicated in lower left corner. Depth scale only valid for true sub-horizontal reflections.

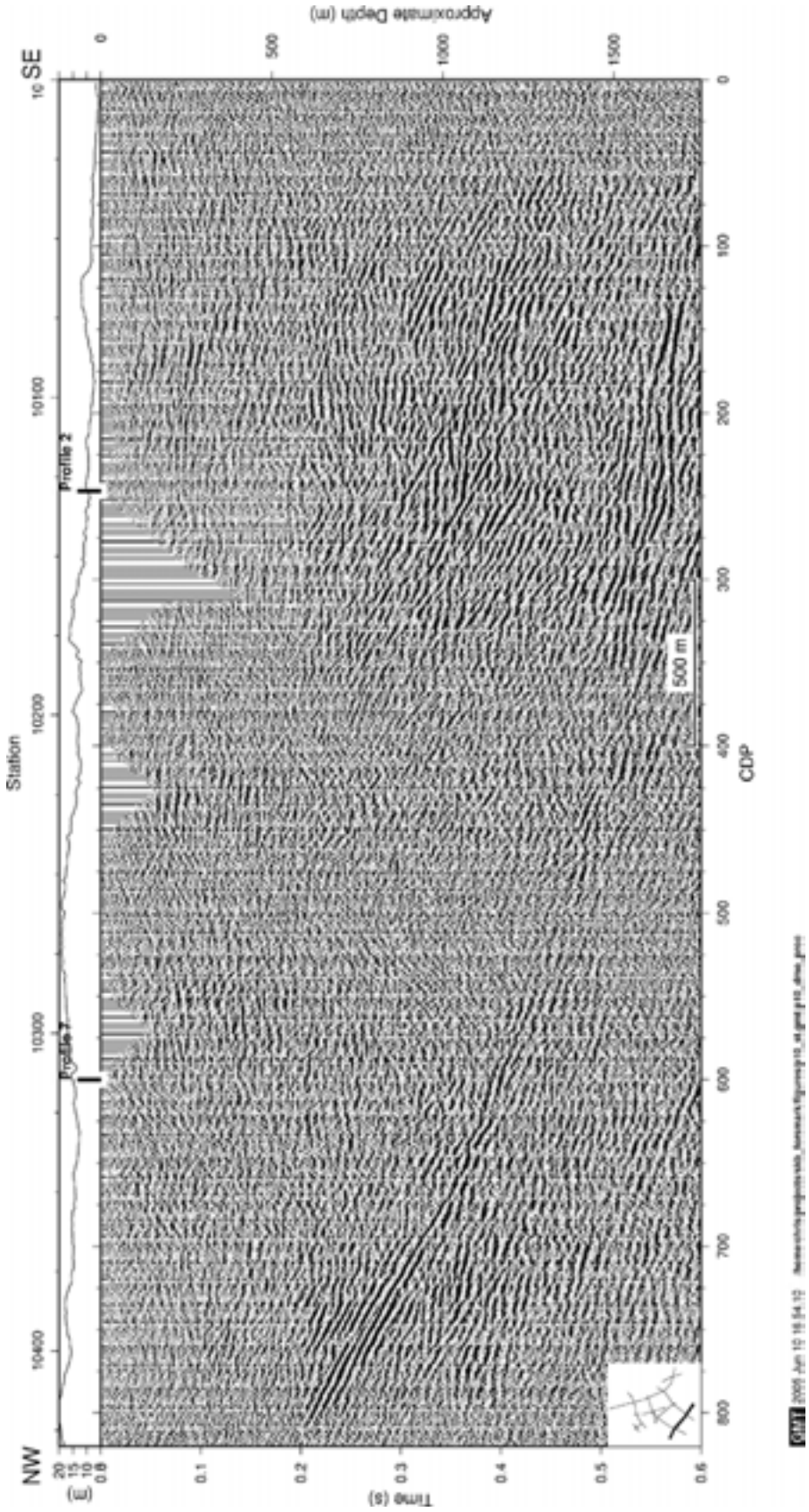

Figure 4-3. Stacked section of profile 10 down to 0.6 seconds. Location of section indicated in lower left corner. Depth scale only valid for true sub-horizontal reflections.

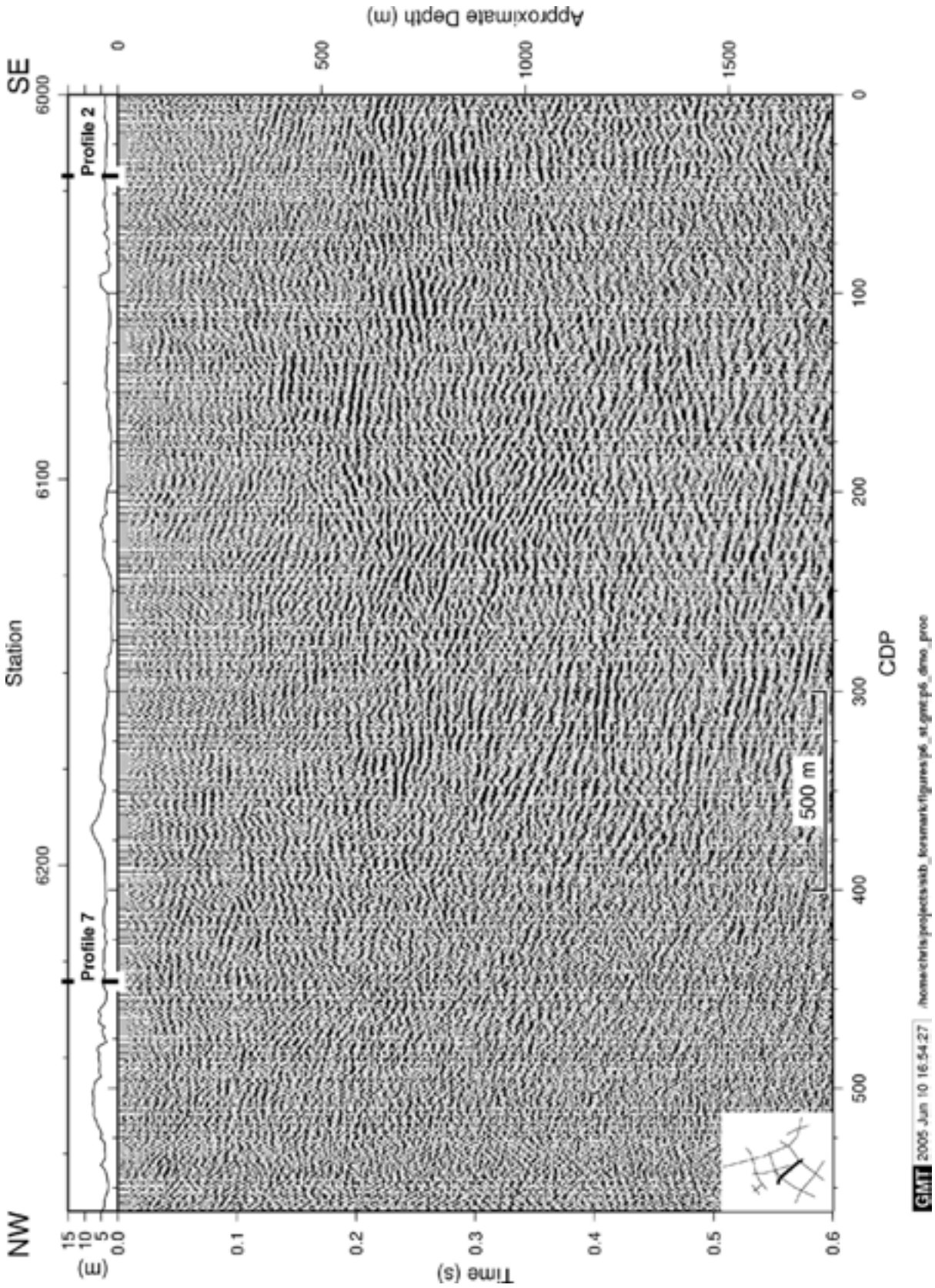

Figure 4-4. Stacked section of profile 6 down to 0.6 seconds. Location of section indicated in lower left corner. Depth scale only valid for true sub-horizontal reflections.

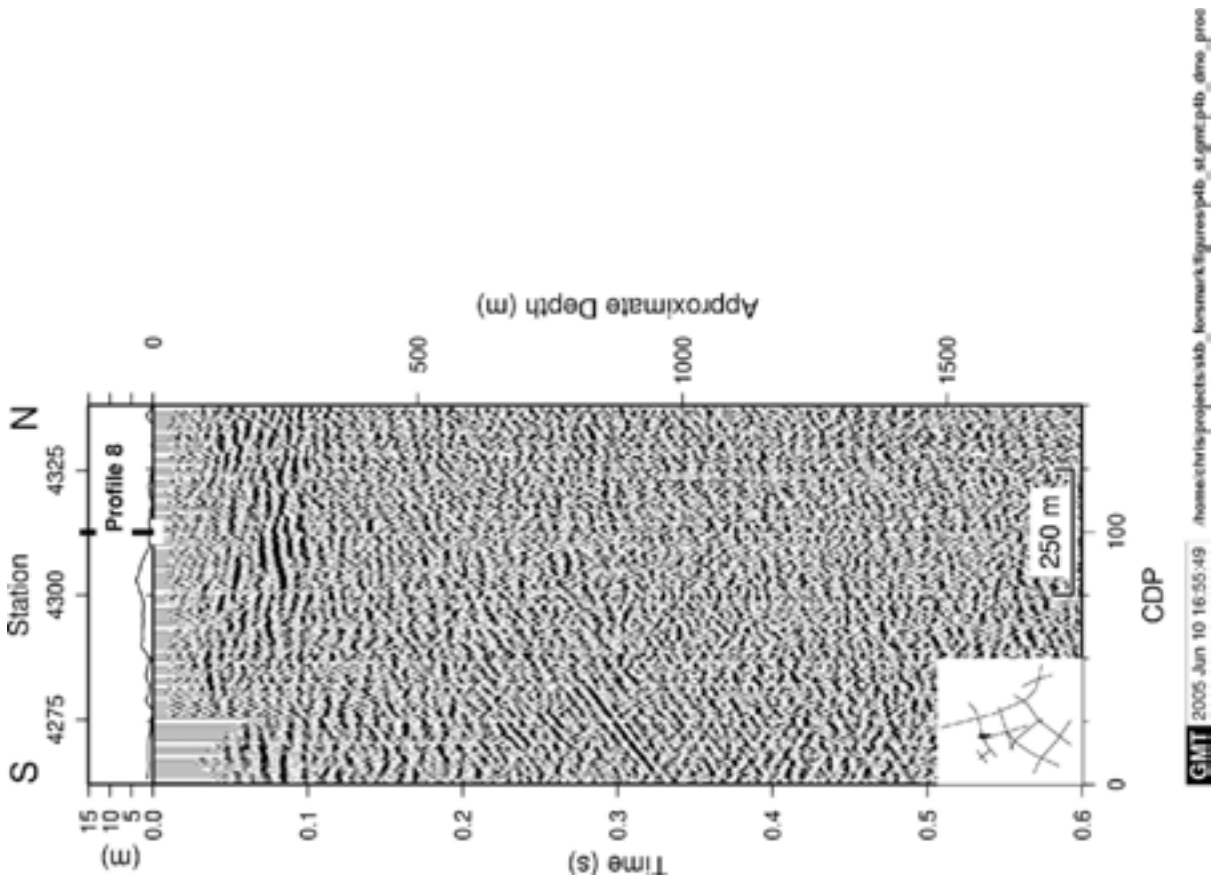

Figure 4-5. Stacked section of profile 4b down to 0.6 seconds. Location of section indicated in lower left corner. Depth scale only valid for true sub-horizontal reflections.

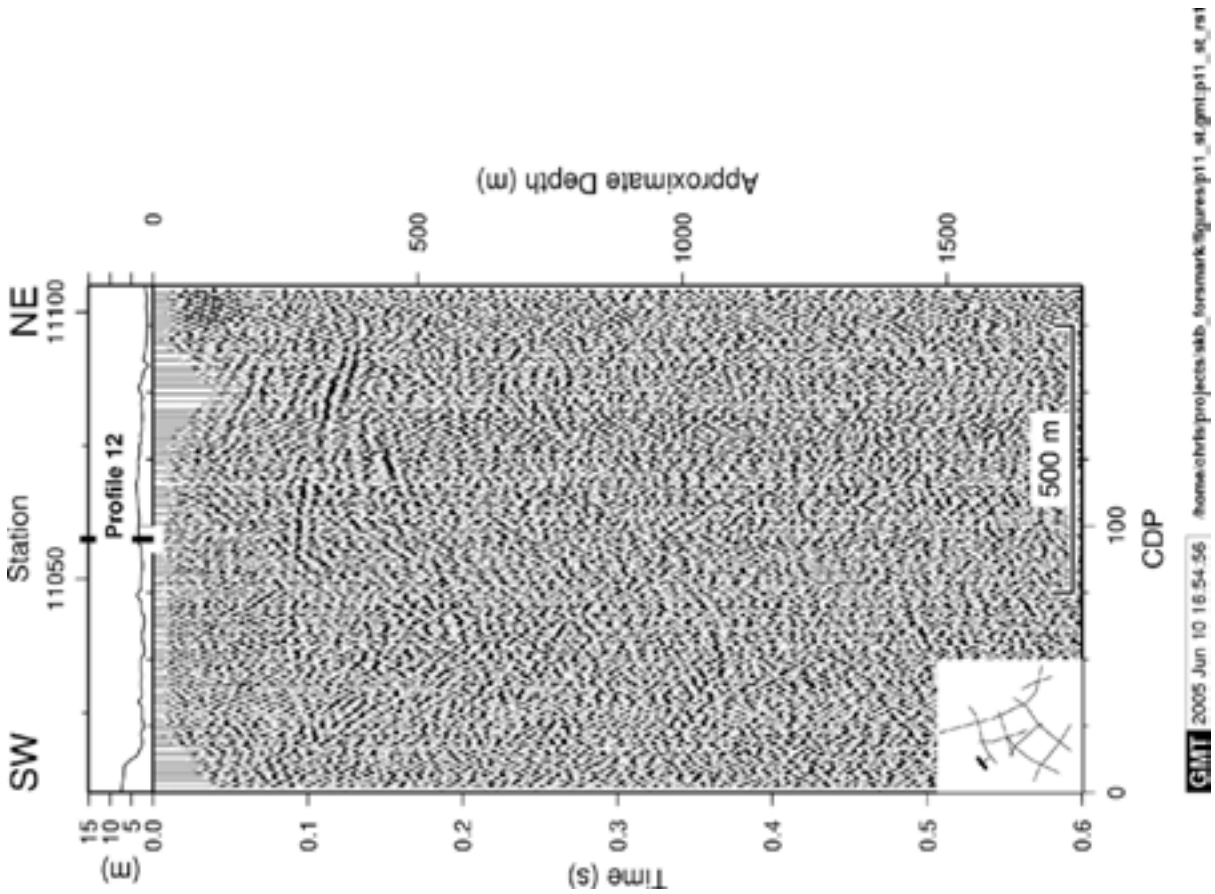

Figure 4-6. Stacked section of profile 11 down to 0.6 seconds. Location of section indicated in lower left corner. Depth scale only valid for true sub-horizontal reflections.

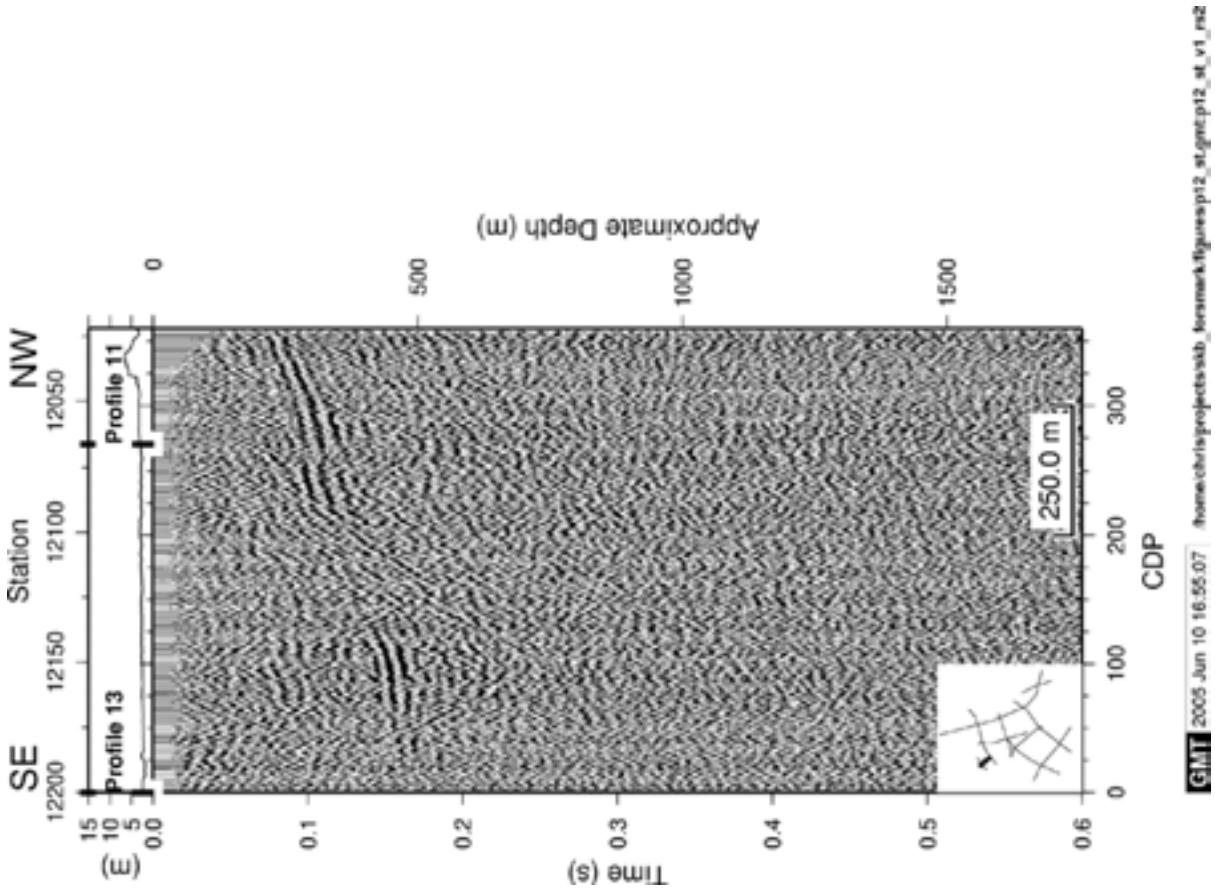

Figure 4-7. Stacked section of profile 12 down to 0.6 seconds. Location of section indicated in lower left corner. Depth scale only valid for true sub-horizontal reflections.

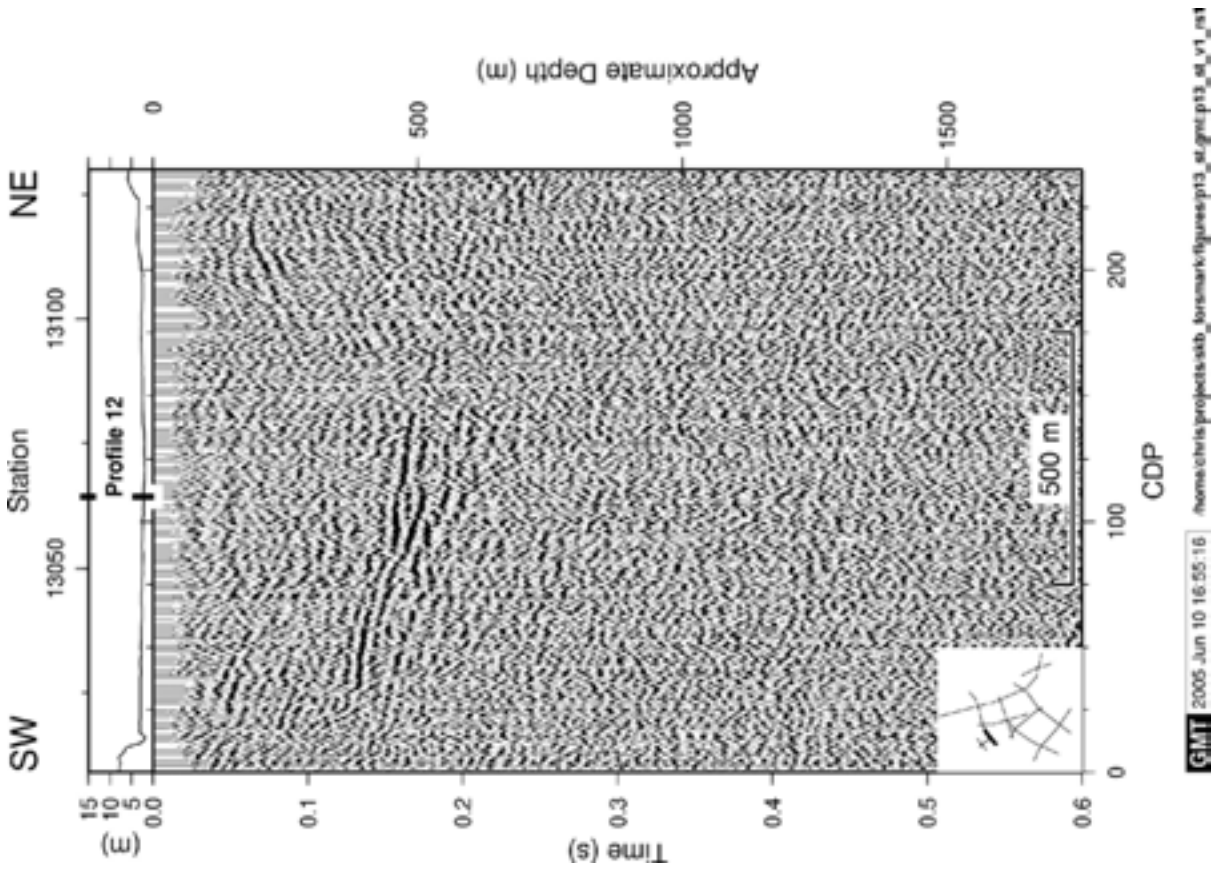

Figure 4-8. Stacked section of profile 13 down to 0.6 seconds. Location of section indicated in lower left corner. Depth scale only valid for true sub-horizontal reflections.

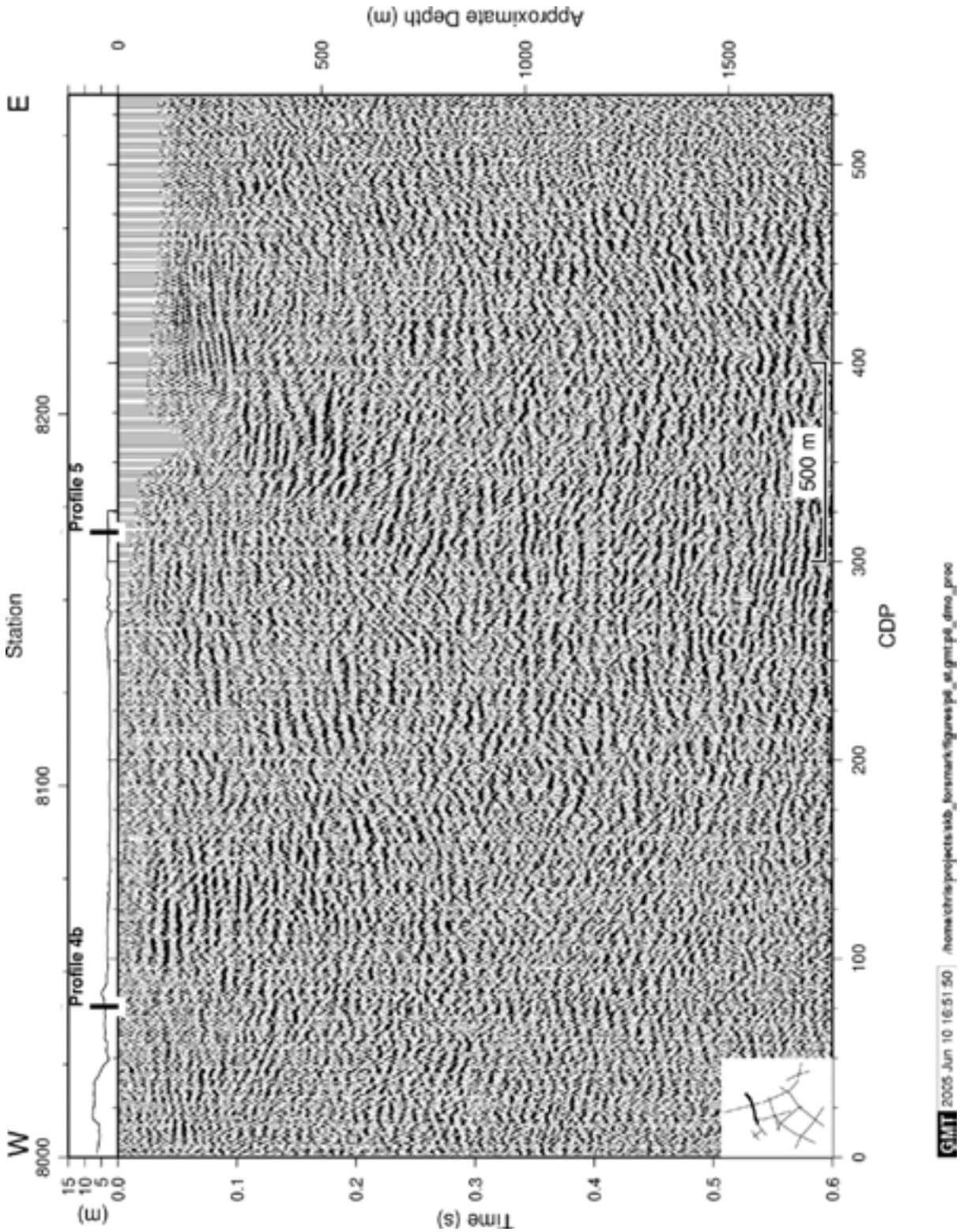

Figure 4-9. Stacked section of profile 8 down to 0.6 seconds. Location of section indicated in lower left corner. Depth scale only valid for true sub-horizontal reflections.

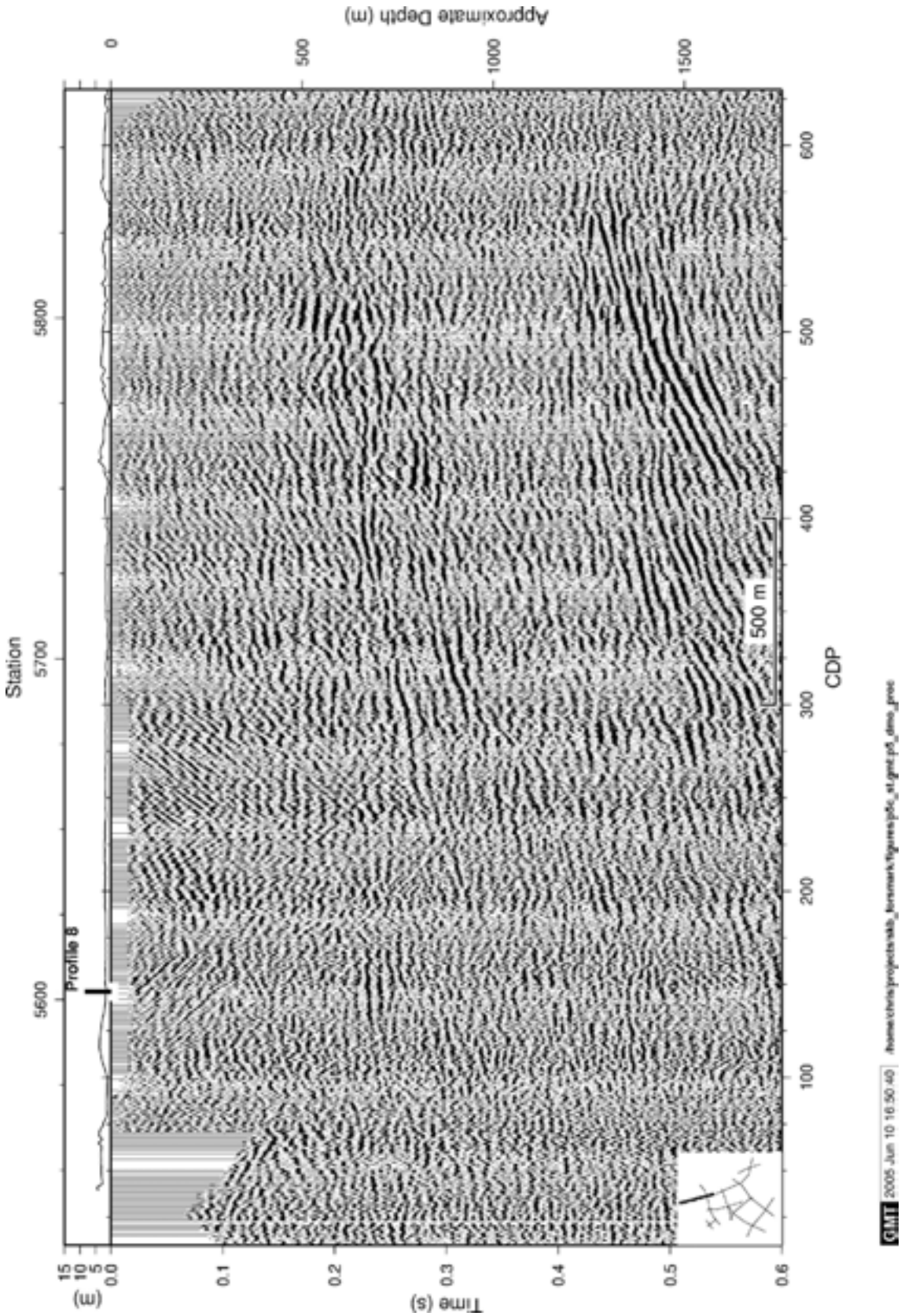

Figure 4-10. Stacked section of profile 5 down to 0.6 seconds. Location of section indicated in lower left corner. Depth scale only valid for true sub-horizontal reflections.

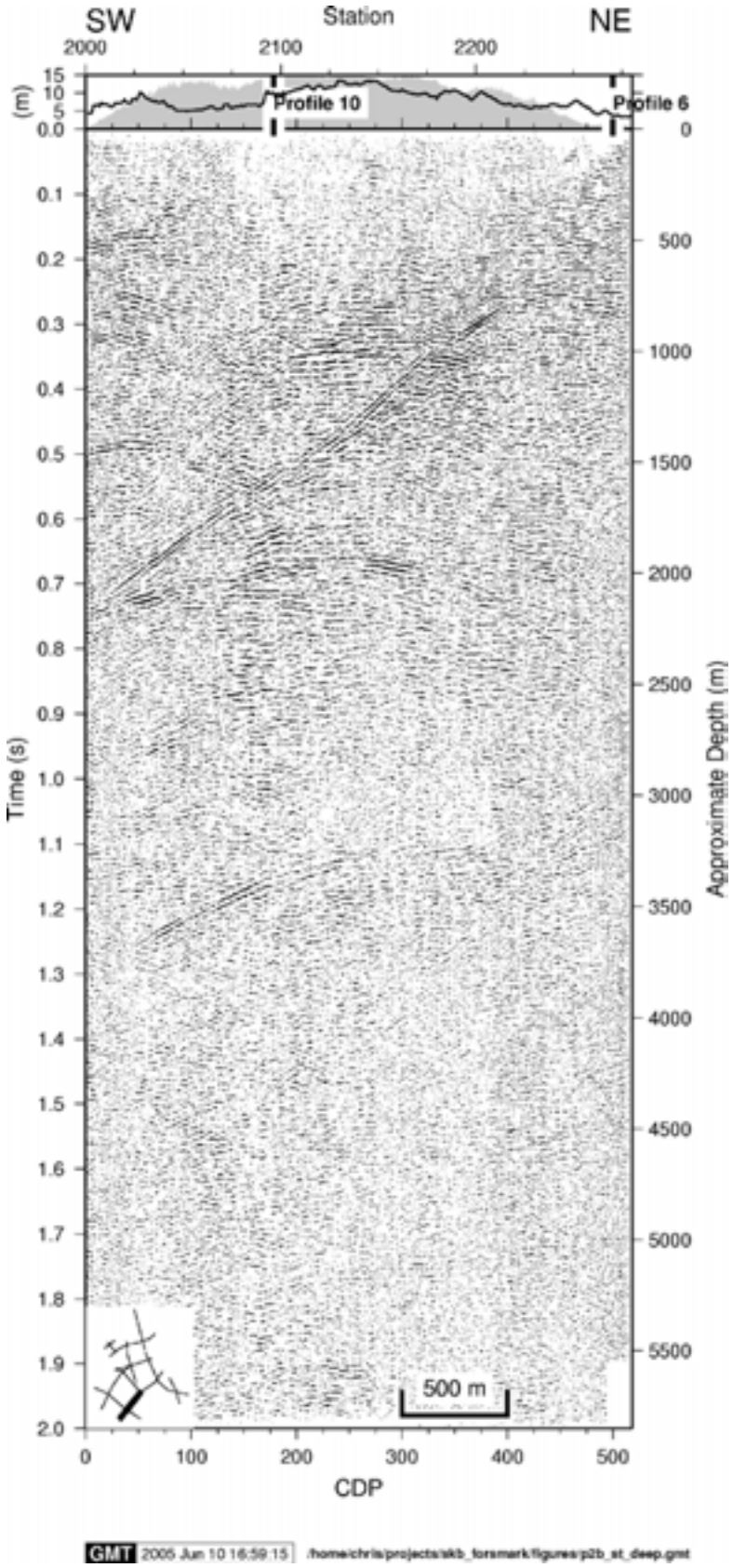

Figure 4-11. Stacked section of profile 2b down to 2.0 seconds. Location of section indicated in lower left corner. Depth scale only valid for true sub-horizontal reflections.

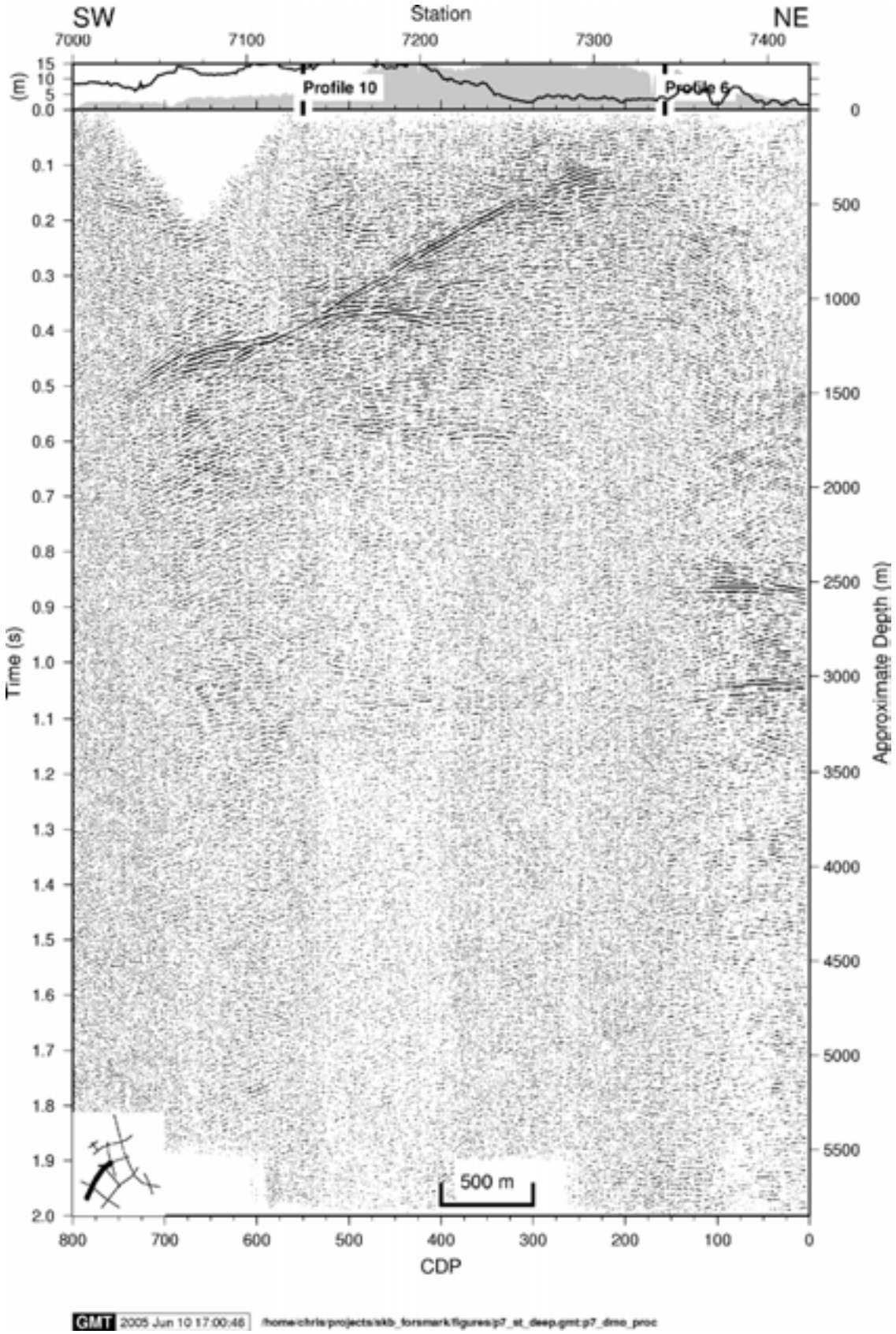

Figure 4-12. Stacked section of profile 7 down to 2.0 seconds. Location of section indicated in lower left corner. Depth scale only valid for true sub-horizontal reflections.

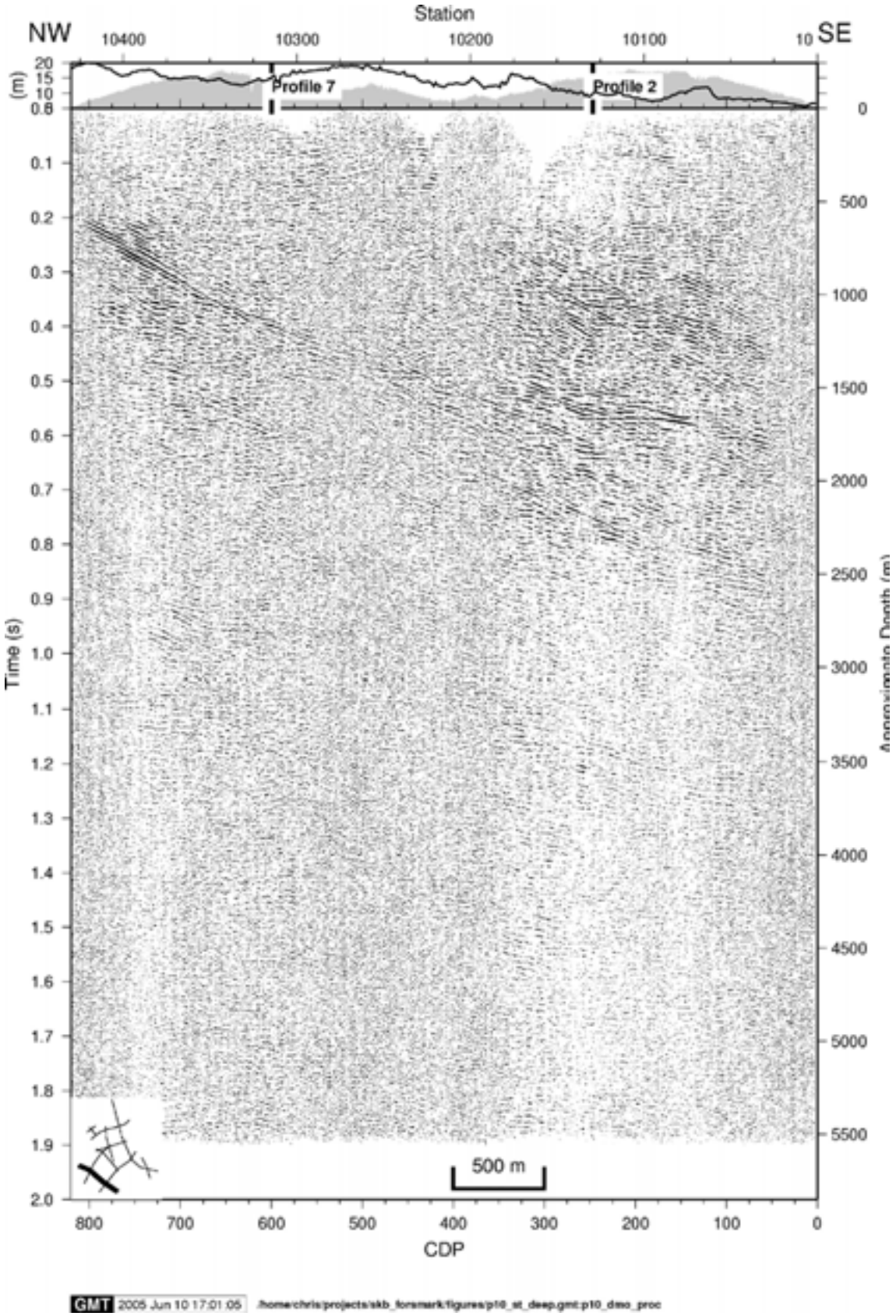

Figure 4-13. Stacked section of profile 10 down to 2.0 seconds. Location of section indicated in lower left corner. Depth scale only valid for true sub-horizontal reflections.

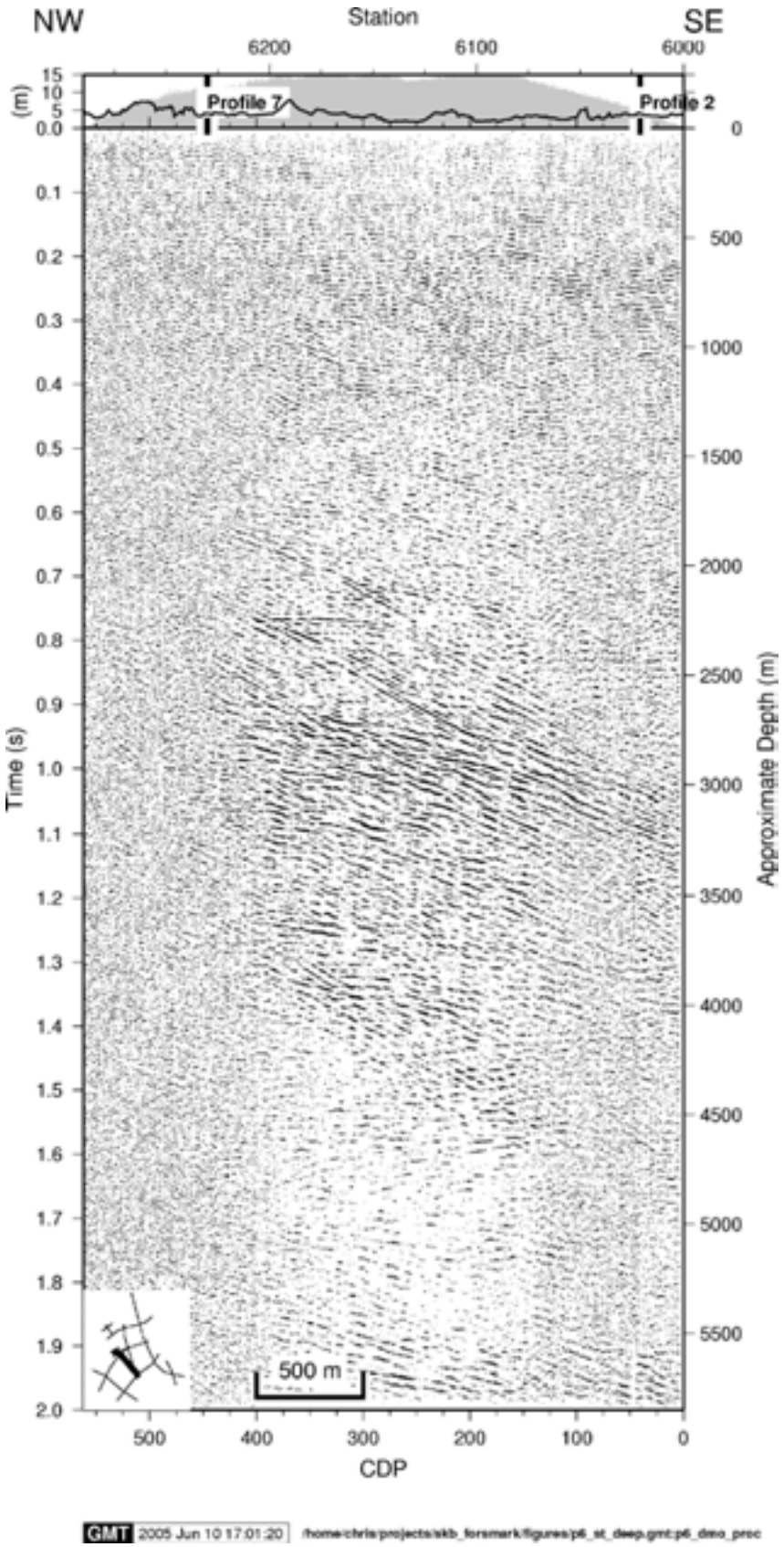

Figure 4-14. Stacked section of profile 6 down to 2.0 seconds. Location of section indicated in lower left corner. Depth scale only valid for true sub-horizontal reflections.

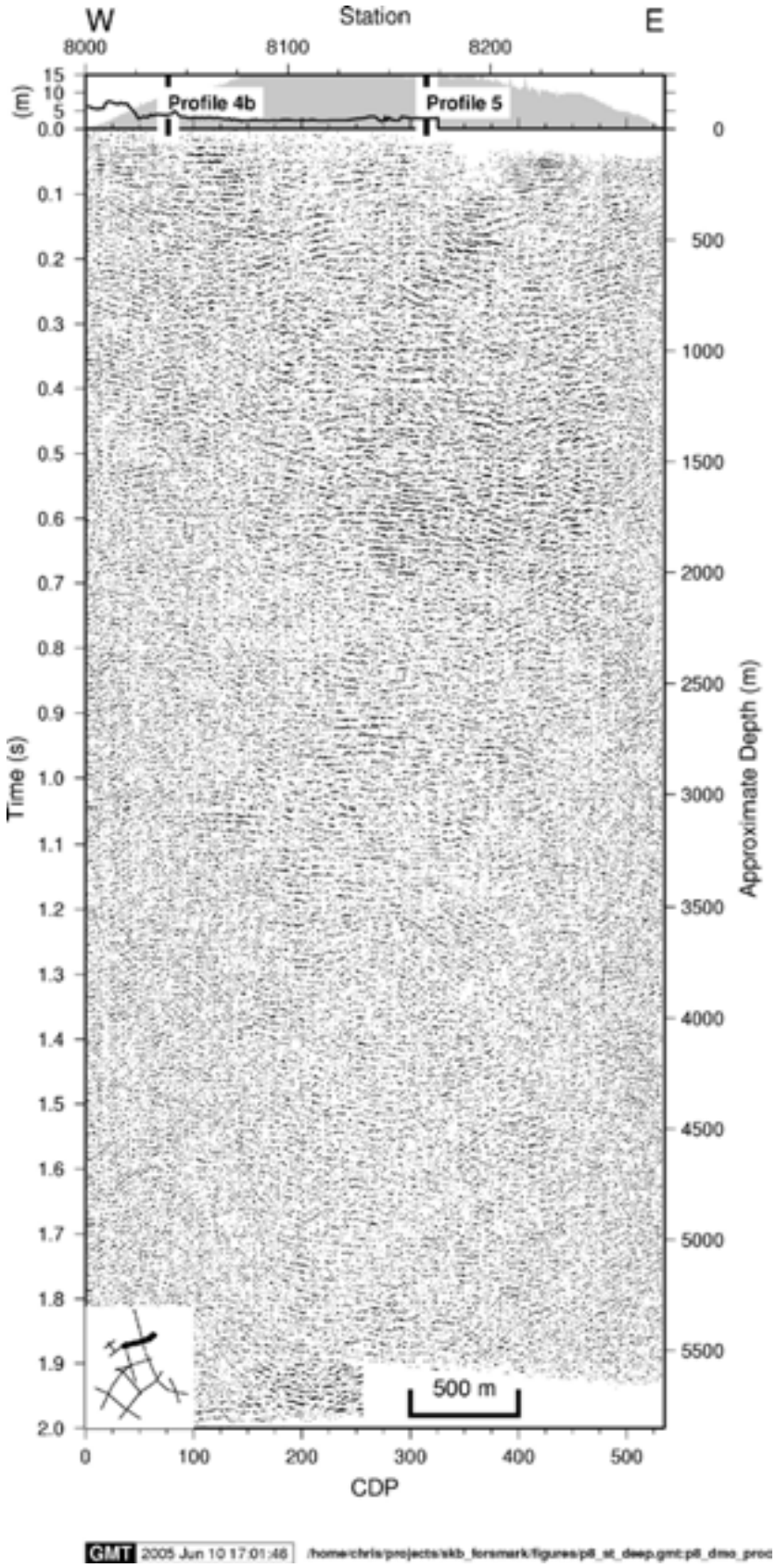

Figure 4-15. Stacked section of profile 8 down to 2.0 seconds. Location of section indicated in lower left corner. Depth scale only valid for true sub-horizontal reflections.

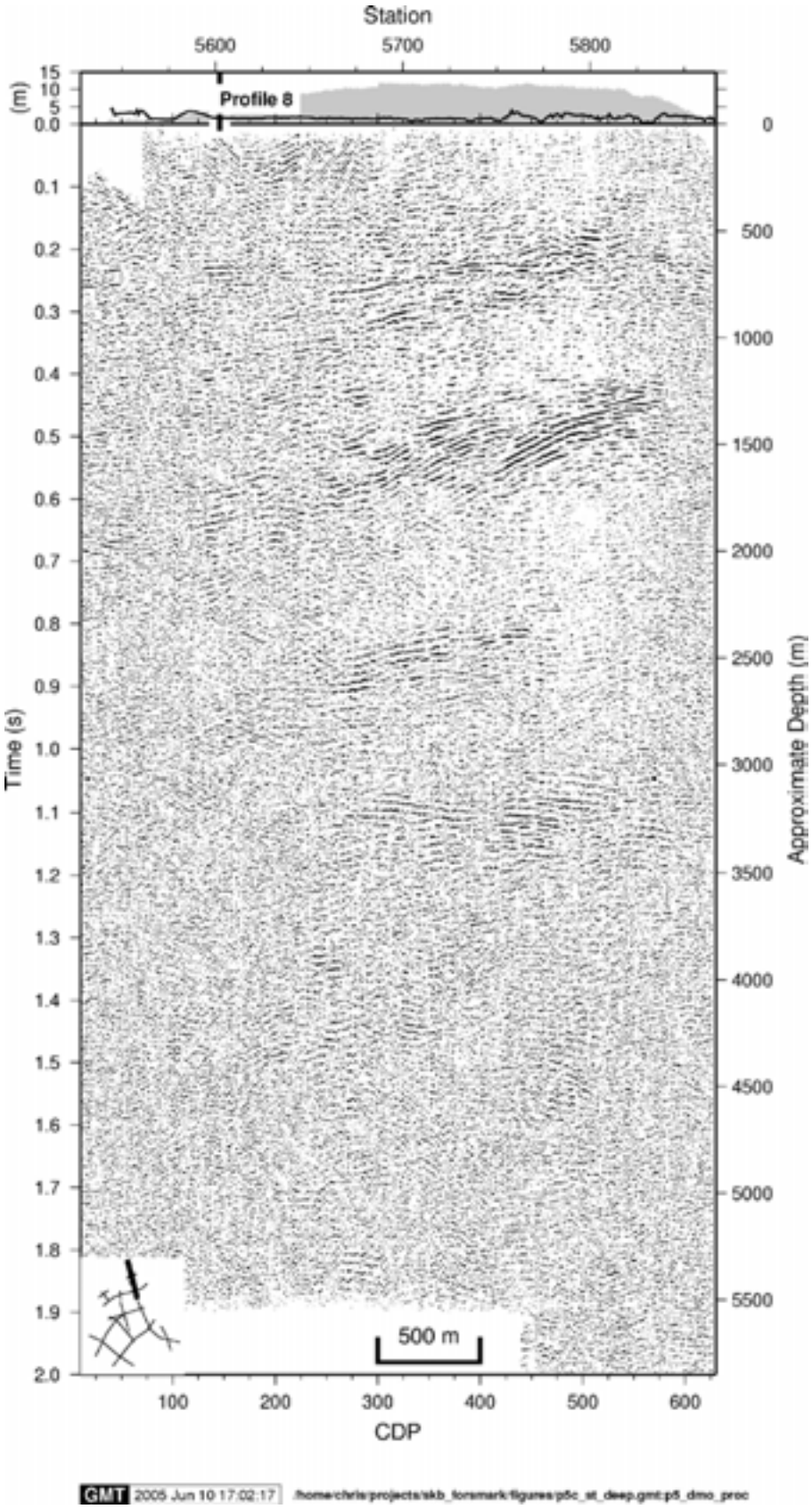

Figure 4-16. Stacked section of profile 5b down to 2.0 seconds. Location of section indicated in lower left corner. Depth scale only valid for true sub-horizontal reflections.

5 Results

5.1 Background

An important aspect of high-resolution seismic studies for nuclear waste disposal is the three dimensional imaging of reflectors and their correlation with borehole data. Fracture zone geometry is often complex and highly three dimensional (Tirén et al., 1999). Ideally, 3D data should be acquired, but for a large area this is a very expensive solution. When only 2D data are available, it is only in the vicinity of crossing lines that it is possible to calculate the true strike and dip of reflectors. Also, if reflections project to the surface on single-line data and can be correlated with a surface feature at the intersection point, then an estimate of the strike and dip can also be made.

In general, reflections may be due to the presence of fracture zones, mafic sheets (sills or dikes), mylonite zones or lithological boundaries at depth. Experience has shown that mafic sheets, in particular, generate distinct high amplitude reflections. Reflections from fracture zones are generally weaker and less distinct. Lateral changes in the reflectivity along the profiles may be due to changes in the geology, but also to changes in acquisition conditions. Noise from the Forsmark power plant, crooked lines (Wu et al., 1995) and changes in the near surface conditions where the source was activated may result in poorer images of reflectors along some portions of the stacked sections.

5.2 Comparison with Stage 1

Profiles 2b and 7 can be regarded as extensions to the south west of profiles 2 and 1, respectively, from Stage 1, while profiles 4b and 5b as extensions to the north of profiles 4 and 5, respectively, from Stage 1. Merged sections of these combined profiles are plotted in Figures 5-1 to 5-4. In general, clear reflections from the Stage 1 sections can be followed on to the Stage 2 sections, but there are some reflectivity patterns that are not consistent. In particular, the upper 0.5 s of profiles 2 and 2b do not merge satisfactorily. Inspection of shot gathers from the 2002 profile 2 shows it may be possible to improve the processing on the southwestern end of this profile, which may give a better match to the newly acquired data.

It is clear that the frequency content of the data along profile 5b is lower than the frequency content along profile 5 from Stage 1 (Figure 5-4). The poorer data quality south of CDP 200 on profile 5b is also apparent on the combined section.

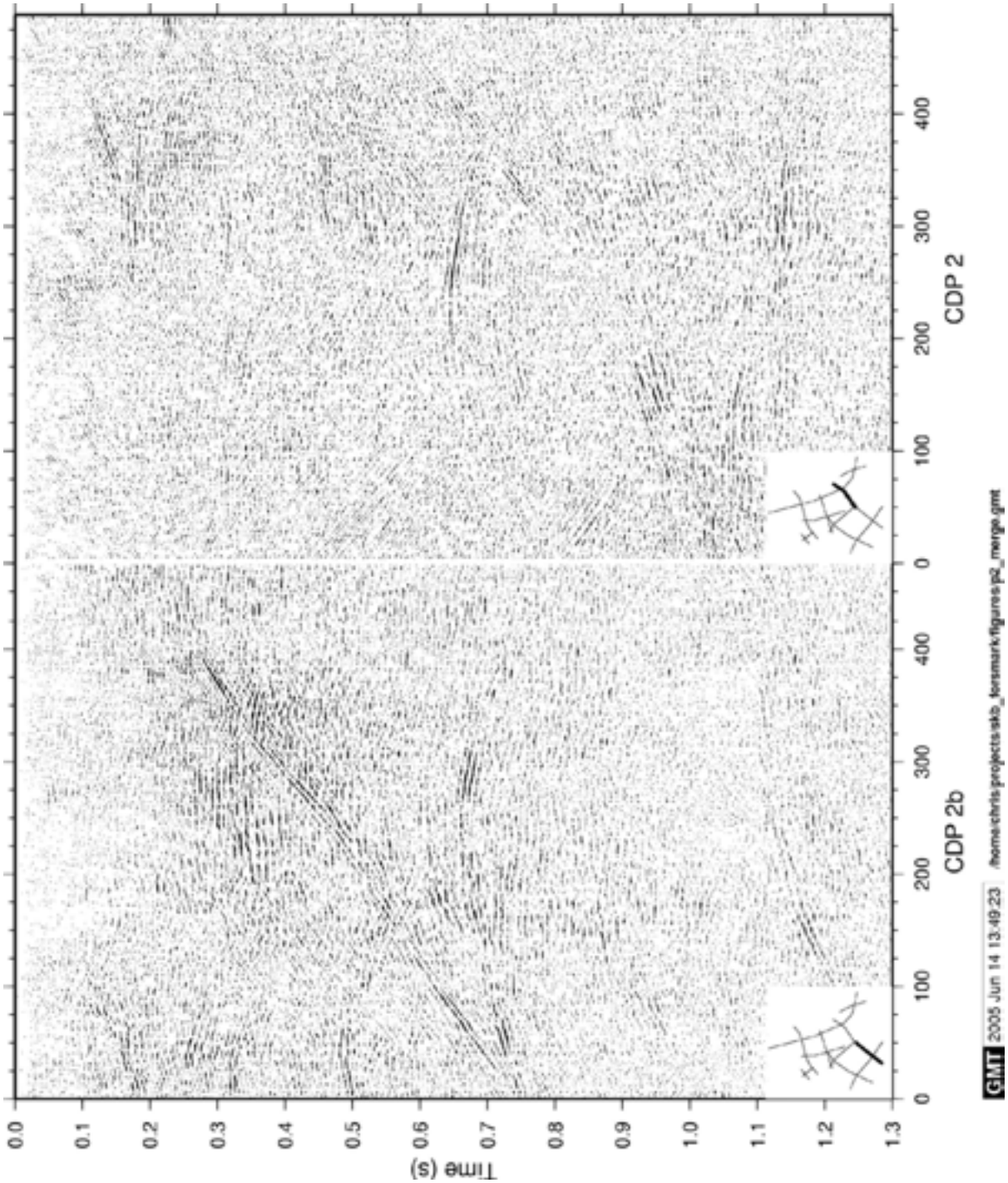

Figure 5-1. Stacked sections of profile 2b acquired in 2004 and profile 2 acquired in 2002 down to 1.3 seconds. Where the profiles overlap, data from profile 2 have been plotted. Location of sections indicated in lower left corners.

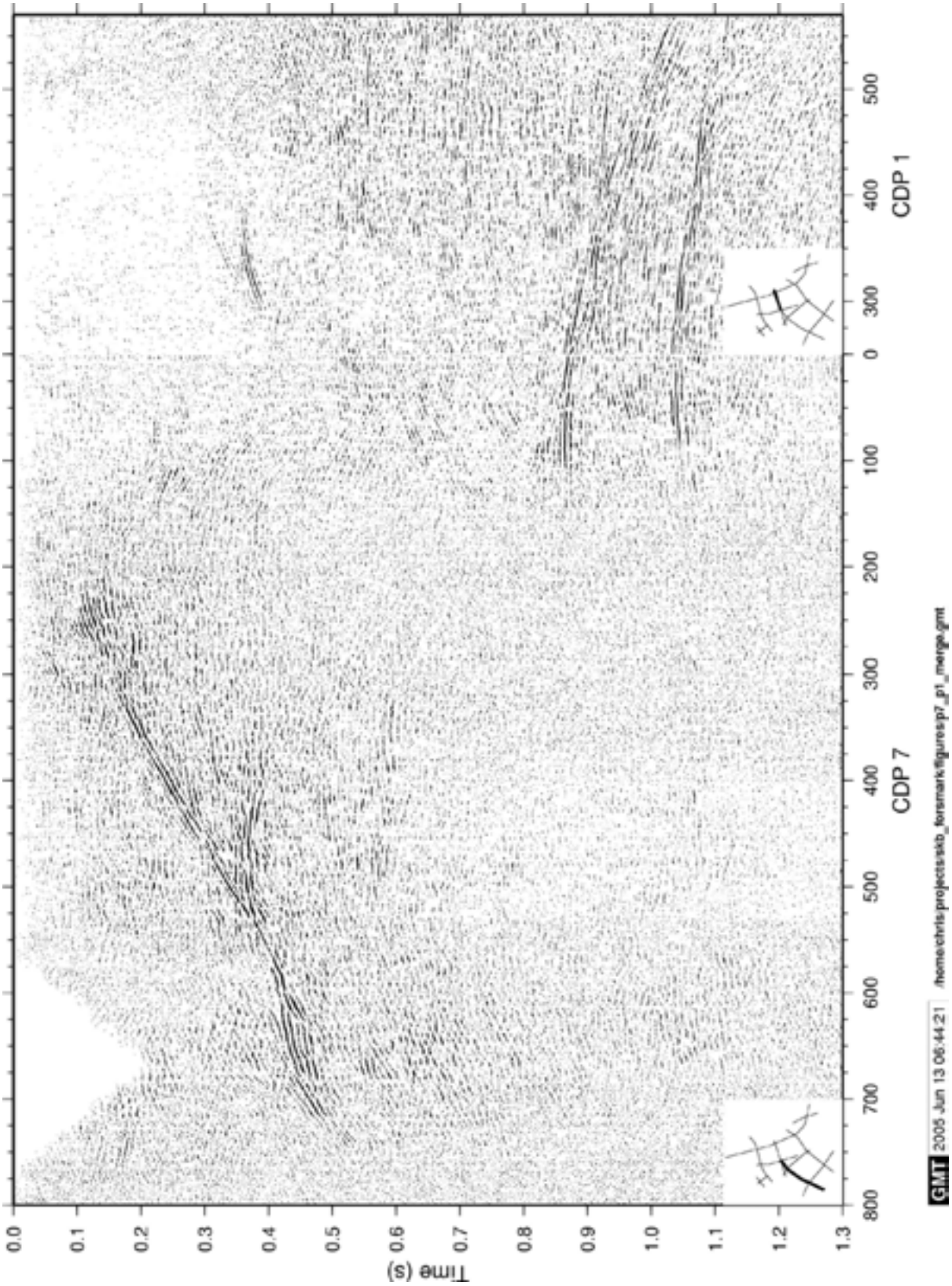

Figure 5-2. Stacked sections of profile 7 acquired in 2004 and north eastern part of profile 1 acquired in 2002 down to 1.3 seconds. Location of sections indicated in lower left corners.

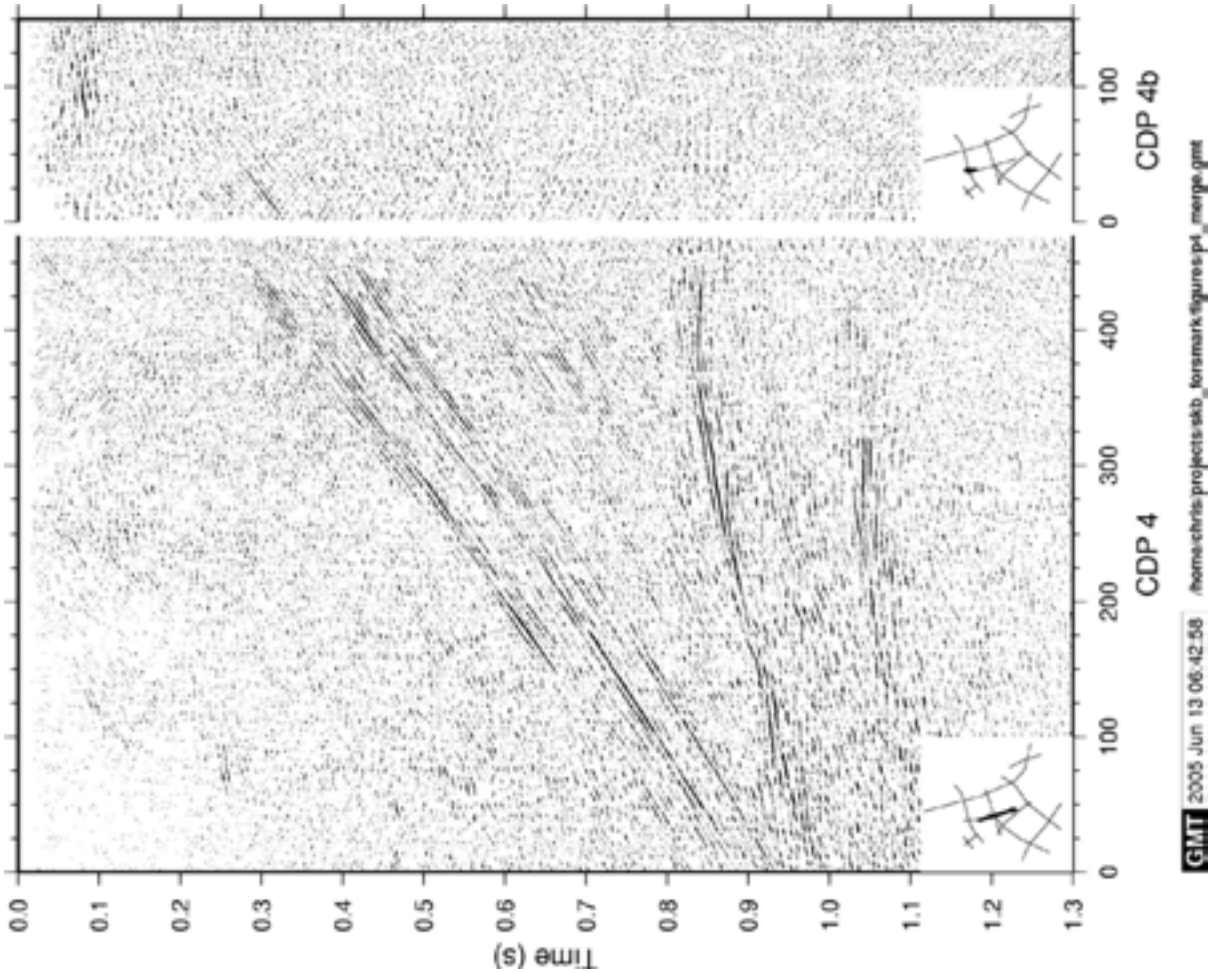

Figure 5-3. Stacked sections of profile 4b acquired in 2004 and profile 4 acquired in 2002 down to 1.3 seconds. Location of sections indicated in lower left corners.

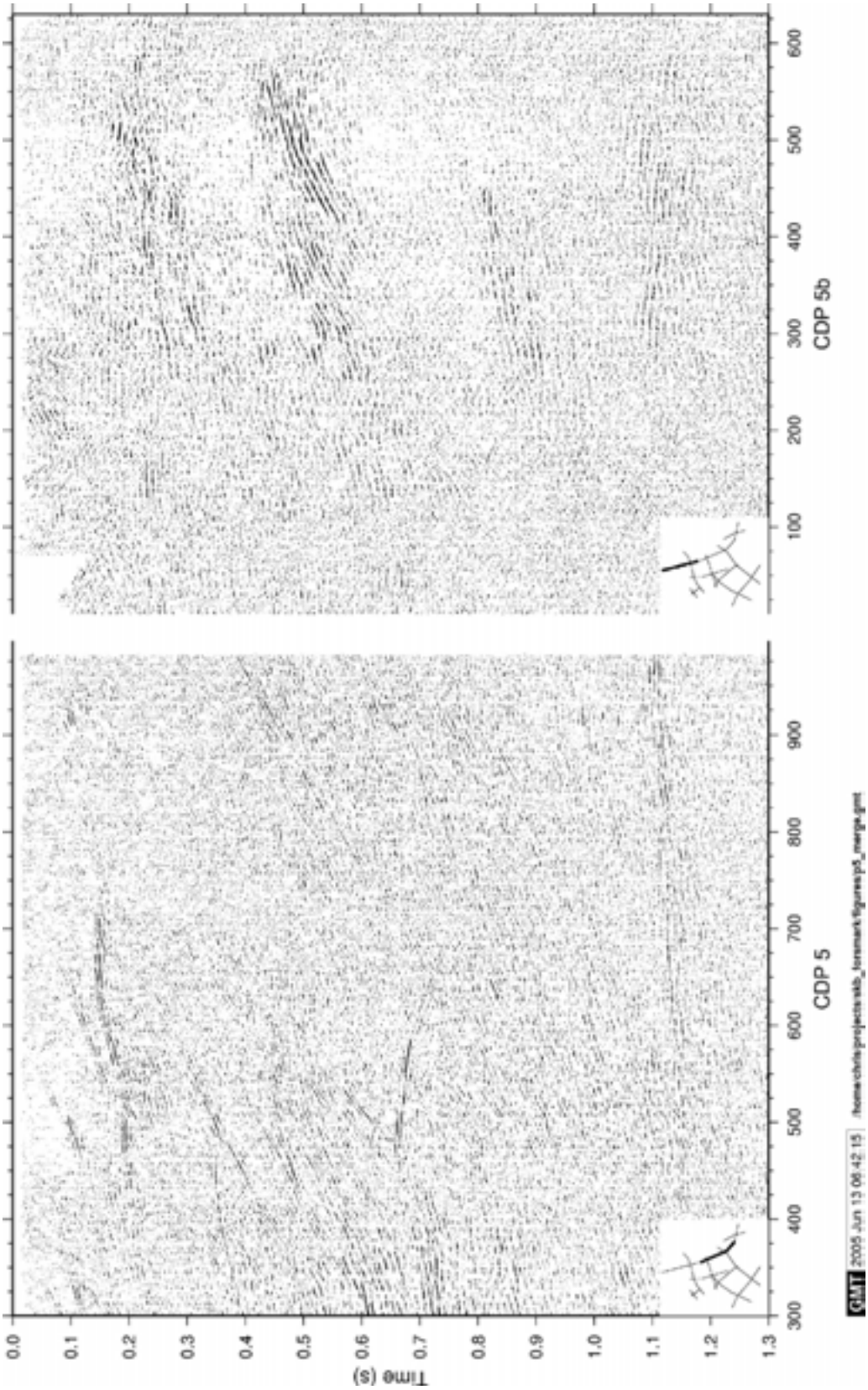

Figure 5-4. Stacked sections of profile 5b acquired in 2004 and the north western part of profile 5 acquired in 2002 down to 1.3 seconds. Location of sections indicated in lower left corners.

5.3 Orientation and extent of reflections

In order to obtain 3D control where the profiles cross, a combination of correlation of reflections between the profiles (Figures 5-5 to 5-11) and seismic modelling (Ayarza et al., 2000) has been used. In principle, a reflection observed on one profile should be observed on a crossing profile at the crossing point at the same traveltime. However, this is not always the case, especially for weaker reflections. Different reflections may have been enhanced in the processing on the different profiles. The crooked line acquisition geometry may also result in destructive stacking of certain reflections, especially those coming from out-of-the-plane of the profile. Also, since numerous reflections are present on some parts of the profiles it can be difficult to uniquely identify one and the same reflection on two crossing profiles due to interference effects.

Table 5-1 lists those reflections that have been oriented in Stage 2 and these are ranked according to the likelihood that the reflector would be encountered in a drilling operation. Reflections A1, A2, C1 and C2 are also observed on the Stage 1 data. The remaining reflections in Table 5-1 are new for the Stage 2 data.

As a check on the picking and the orientation, reflections from these interfaces have been modelled, assuming that the interfaces are planes, and then compared with the observed data in order to obtain some idea of the lateral extent of the reflecting interfaces (Figures 5-12 to 5-18). When the reflection is not observed on the section or its position does not match that expected from the modelling, then the assumption of the reflector being a plane may have broken down. The A0 reflection is not listed in Table 5-1, but is also plotted since it represents the base of the A1 package and is sometimes more clearly seen in the sections.

The most prominent reflections on the Stage 2 profiles are the J1, J2 and K1 reflection in the south west. These are most clearly observed on profiles 2b, 7 and 10 (Figures 5-19 to 5-21). The orientations of the J2 and K1 reflections are somewhat uncertain due to that they arrive at the same time where profiles 10 and 7 cross one another and, thus, interfere with one another. J3 represents (Figure 5-12) a set of more steeply dipping reflections observed on profiles 2b and 10. Several of these are present and have a similar strike to J1 and J2, but none of them can be traced to the surface.

More diffuse sub-horizontal reflections are also present in the upper 0.4 s on the south eastern part of profile 10 and on the north eastern part of profile 2b (Figures 5-19 and 5-21). G5 and G6 mark the approximate top and bottom of this reflectivity. G7 has a similar orientation to G5 and G6, but is more distinct and shallower (Figures 5-19 and 5-21).

Although not as clearly imaged as on the Stage 1 data, the A2 reflection appears present on the northernmost parts of profiles 6 and 7 (Figure 5-14). It can followed south to about CDP 300 on profile 7 and to about CDP 350 on profile 6.

The A1 reflector produced the most prominent reflection on the Stage 1 data. Reflections consistent with its orientation are clearly seen on all profiles except for profiles 11,12, and 13. This suggests that the A1 reflector does not exist under the power plant. Further east, along profile 4b, it appears to be cut off by sub-horizontal reflections before reaching the surface (Figure 5-17). Signs of A1 can be found along entire profile 8 (Figure 5-22) in the form of sub-horizontal reflections. This is to be expected for a profile running parallel to the strike of a complex dipping reflecting zone. Although data quality are poor, the A1 reflection appears to reach the surface along profile 5b close to CDP 250 (Figure 5-23).

Below the power plant, 2 new reflectors are indicated, B8 and B9 (Figures 5-15 and 5-16). Reflections from B8 are well defined, whereas those from B9 are not as clear. However, B9

can almost be traced to the surface along profile 13.

The zone of sub-horizontal reflections that appear to stop the A1 reflection from reaching the surface on profile 4b have been labelled as L1 and L2 (Figure 5-17) with L1 representing the top of the zone and L2 the bottom. Their orientation is somewhat uncertain, but they appear to dip gently in the opposite direction to the A1 reflection zone.

The crust becomes quite reflective below the northern part of profile 5b (Figure 5-23). This reflectivity appears to dip within the plane of profile 5c since mostly sub-horizontal reflections are observed on profile 8 (Figure 5-22) at corresponding times. The tops of the two most reflective zones (M1 and M2 in Figure 5-23) dip gently to the north.

None of the new reflections identified in the Stage 2 profiles can be reliably traced to the surface, with the possible exception of the B9 reflection on profile 13. This is due to either the profiles not being long enough or that the reflections cannot be followed to the surface on the profiles. In the latter case, they are either cut by other reflections or simply become diffuse. However, it is still of interest to project the orientations of the reflections to the surface and compare with the topography (Figure 5-24) and the magnetic map (Figure 5-25).

For completeness, Table 5-2 lists all reflectors that have been identified in Stage 1 and Stage 2 with the exception of the group D reflectors that were speculated upon in the Stage 1 report (Juhlin et al., 2002a). These have been removed since it was not possible to confirm their existence in the Stage 2 data. Projections of reflections to the surface for Stage 1 and Stage 2 onto the topographic and magnetic maps are shown in Figures 5-26 and 5-27.

Table 5-1. Orientation of reflectors from Stage 2 as determined in this report. Distance refers to distance from the arbitrary origin (6699 km N, 1633 km W) to the closest point on the reflector at the surface. Depth refers to depth below the surface at this origin. Strike is measured clockwise from north. Rank indicates how sure the observation of each reflection is on profiles that the reflection is observed on; 1 – definite, 2- probable, 3-possible.

Reflector	*Strike*	*Dip*	*Distance (m)*	*Depth (m)*	*Rank*	*Profiles observed on*
A1	75	45	3100		2	2b, 4b, 5b?, 6, 7, 8, 10
A2	80	22	790		2	6, 7
B8	15	22	4400		1	11, 12, 13
B9	-5	38	3150		2	11, 12, 13, 4b?
C1	15	20		3300	1	2b, 4b, 5b, 6, 7. 8, 10
C2	-5	10		3300	1	2b, 4b, 5b, 6, 7, 8, 10
G5	100	12		200	3	2b, 6, 10
G6	100	12		550	3	2b, 6, 10
G7	100	12		-400	3	6, 10
J1	115	48	-1050		1	2b, 10
J2	100	37	-150		1	7, 10
J3	90	70	-1500		2	2b, 10
K1	50	40	2800		1	7, 10
L1	-105	7	-400		2	4, 8
L2	-105	7	-1600		2	4, 8
M1	80	11	6900		2	5, 8
M2	80	11	10900		2	5, 8

Table 5-2. Orientation of reflectors from Stage 2 as determined from this report and from Stage 1 as determined from the surface seismic in P-04-158 (Juhlin and Bergman, 2004). Distance refers to distance from the arbitrary origin (6699 km N, 1633 km W) to the closest point on the reflector at the surface. Depth refers to depth below the surface at this origin. Strike is measured clockwise from north. Rank indicates how sure the observation of each reflection is on profiles that the reflection is observed on; 1 – definite, 2- probable, 3-possible.

Reflector	*Strike*	*Dip*	*Distance (m)*	*Depth (m)*	*Rank*	*Profiles observed on*
A1	75	45	3100		2	1, 2, 2b, 3, 4, 4b, 5, 5b?, 6, 7, 8, 10
A2	80	22	790		1	2, 4, 5, 6, 7
A3	50	23	-50		1	3, 5
A4	65	25	-950		1	3, 5
A5	75	30	-1450		1	3, 5
A6	75	30	-1875		1	3, 5
A7	55	23	-780		1	3, 5
B1	30	25	-600		1	3, 5
B2	30	25	800		1	2?, 3, 5
B3	30	21	1550		1	2?, 3, 4?, 5
B4	50	28	1460		1	2, 3, 4?,5
B5	50	25	2600		1	3, 4?, 5
B6	30	32	-250		1	3, 5
B7	25	20	1700		2	1, 5
B8	15	22	4400		1	11, 12, 13
B9	-5	38	3150		2	11, 12, 13, 4b?
C1	15	20		3300	1	1, 2, 2b, 3, 4, 4b, 5, 5b?, 6, 7, 8, 10
C2	355	10		3300	1	1, 2, 2b, 3, 4, 4b, 5, 5b?, 6, 7, 8, 10
E1	270	9		2020	2	2, 5
F1	20	20		400	2	2, 5
G1	180	3		100	3	1, 4
G2	180	3		200	3	1, 4
G3	0	2		1120	3	1, 4
G4	0	2		1220	3	1, 4
G5	100	12		200	3	2b, 6, 10
G6	100	12		550	3	2b, 6, 10
G7	100	12		-400	3	6, 10
H1	123	70	-150		2	1, 2?, 4
H2	123	70	-50		2	1, 2?, 4
I1	30	70	-1100		2	3, 5
J1	115	48	-1050		1	2b, 10
J2	100	37	-150		1	7, 10
J3	90	70	-1500		2	2b, 10
K1	50	40	2800		1	7, 10
L1	-105	7	-400		2	4, 8
L2	-105	7	-1600		2	4, 8
M1	80	11	6900		2	5, 8
M2	80	11	10900		2	5, 8

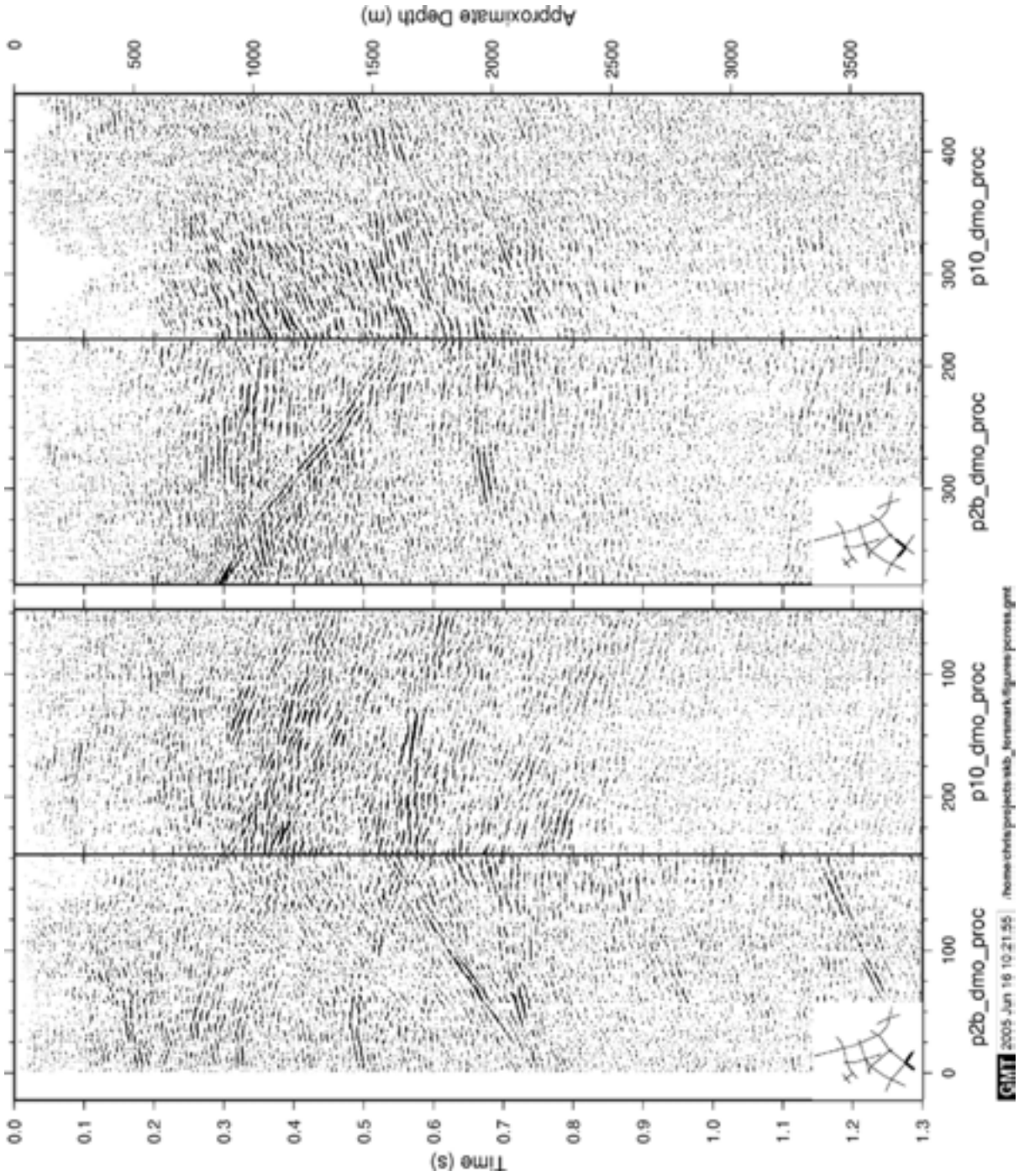

Figure 5-5. Correlation of stacks from profiles 10 and 2b at their crossing point (Figure 3-1). Horizontal numbering is CDP.

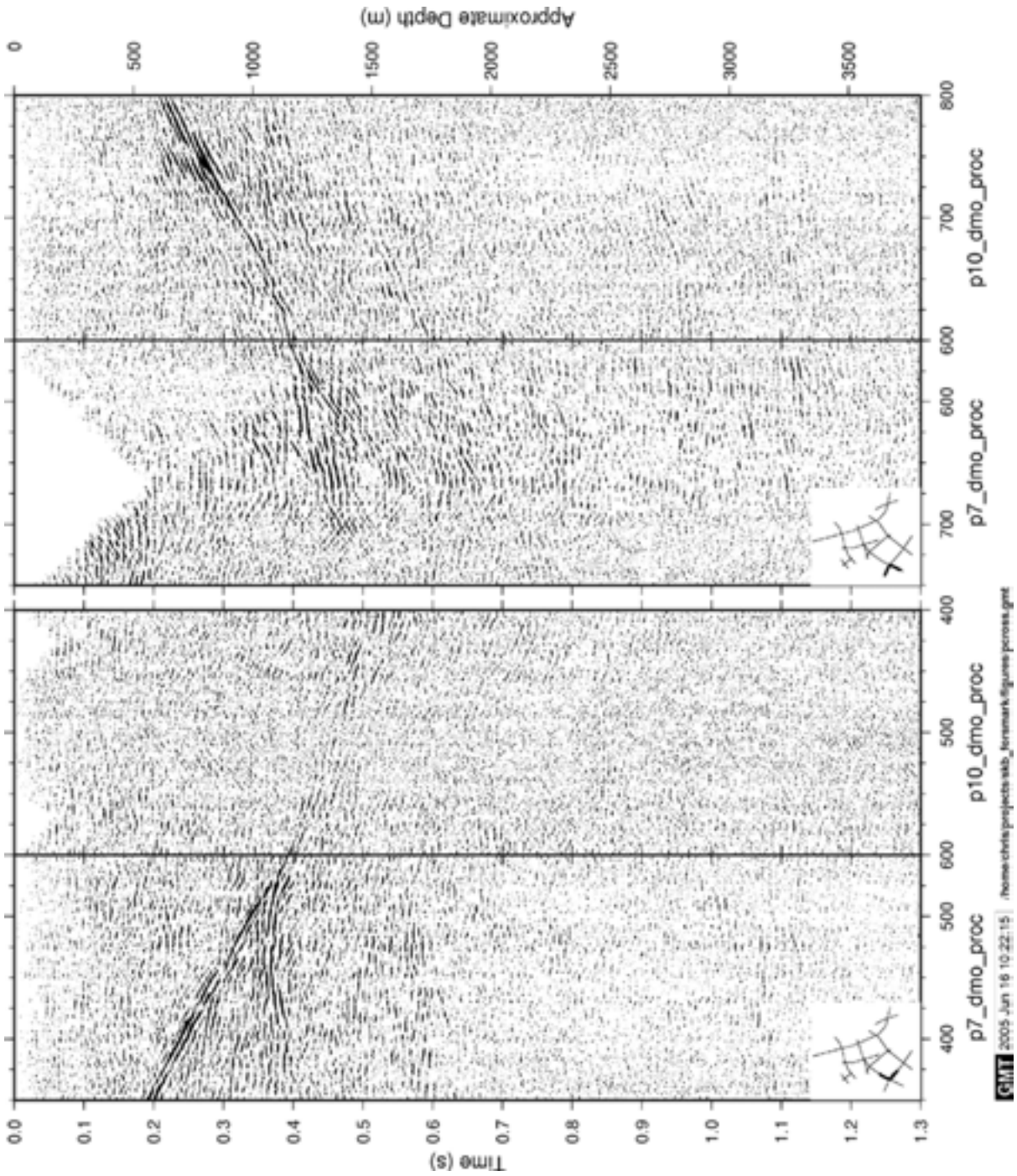

Figure 5-6. Correlation of stacks from profiles 10 and 7 at their crossing point (Figure 3-1). Horizontal numbering is CDP.

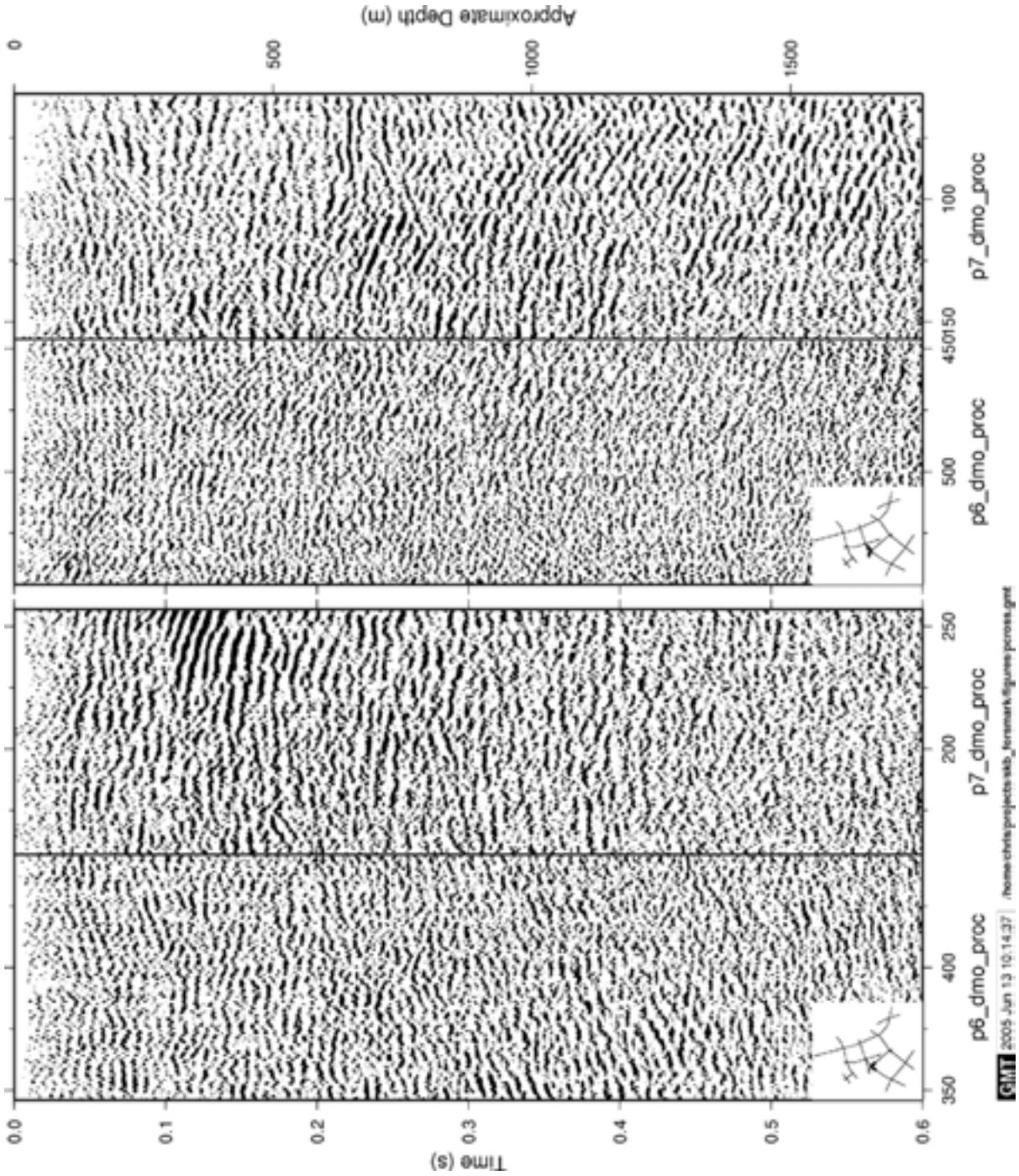

Figure 5-7. Detailed correlation of stacks from profiles 7 and 6 at their crossing point (Figure 3-1). Horizontal numbering is CDP.

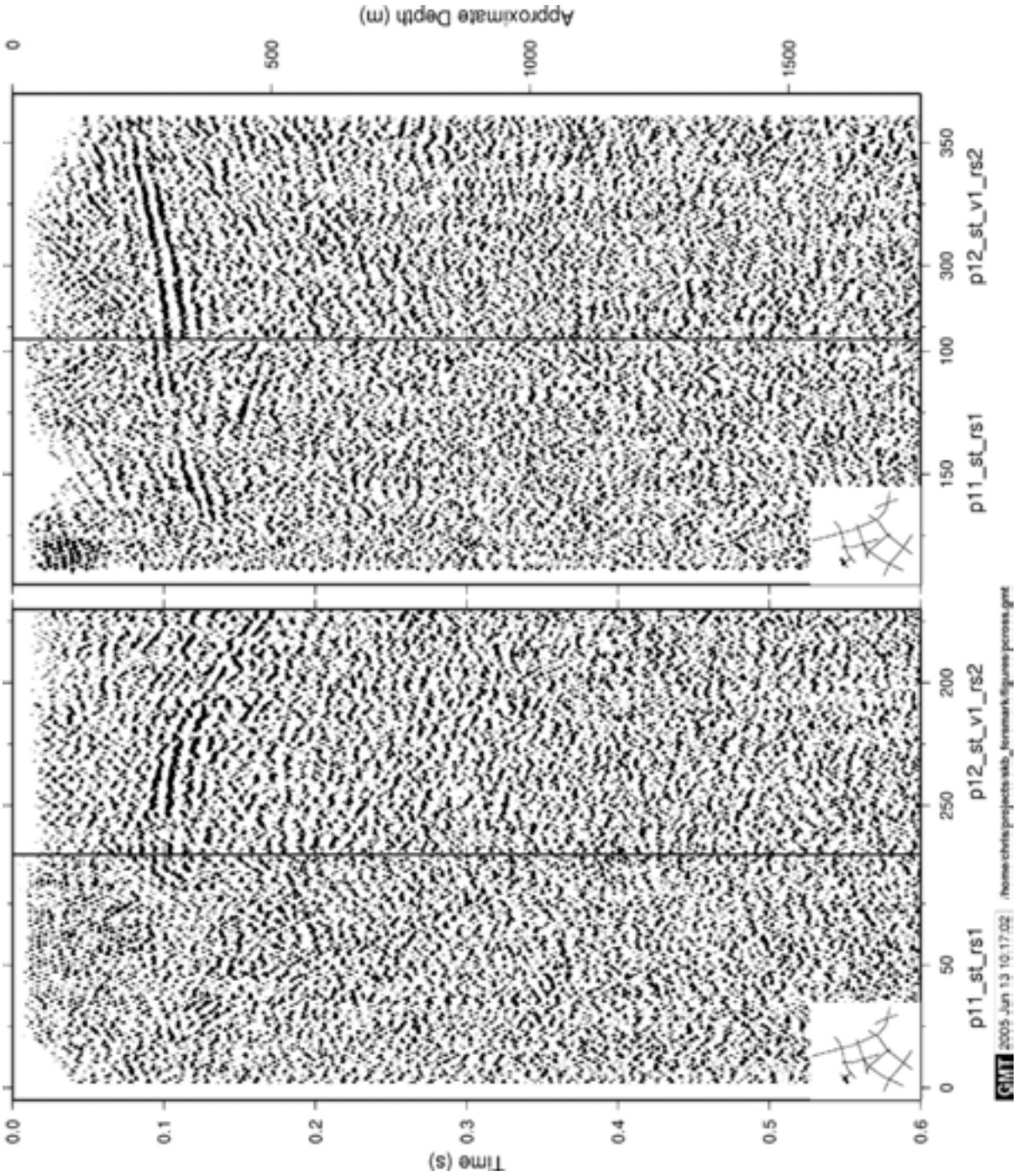

Figure 5-8. Detailed correlation of stacks from profiles 11 and 12 at their crossing point (Figure 3-1). Horizontal numbering is CDP.

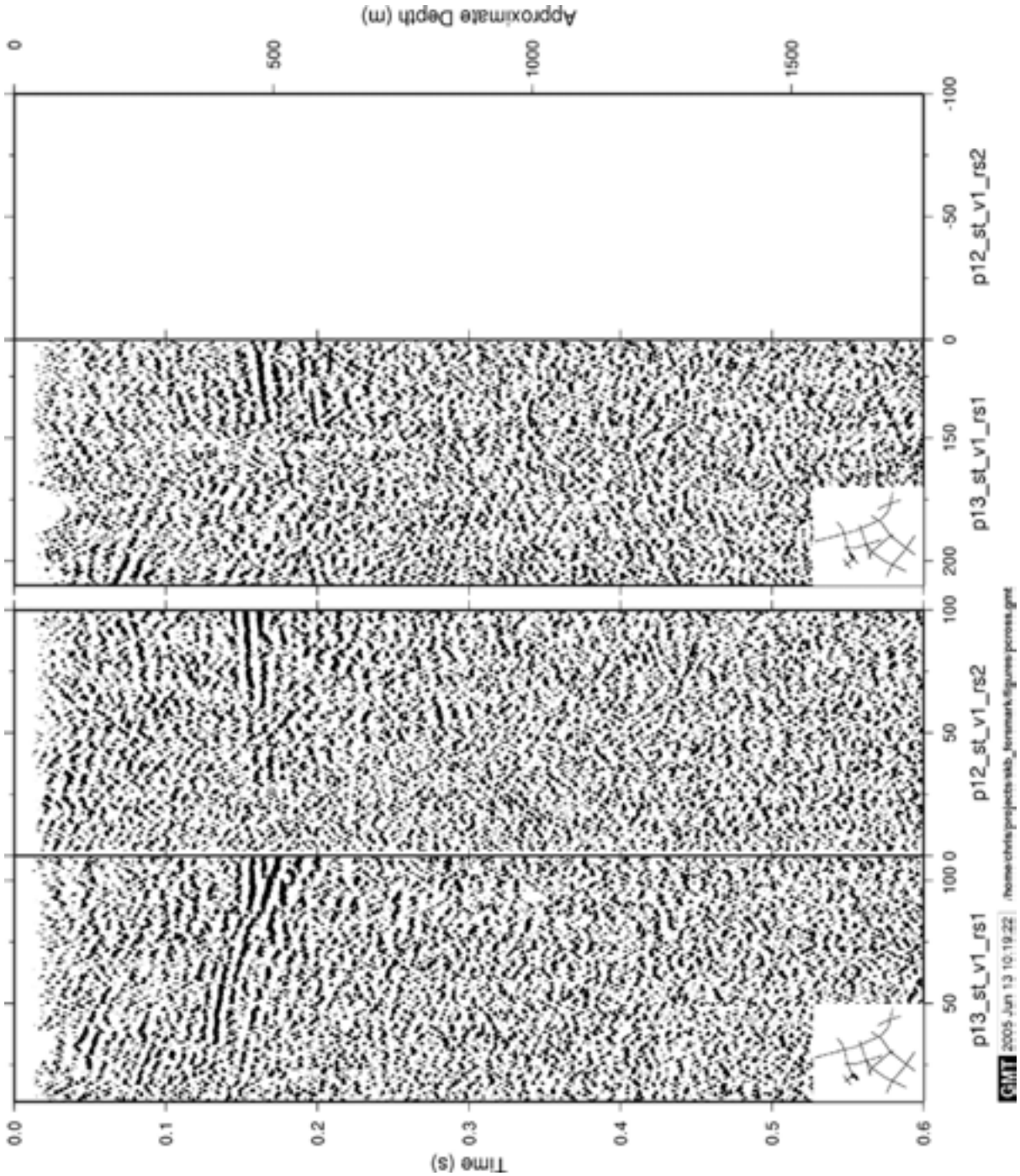

Figure 5-9. Correlation of stacks from profiles 12 and 13 at their crossing point (Figure 3-1). Horizontal numbering is CDP.

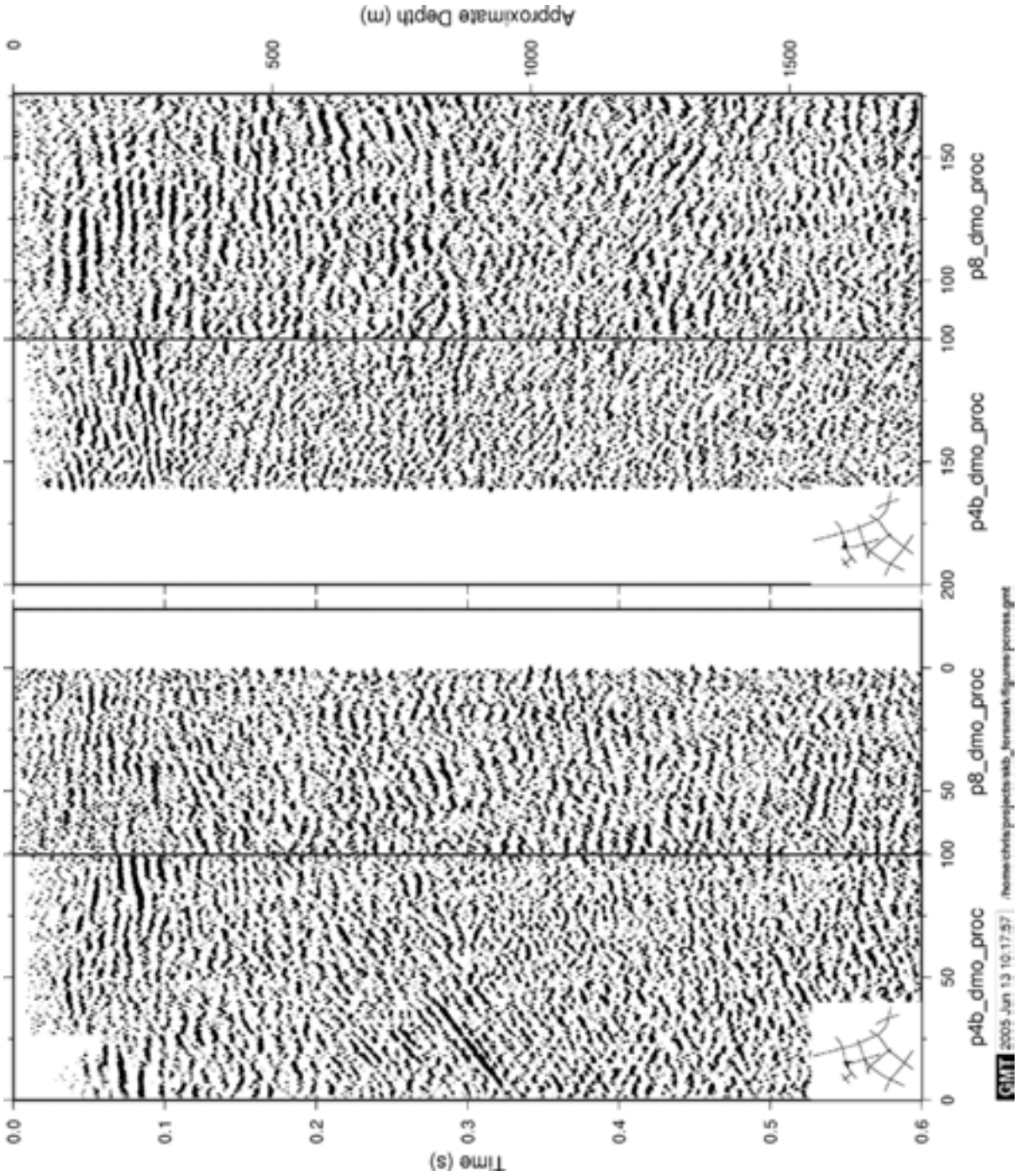

Figure 5-10. Detailed correlation of stacks from profiles 4b and 8 at their crossing point (Figure 3-1). Horizontal numbering is CDP.

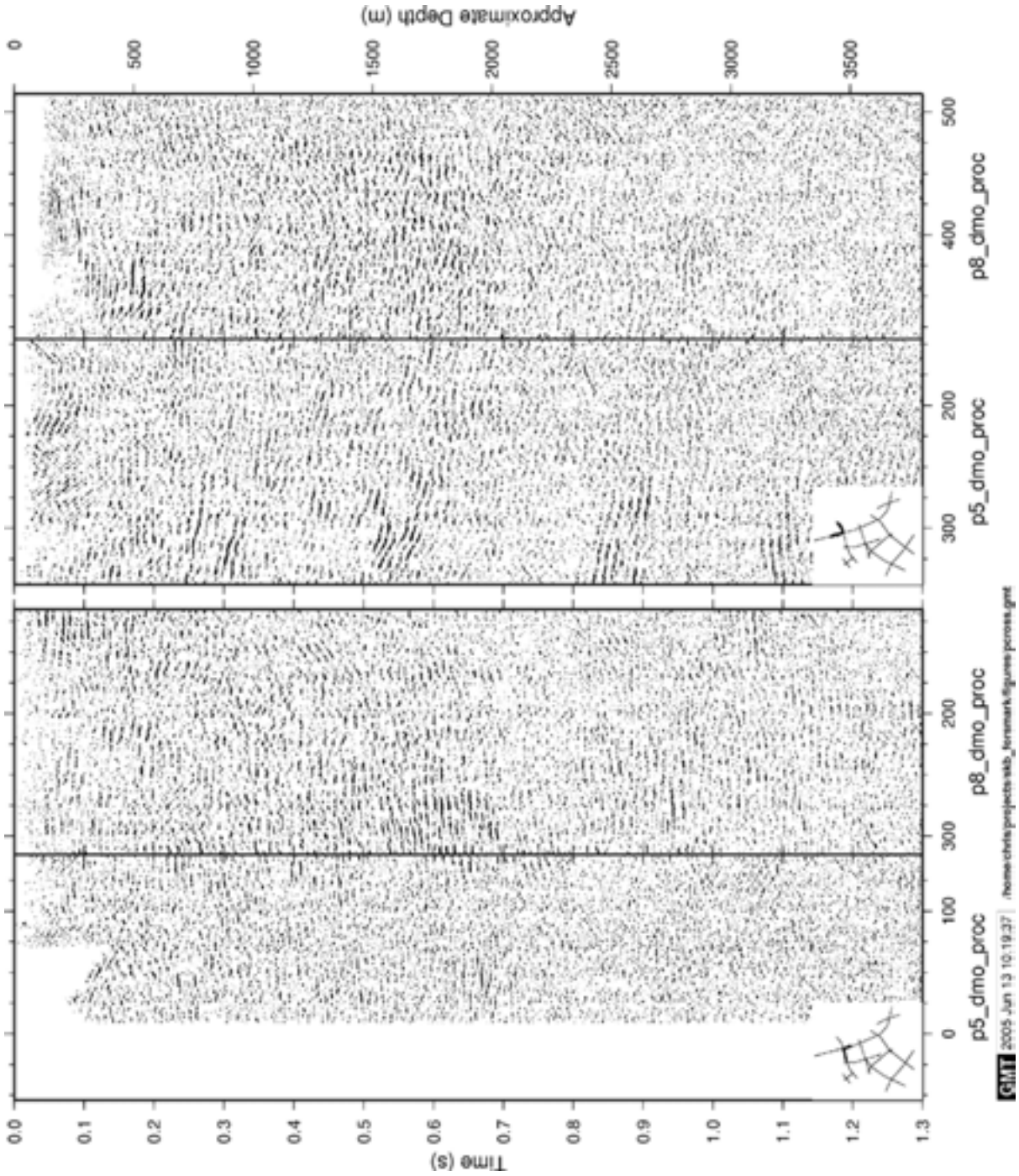

Figure 5-11. Correlation of stacks from profiles 8 and 5b at their crossing point (Figure 3-1). Horizontal numbering is CDP.

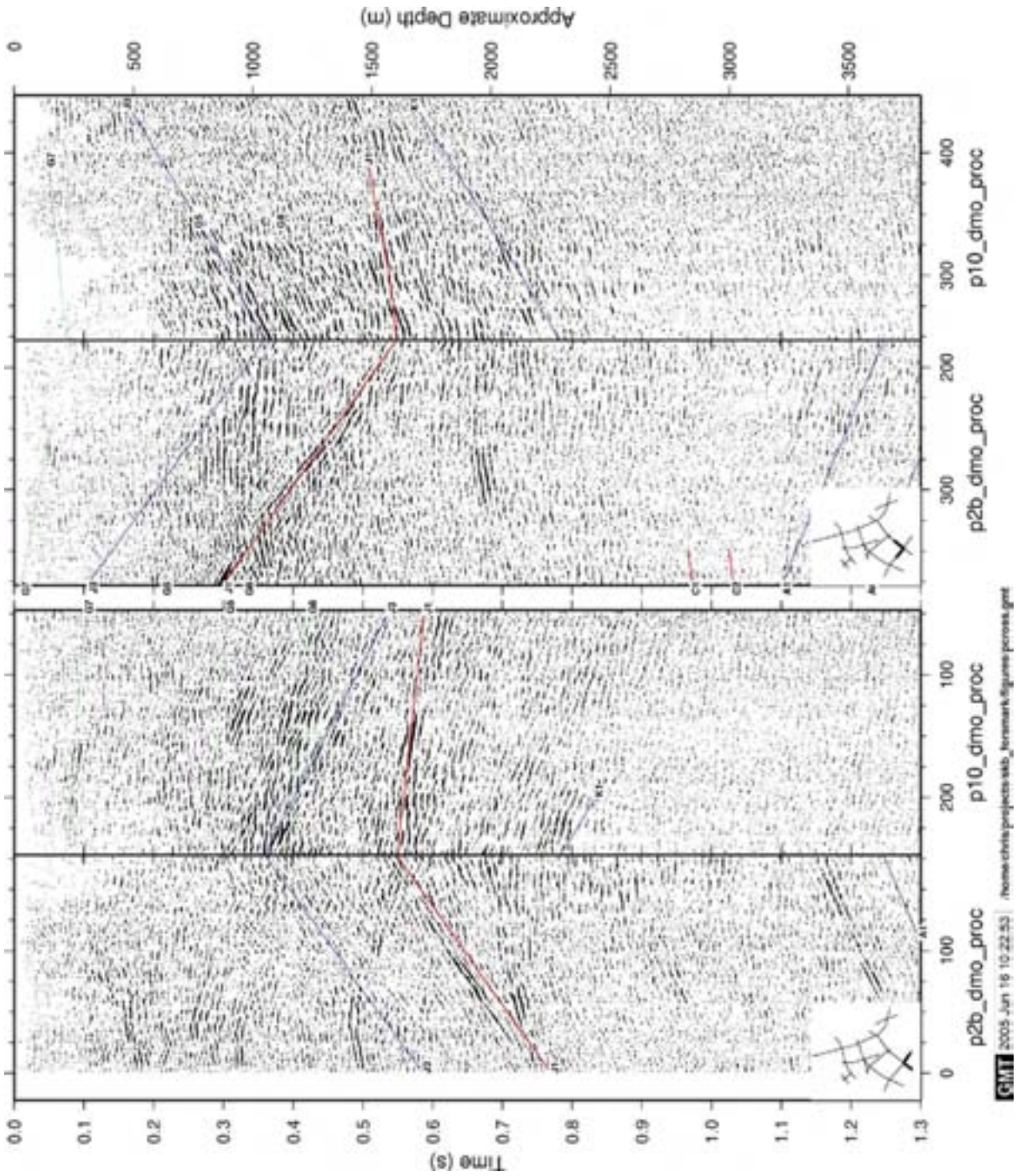

Figure 5-12. Correlation of stacks from profiles 10 and 2b at their crossing point (Figure 3-1) and comparison with modeling the reflectors defined in Table 5-1. Modeling of reflectors is coded as follows: red-rank 1, blue-rank 2, green-rank 3. Note that these lines are where reflections are expected to be observed on the seismic sections based on the strike and dips given in Table 5-1, they are ***not*** *picked reflections. Location of section indicated in lower left corner. Depth scale only valid for true sub-horizontal reflections. Horizontal numbering is CDP.*

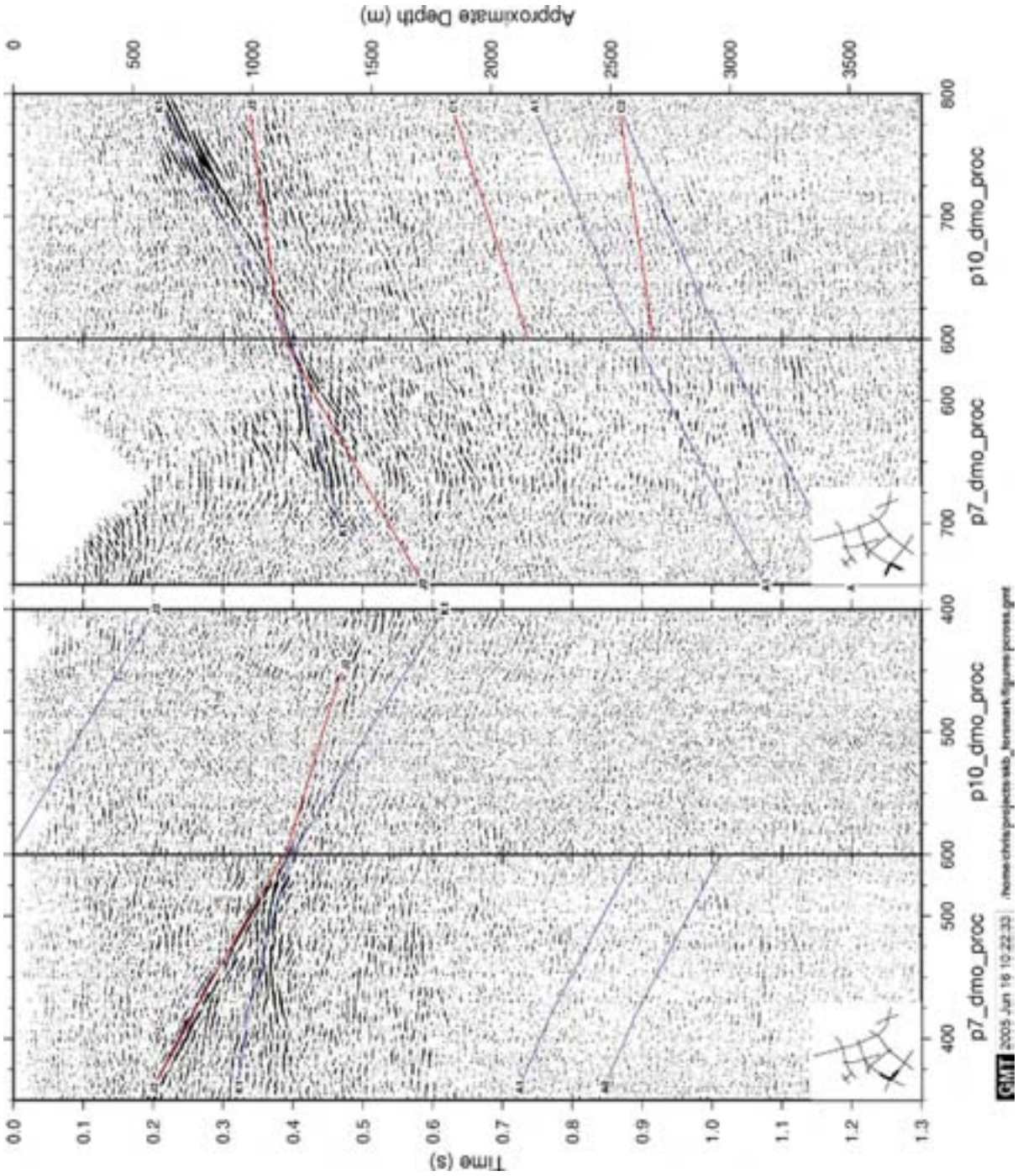

Figure 5-13. Correlation of stacks from profiles 10 and 7 at their crossing point (Figure 3-1) and comparison with modeling the reflectors defined in Table 5-1. Modeling of reflectors is coded as follows: red-rank 1, blue-rank 2, green-rank 3. Note that these lines are where reflections are expected to be observed on the seismic sections based on the strike and dips given in Table 5-1, they are ***not*** *picked reflections. Location of section indicated in lower left corner. Depth scale only valid for true sub-horizontal reflections. Horizontal numbering is CDP.*

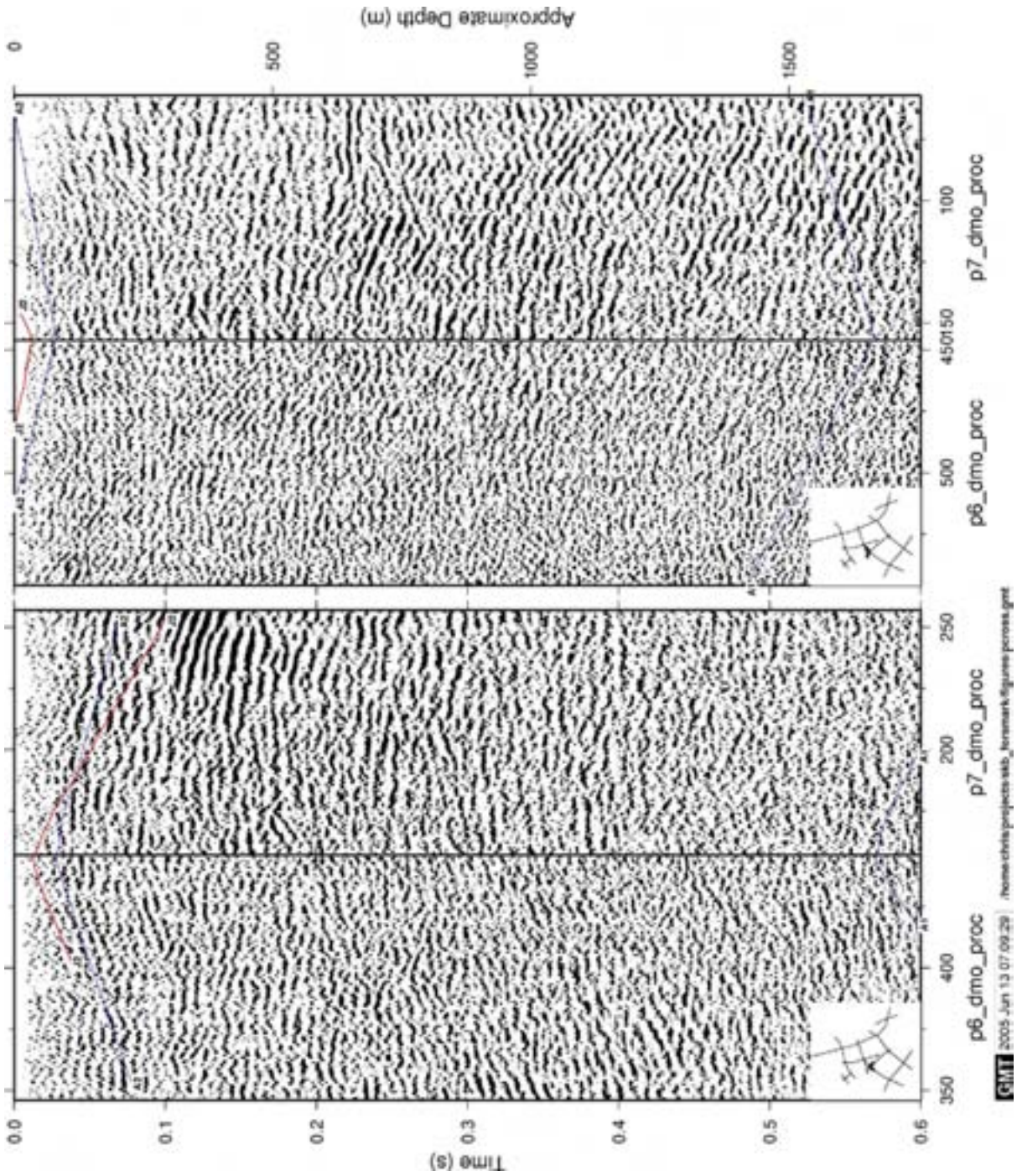

Figure 5-14. Detailed correlation of stacks from profiles 7 and 6 at their crossing point (Figure 3-1) and comparison with modeling the reflectors defined in Table 5-1. Modeling of reflectors is coded as follows: red-rank 1, blue-rank 2, green-rank 3. Note that these lines are where reflections are expected to be observed on the seismic sections based on the strike and dips given in Table 5-1, they are ***not*** *picked reflections. Location of section indicated in lower left corner. Depth scale only valid for true sub-horizontal reflections. Horizontal numbering is CDP.*

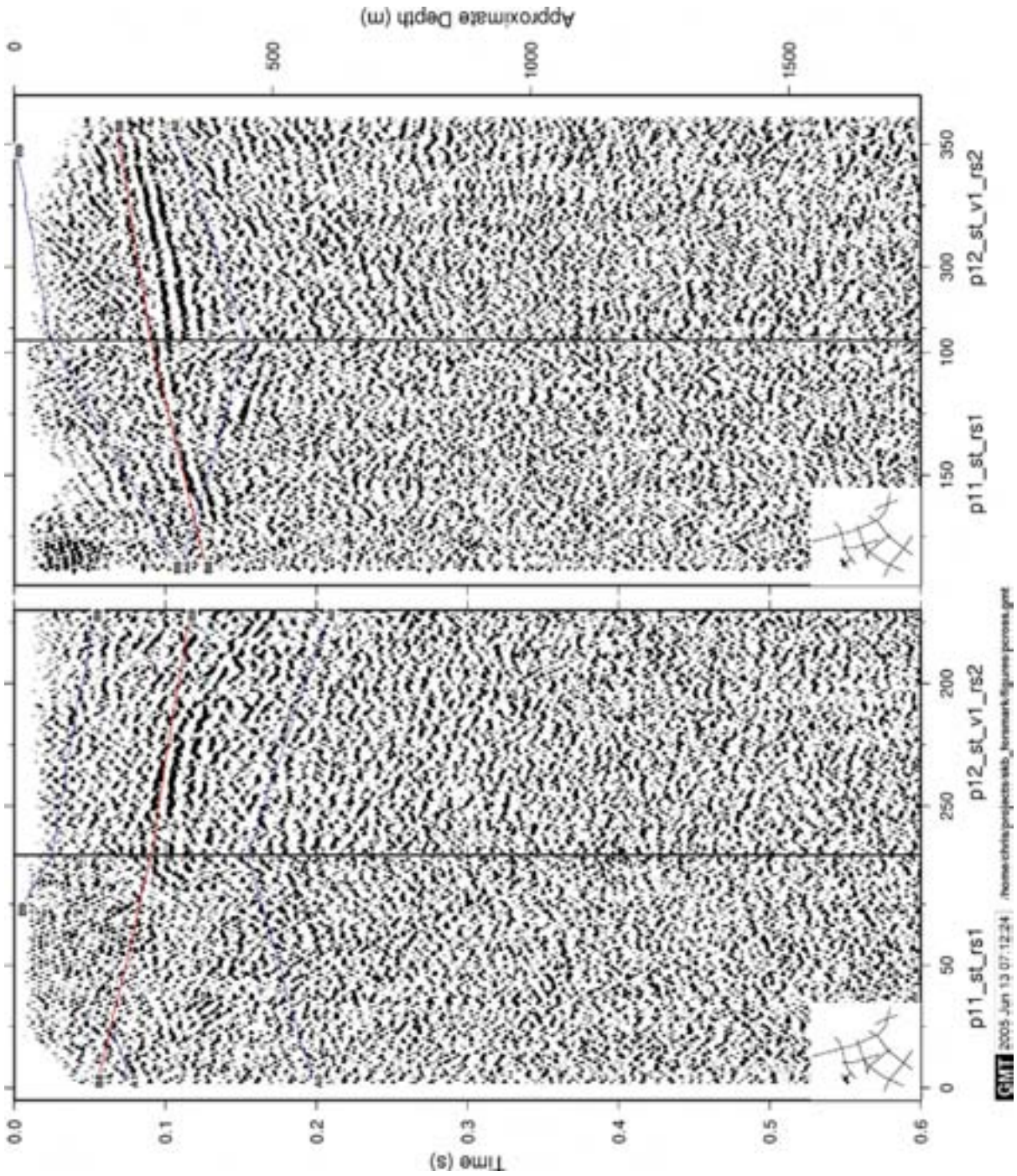

Figure 5-15. Detailed correlation of stacks from profiles 11 and 12 at their crossing point (Figure 3-1) and comparison with modeling the reflectors defined in Table 5-1. Modeling of reflectors is coded as follows: red-rank 1, blue-rank 2, green-rank 3. Note that these lines are where reflections are expected to be observed on the seismic sections based on the strike and dips given in Table 5-1, they are ***not*** *picked reflections. Location of section indicated in lower left corner. Depth scale only valid for true sub-horizontal reflections. Horizontal numbering is CDP.*

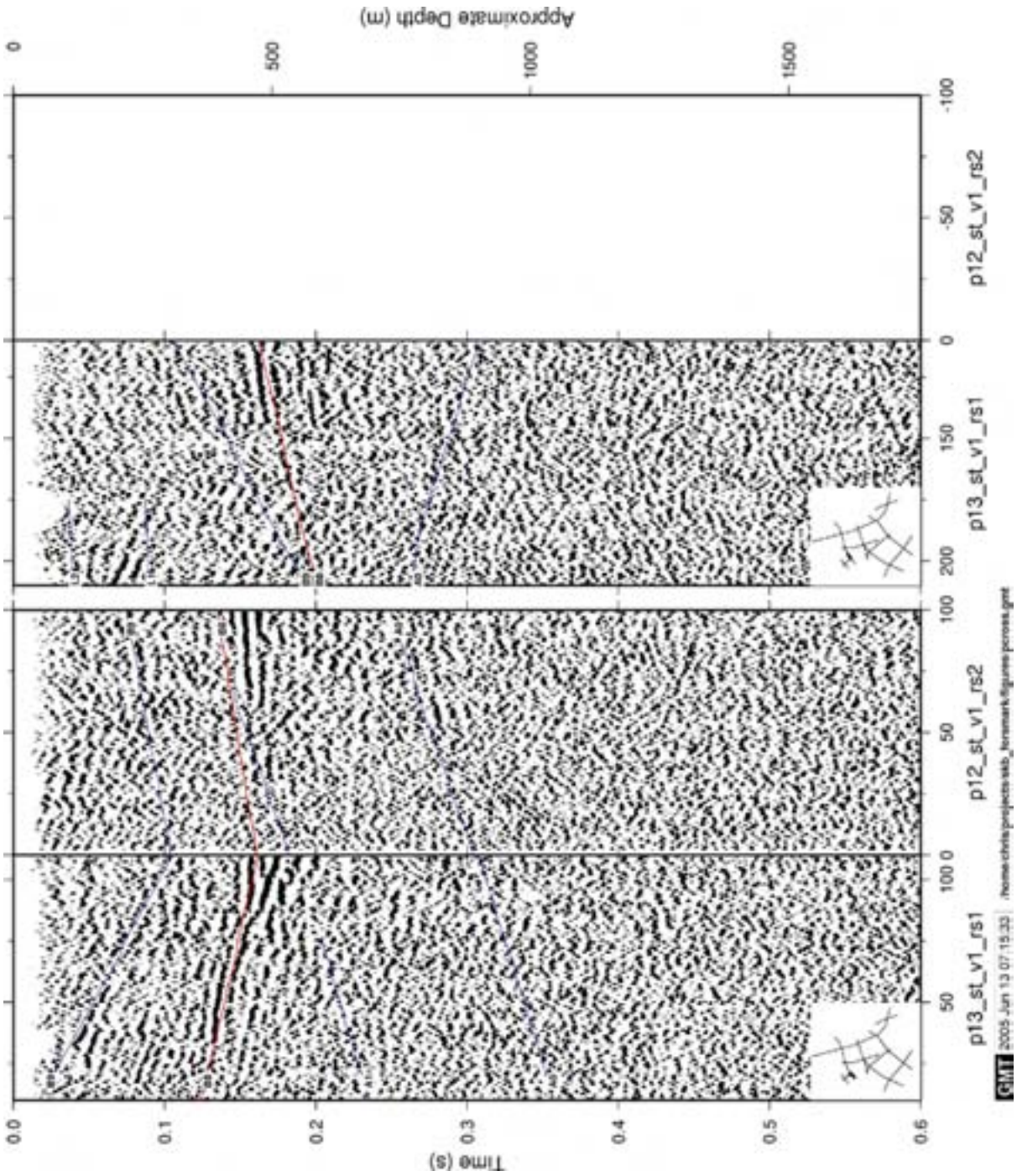

Figure 5-16. Correlation of stacks from profiles 12 and 13 at their crossing point (Figure 3-1) and comparison with modeling the reflectors defined in Table 5-1. Modeling of reflectors is coded as follows: red-rank 1, blue-rank 2, green-rank 3. Note that these lines are where reflections are expected to be observed on the seismic sections based on the strike and dips given in Table 5-1, they are ***not*** *picked reflections. Location of section indicated in lower left corner. Depth scale only valid for true sub-horizontal reflections. Horizontal numbering is CDP.*

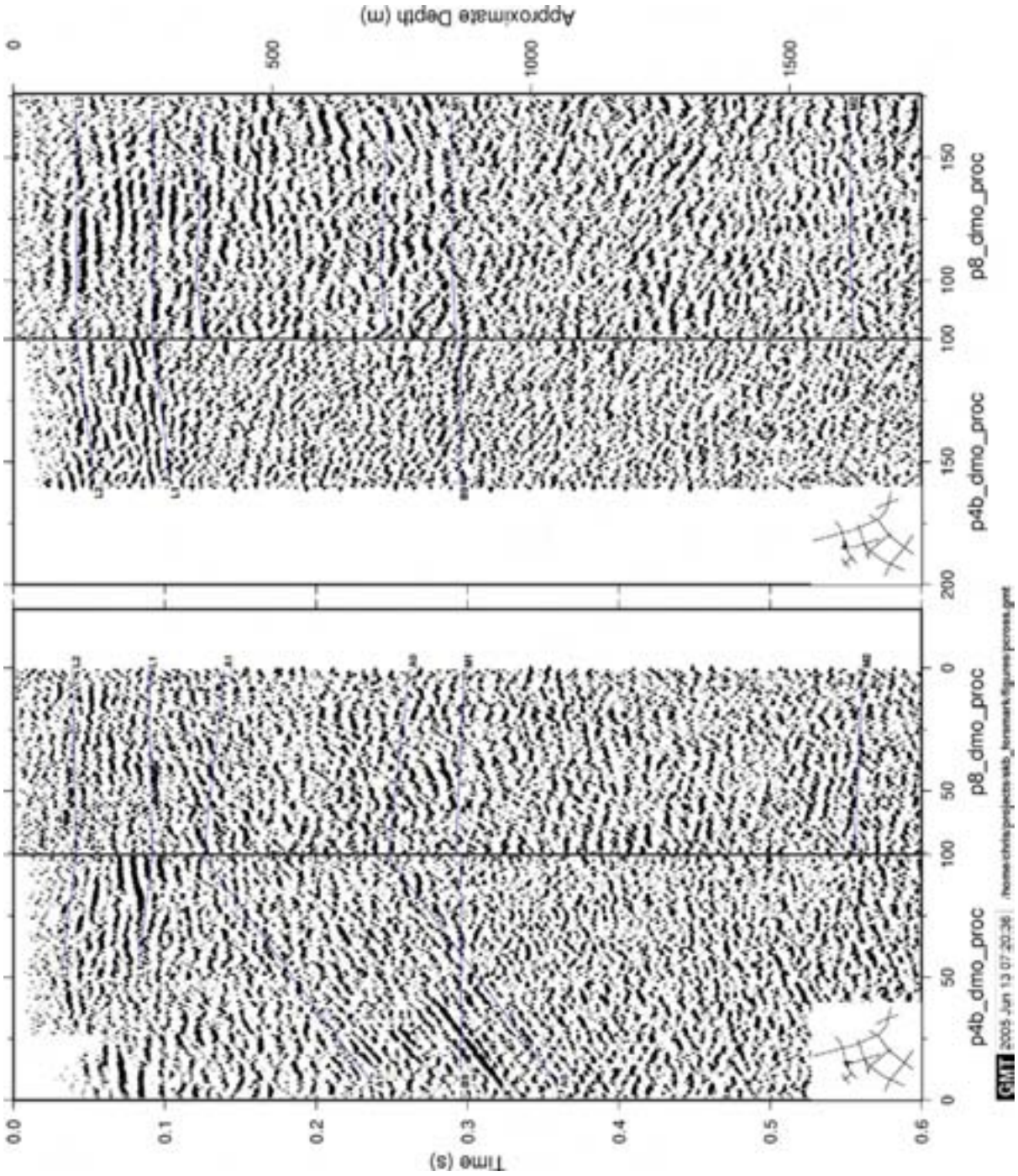

Figure 5-17. Detailed correlation of stacks from profiles 4b and 8 at their crossing point (Figure 3-1) and comparison with modeling the reflectors defined in Table 5-1. Modeling of reflectors is coded as follows: red-rank 1, blue-rank 2, green-rank 3. Note that these lines are where reflections are expected to be observed on the seismic sections based on the strike and dips given in Table 5-1, they are ***not*** *picked reflections. Location of section indicated in lower left corner. Depth scale only valid for true sub-horizontal reflections. Horizontal numbering is CDP.*

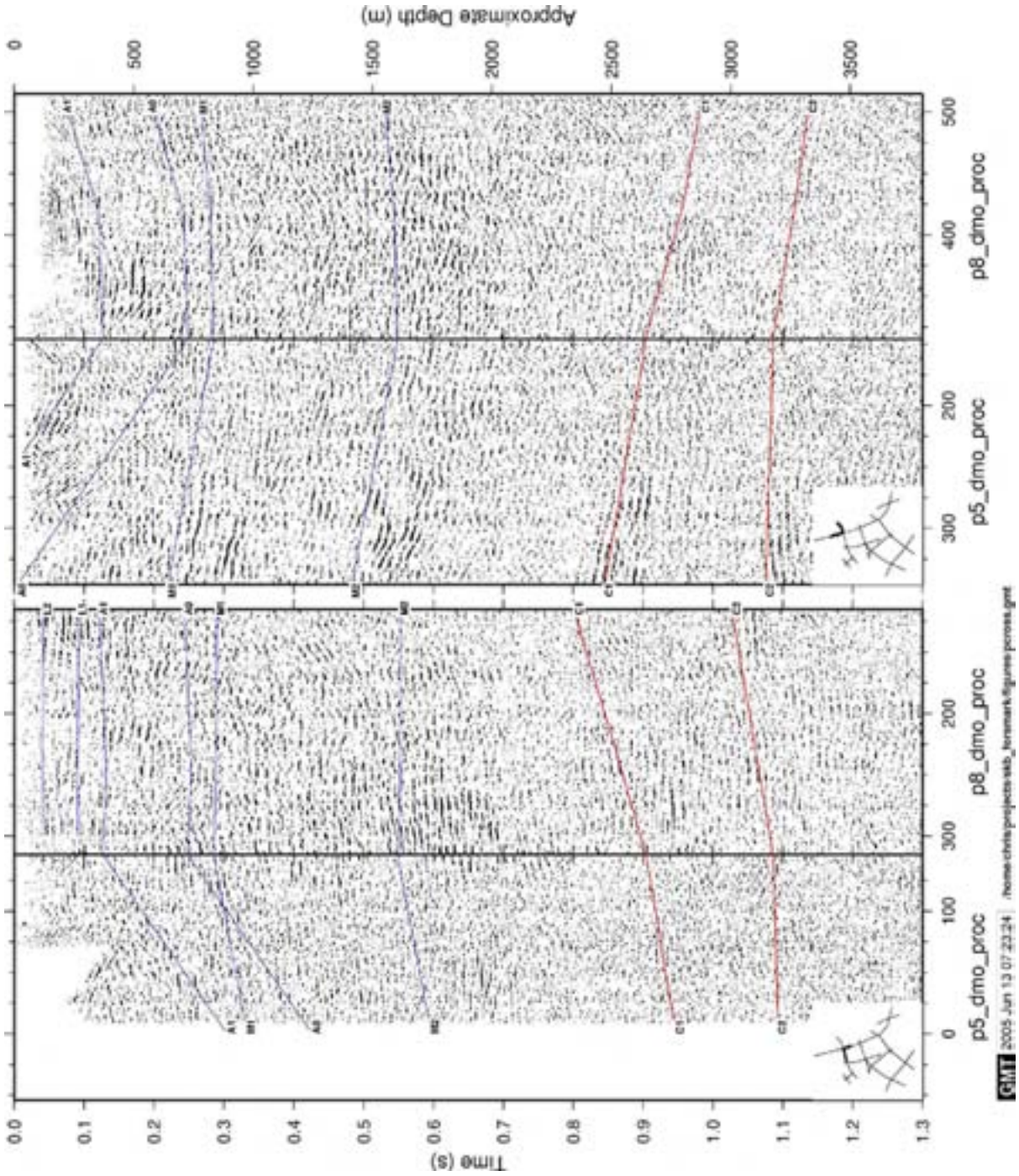

Figure 5-18. Correlation of stacks from profiles 8 and 5b at their crossing point (Figure 3-1) and comparison with modeling the reflectors defined in Table 5-1. Modeling of reflectors is coded as follows: red-rank 1, blue-rank 2, green-rank 3. Note that these lines are where reflections are expected to be observed on the seismic sections based on the strike and dips given in Table 5-1, they are ***not*** *picked reflections. Location of section indicated in lower left corner. Depth scale only valid for true sub-horizontal reflections. Horizontal numbering is CDP.*

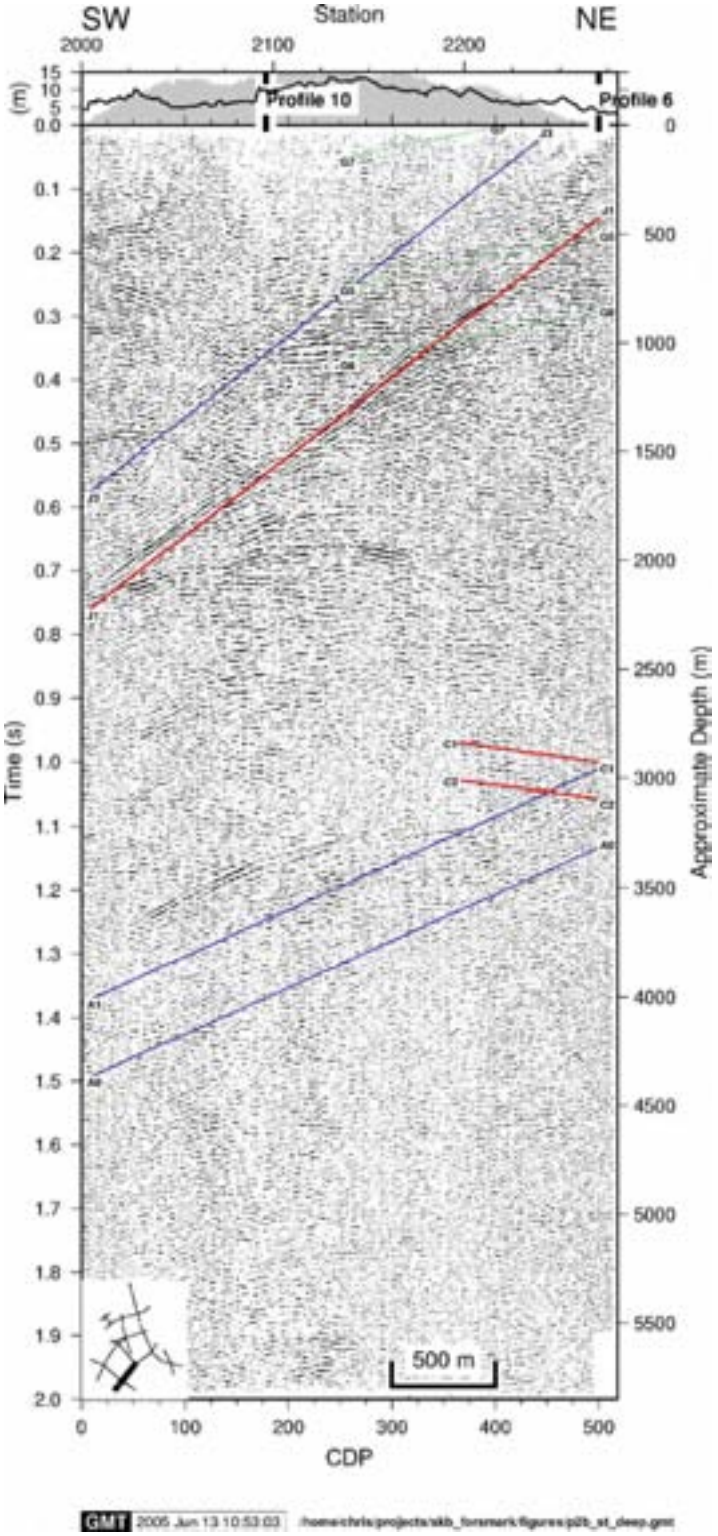

Figure 5-19. Stacked section of profile 2b and comparison with modeling the reflectors defined in Table 5-1. Modeling of reflectors is coded as follows: red-rank 1, blue-rank 2, green-rank 3. Note that these lines are where reflections are expected to be observed on the seismic sections based on the strike and dips given in Table 5-1, they are ***not*** *picked reflections. Location of section indicated in lower left corner. Depth scale only valid for true sub-horizontal reflections. Horizontal numbering is CDP.*

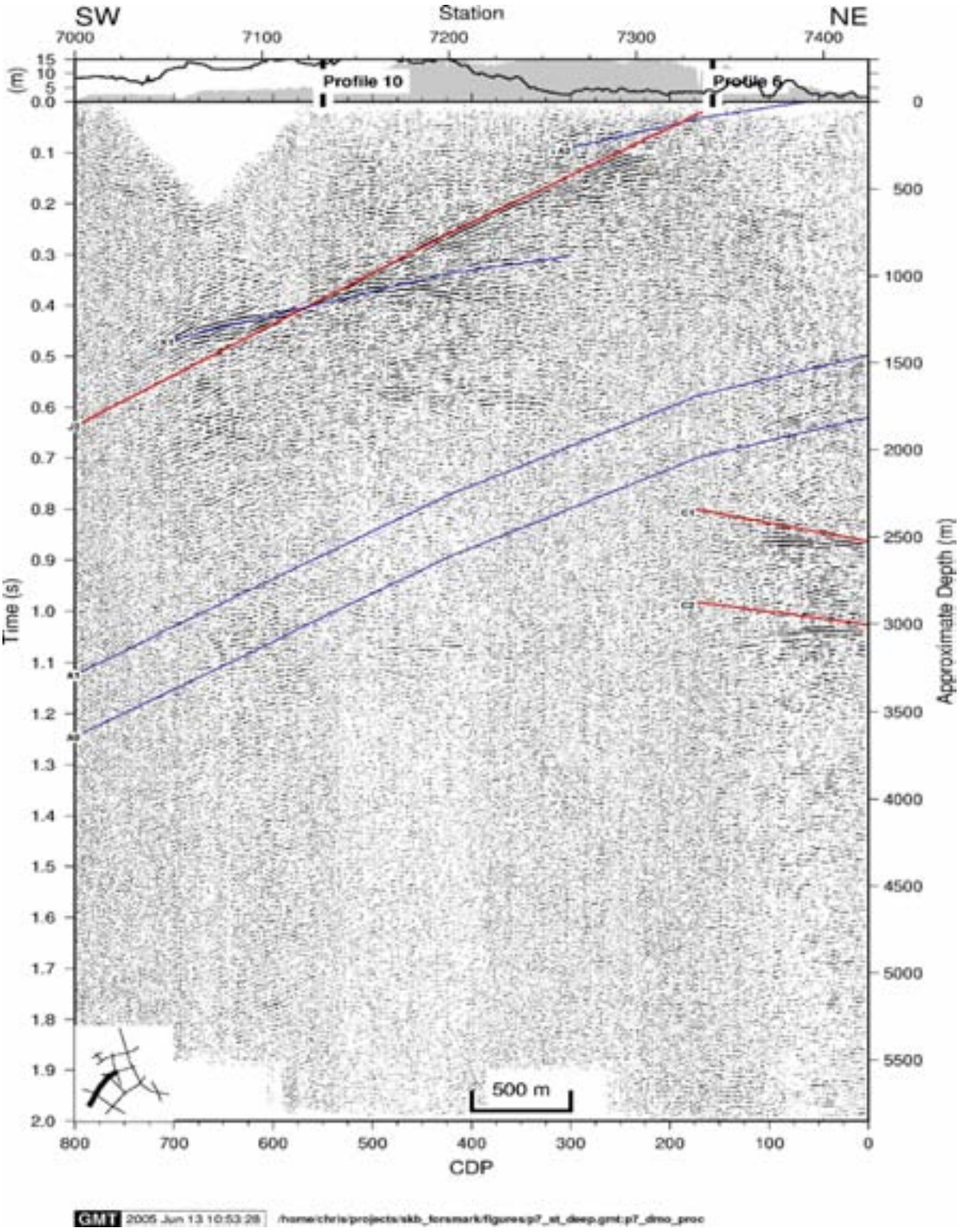

Figure 5-20. Stacked section of profile 7 and comparison with modeling the reflectors defined in Table 5-1. Modeling of reflectors is coded as follows: red-rank 1, blue-rank 2, green-rank 3. Note that these lines are where reflections are expected to be observed on the seismic sections based on the strike and dips given in Table 5-1, they are ***not*** *picked reflections. Location of section indicated in lower left corner. Depth scale only valid for true sub-horizontal reflections. Horizontal numbering is CDP.*

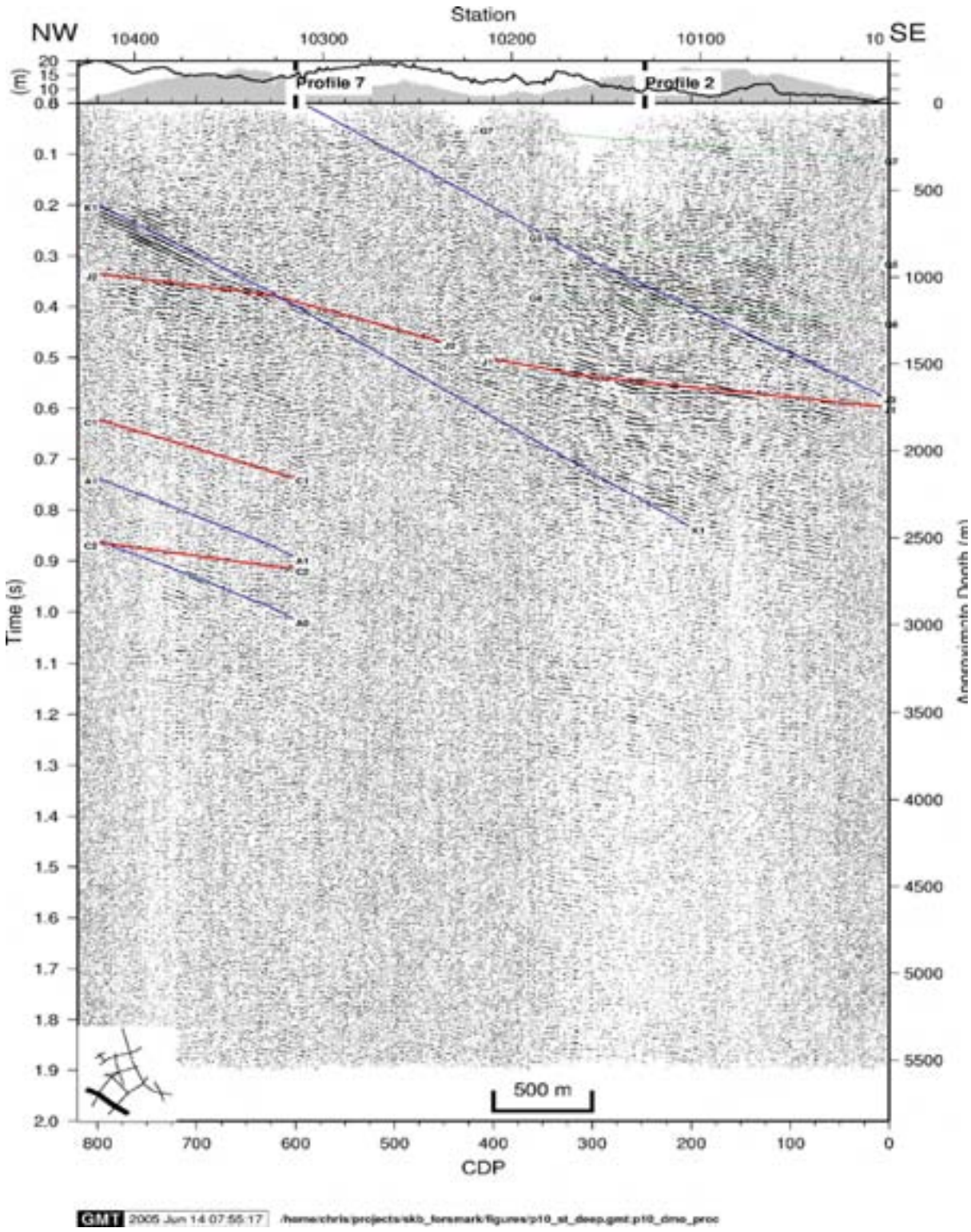

Figure 5-21. Stacked section of profile 10 and comparison with modeling the reflectors defined in Table 5-1. Modeling of reflectors is coded as follows: red-rank 1, blue-rank 2, green-rank 3. Note that these lines are where reflections are expected to be observed on the seismic sections based on the strike and dips given in Table 5-1, they are ***not*** *picked reflections. Location of section indicated in lower left corner. Depth scale only valid for true sub-horizontal reflections. Horizontal numbering is CDP.*

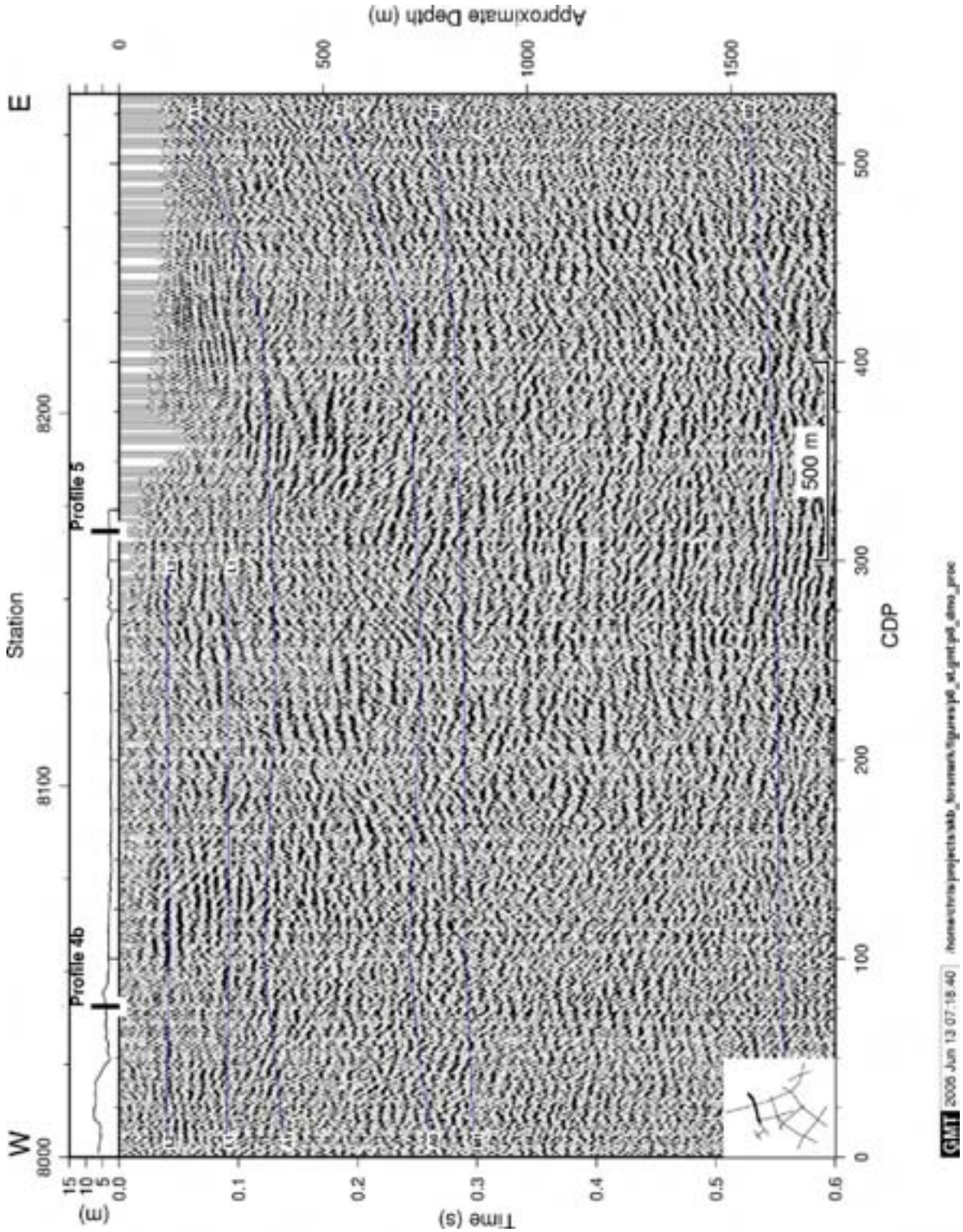

Figure 5-22. Stacked section of profile 8 and comparison with modeling the reflectors defined in Table 5-1. Modeling of reflectors is coded as follows: red-rank 1, blue-rank 2, green-rank 3. Note that these lines are where reflections are expected to be observed on the seismic sections based on the strike and dips given in Table 5-1, they are ***not*** *picked reflections. Location of section indicated in lower left corner. Depth scale only valid for true sub-horizontal reflections. Horizontal numbering is CDP.*

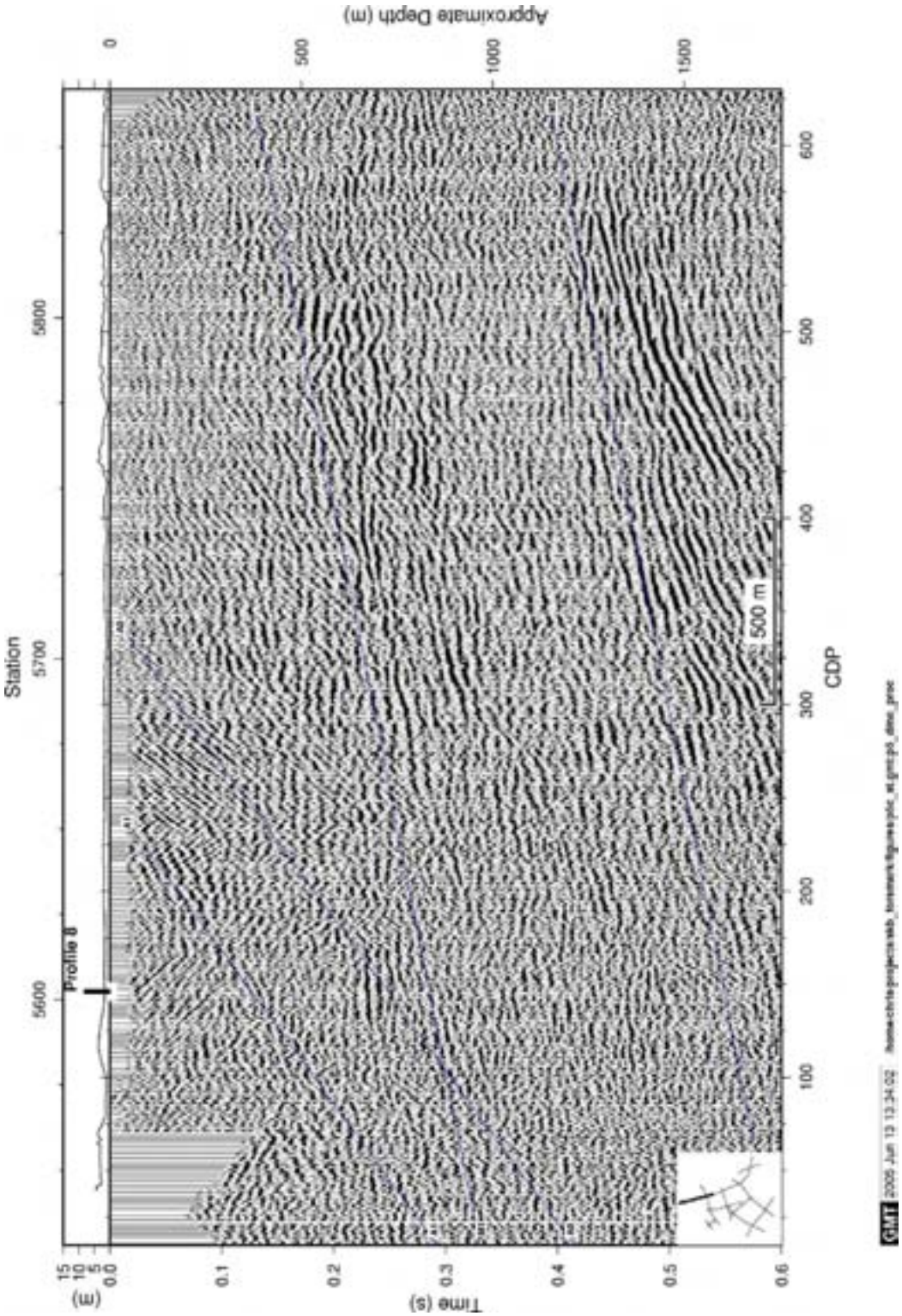

Figure 5-23. Stacked section of profile 5b and comparison with modeling the reflectors defined in Table 5-1. Modeling of reflectors is coded as follows: red-rank 1, blue-rank 2, green-rank 3. Note that these lines are where reflections are expected to be observed on the seismic sections based on the strike and dips given in Table 5-1, they are ***not*** *picked reflections. Location of section indicated in lower left corner. Depth scale only valid for true sub-horizontal reflections. Horizontal numbering is CDP.*

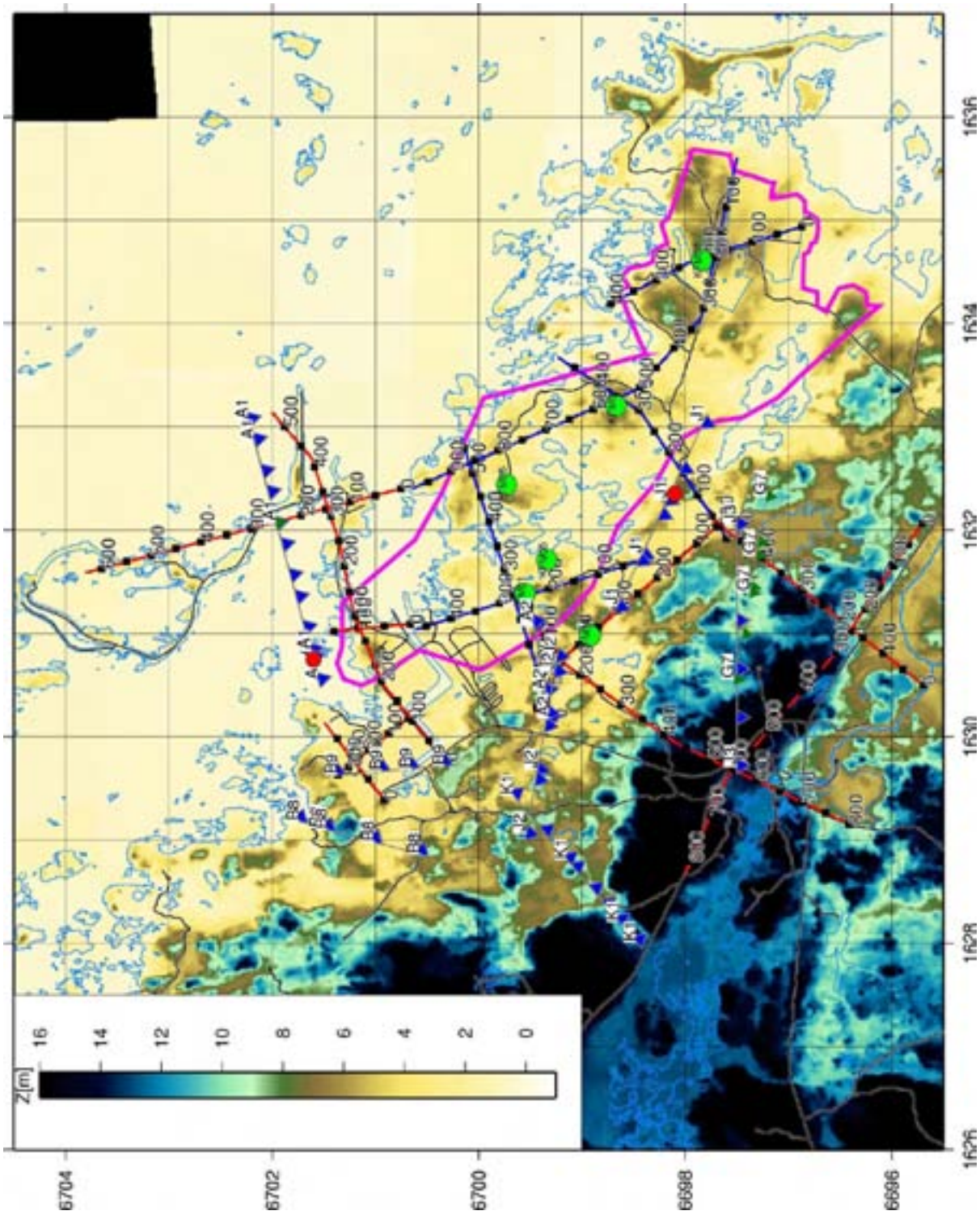

Figure 5-24. Projected reflector intersections with the surface as picked in Stage 2 and plotted on the topographic map. All indicated reflectors correspond to relatively thin zones (5-15 m thick), except for A1. Shown also are where the A1 and the J1 reflectors project to the surface (red dots) along the extension of their respective profiles. Reflectors are coded as follows: red-rank 1, blue-rank 2, green-rank 3.

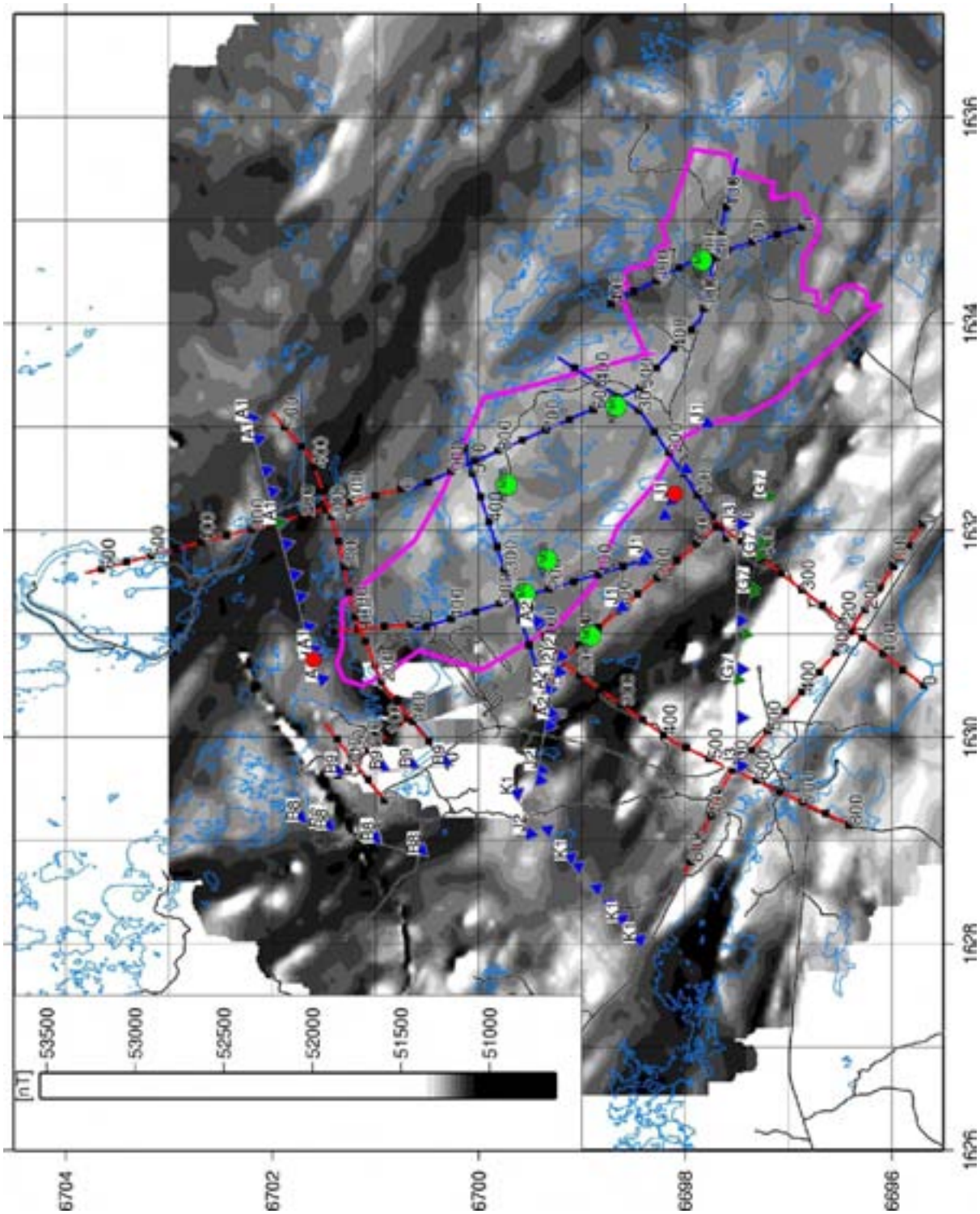

Figure 5-25. Projected reflector intersections with the surface as picked in Stage 2 and plotted on the magnetic map. All indicated reflectors correspond to relatively thin zones (5-15 m thick), except for A1. Shown also are where the A1 and the J1 reflectors project to the surface (red dots) along the extension of their respective profiles. Reflectors are coded as follows: red-rank 1, blue-rank 2, green-rank 3.

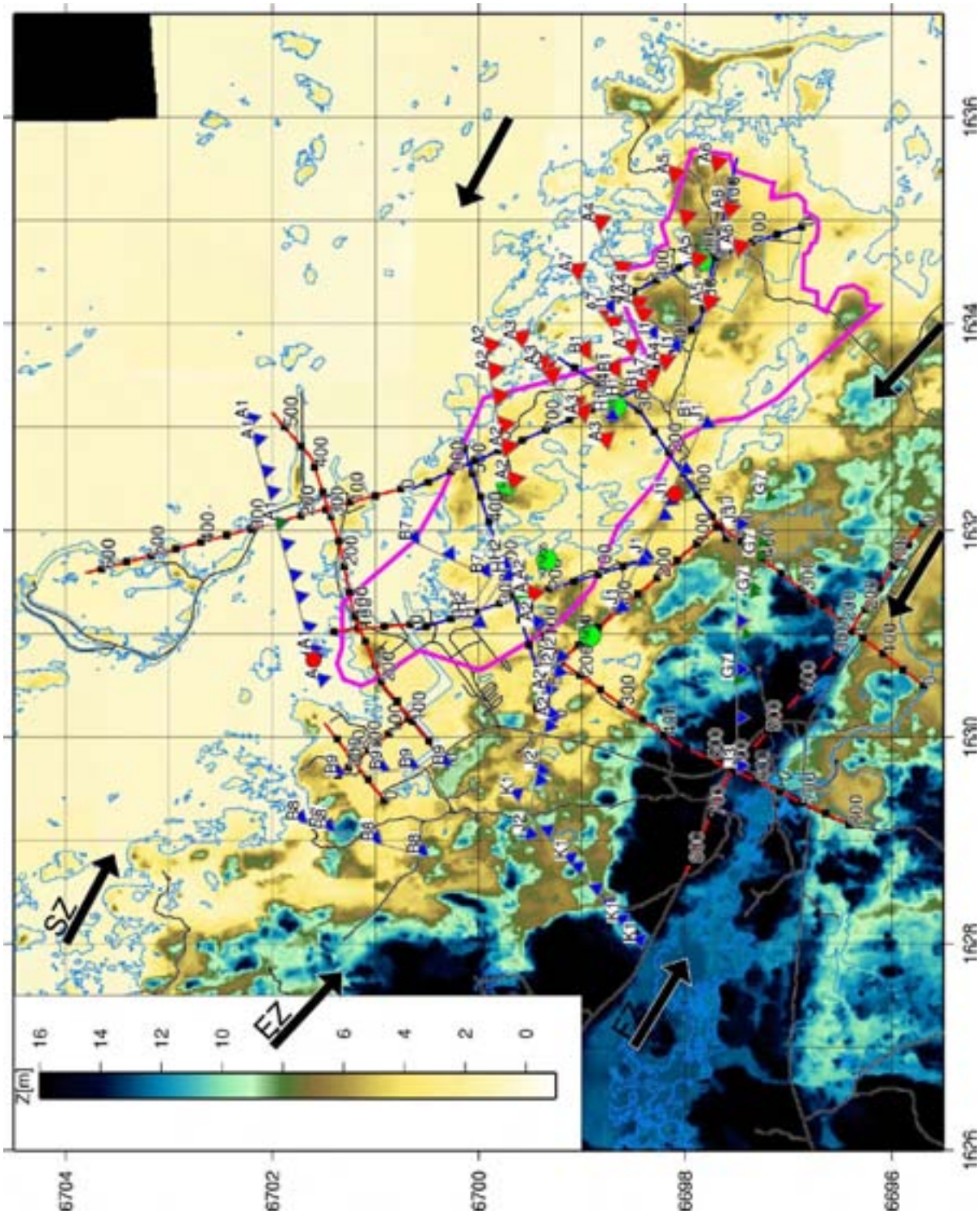

Figure 5-26. Projected reflector intersections with the surface as picked in Stage 1 and Stage 2 and plotted on the topographic map. All indicated reflectors correspond to relatively thin zones (5-15 m thick), except for A1. Shown also are where the A1 and the J1 reflectors project to the surface (red dots) along the extension of their respective profiles. Reflectors are coded as follows: red-rank 1, blue-rank 2, green-rank 3. FZ - Forsmark zone, EZ – Eckarfjärden zone, SZ – Singö zone.

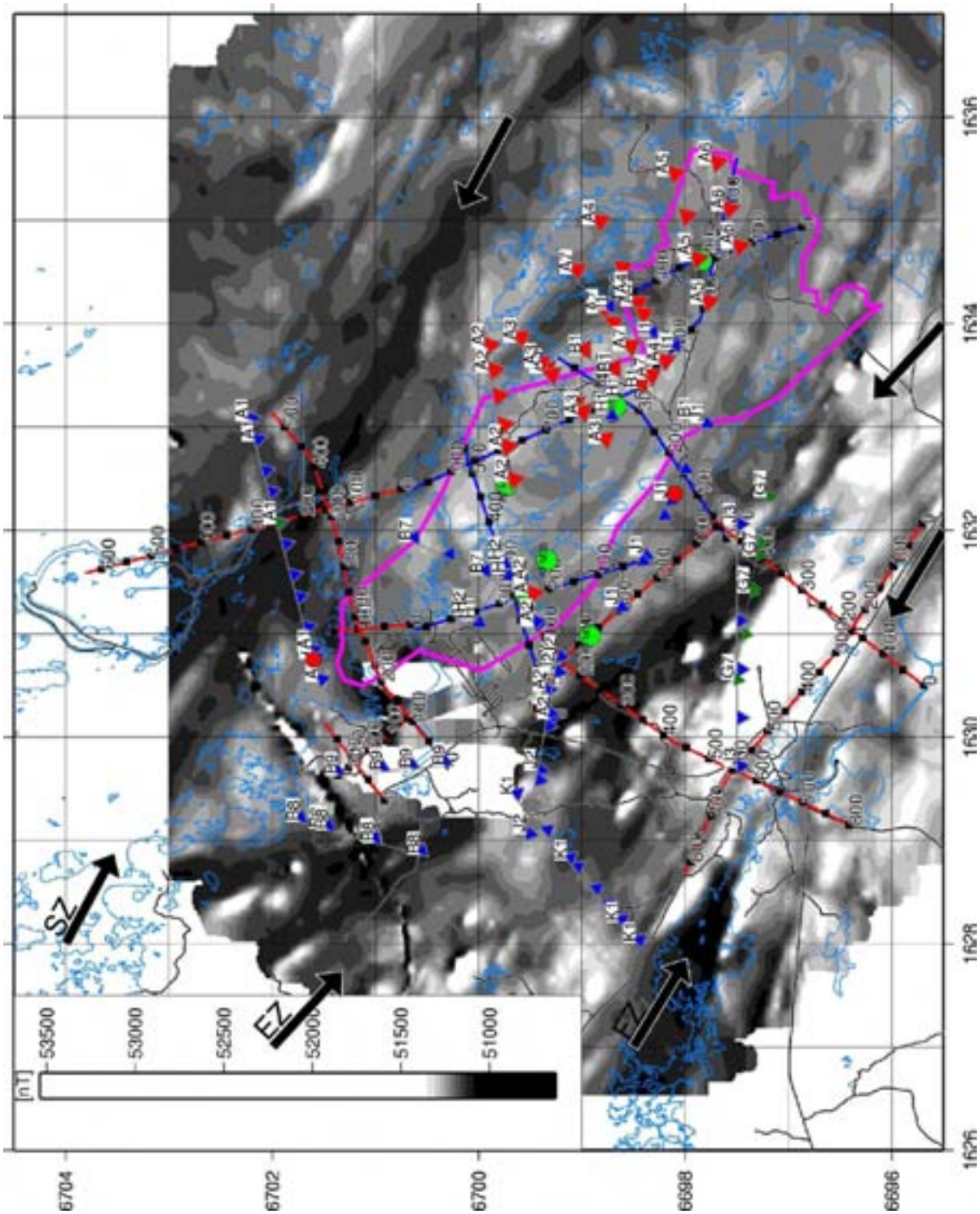

Figure 5-27. Projected reflector intersections with the surface as picked in Stage 1 and Stage 2 and plotted on the magnetic map. All indicated reflectors correspond to relatively thin zones (5-15 m thick), except for A1. Shown also are where the A1 and the J1 reflectors project to the surface (red dots) along the extension of their respective profiles. Reflectors are coded as follows: red-rank 1, blue-rank 2, green-rank 3. FZ - Forsmark zone, EZ – Eckarfjärden zone, SZ – Singö zone.

5.4 Migrated sections

Most observed reflections on the profiles have an out-of-the-plane of the profile dip component. The migration process will only migrate properly those reflections which lie completely within-the-plane of the profiles. If the out-of-the-plane component is small then reflections will migrate to approximately their correct spatial position if the correct velocity is used. From geometrical considerations, steeply dipping reflections will have a limited out-of-the-plane component. Therefore, the merged profiles shown in Figures 5-19 to 5-22 have been migrated (Figures 5-28 to 5-31). These plots show the J1, J2 and A1 reflectors in their approximately correct spatial position below the profiles. They also show that many of the diffractions have collapsed to the edges of high amplitude reflectors. However, the reader should keep in mind that many of the reflections are from out-of-the-plane of the profile and, therefore, the migrated sections cannot be regarded as vertical slices below the profiles. Instead the depth scale should be regarded as distance from the surface to the reflector. The approximate depth scale shown in the figures is based on an average velocity for the area and is only valid for reflections striking perpendicular to the plane of the profile. Note also that there is considerable migration noise from those portions of the profiles where the data quality is poorer.

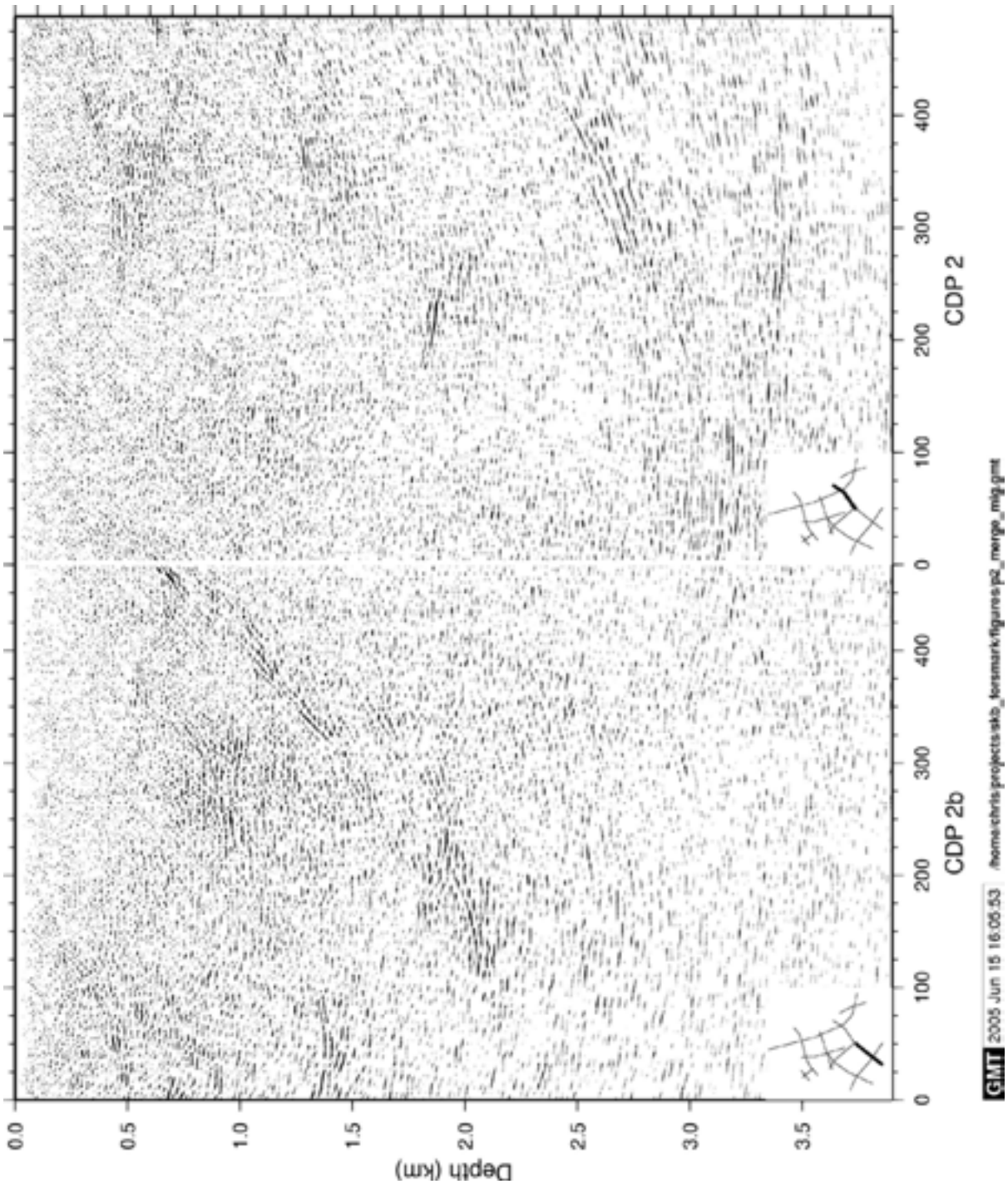

Figure 5-28. Migrated section of profile 2b acquired in 2004 and profile 2 acquired in 2002 down to 3.9 km. Location of sections indicated in lower left corners. Depth scale only valid for reflections originating from within the plane-of-the-profile.

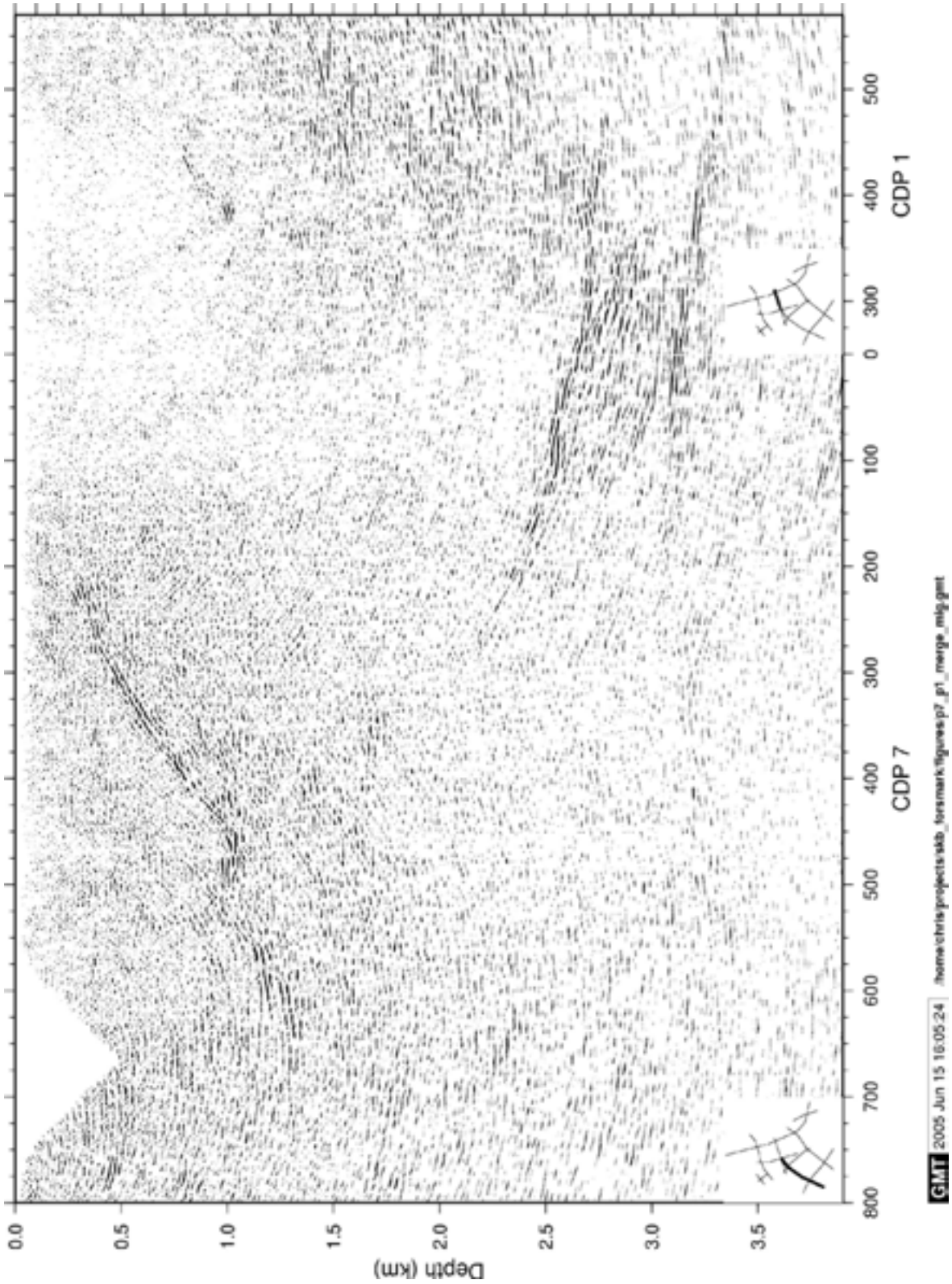

Figure 5-29. Migrated section of profile 7 acquired in 2004 and north eastern part of profile 1 acquired in 2002 down to 1.3 seconds. Location of sections indicated in lower left corners. Depth scale only valid for reflections originating from within the plane-of-the-profile.

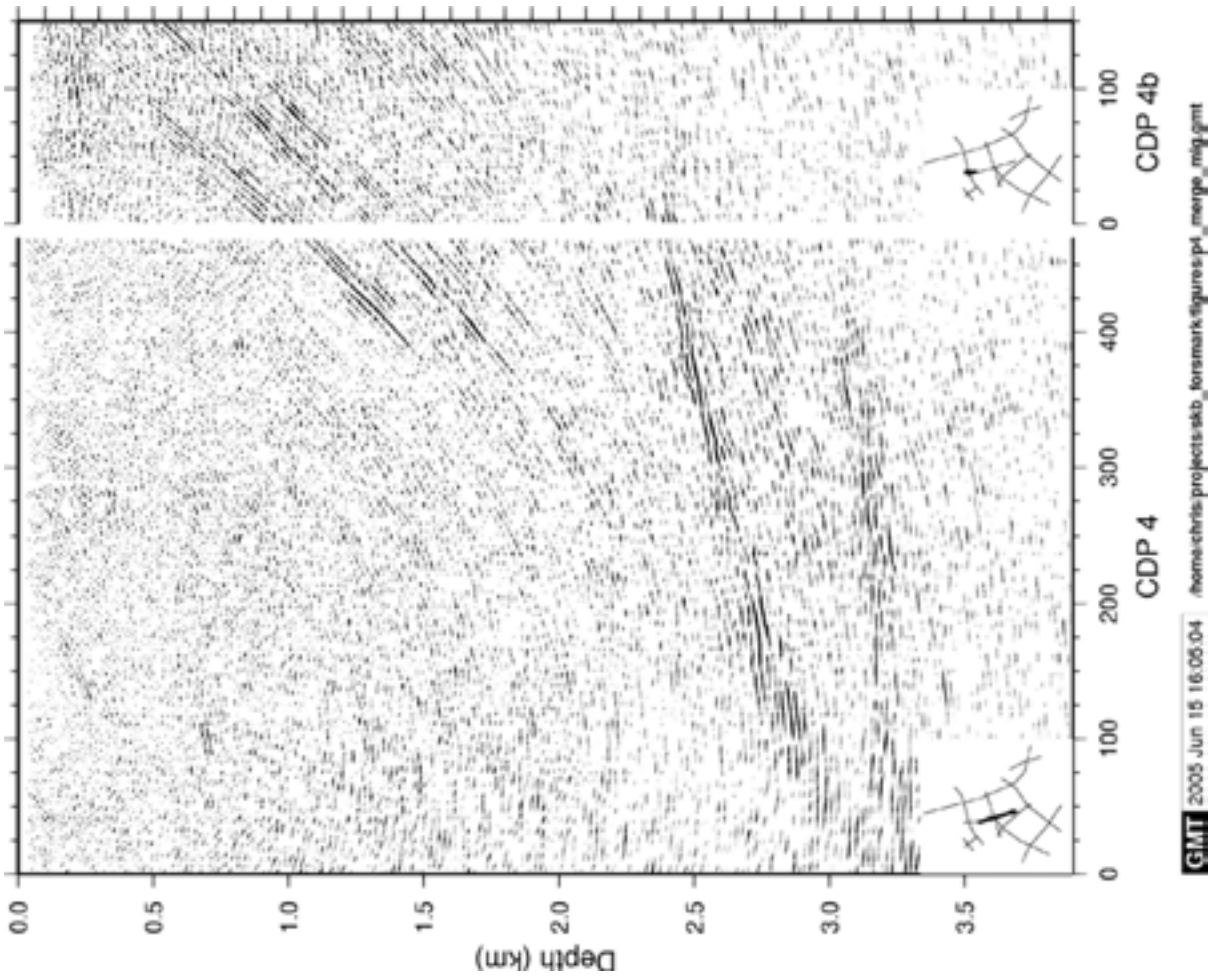

Figure 5-30. Migrated section of profile 4b acquired in 2004 and profile 4 acquired in 2002 down to 1.3 seconds. Location of sections indicated in lower left corners. Depth scale only valid for reflections originating from within the plane-of-the-profile.

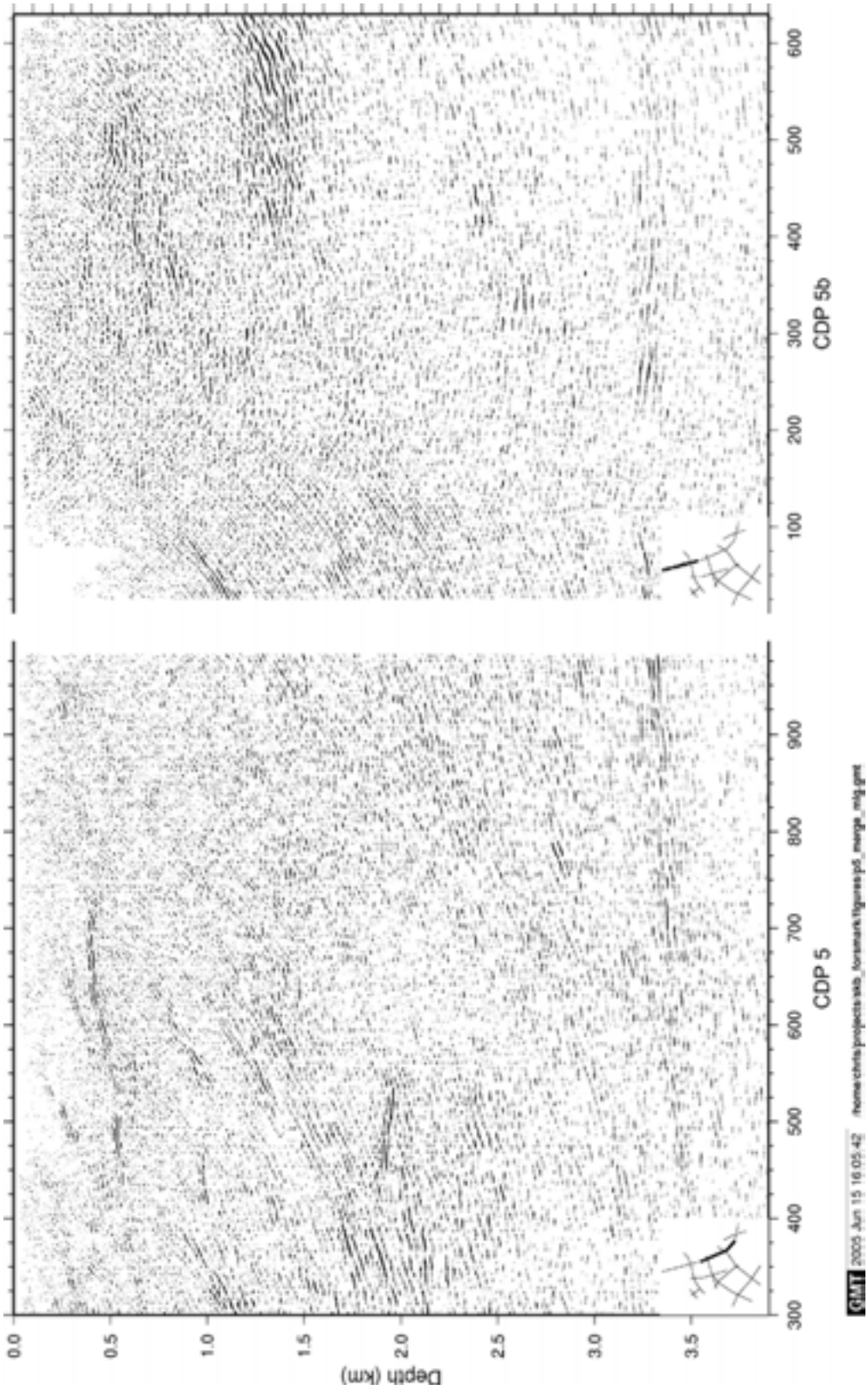

Figure 5-31. Migrated section of profile 5b acquired in 2004 and northern part of profile 5 acquired in 2002 down to 1.3 seconds. Location of sections indicated in lower left corners. Depth scale only valid for reflections originating from within the plane-of-the-profile.

6 Discussion and conclusions

6.1 Acquisition

The combined use of explosives and VIBISIST as sources proved to be a viable alternative to using only an explosive source. The VIBSIST source can be used in areas where explosives cannot be used. The two sources provide data that are of comparable quality. If the VIBSIST source can adapted to function in the terrain, then this could lower the cost of 3D surveys considerably.

The stacked sections contain some gaps due to the shooting geometry, for example over the Forsmark Zone on profile profile 7, and where there is not enough overlap between existing and new profiles, for example the merged profile 5 and profile 5b. Future seismic acquisition should avoid such gaps by choosing profiles where a regular geometry can be used and ensuring that there is enough overlap between existing and new profiles.

Data quality near the power plant and along parts of of profile 8 and profile 5b was poorer due to noise from the power plant and probably also due to near surface conditions. These factors cannot be controlled, however, acquiring data with a shorter spacing between sources and receivers (profile 12) results in a better stacked section under these conditions.

6.2 Processing

Pre-processing of the VIBSIST data is a time consuming operation. The lack of an exact time break required extra efforts to ensure that sources had a consistent starting time. More effort needs to be put into streamlining the pre-processing of the VIBISIST data. Once the pre-processing is complete, the VIBSIST data are treated the same as the explosive source data. The frequency content of the VIBISIST data is slightly lower than the explosive source data, but not enough to warrant use of different filters. It is more the near-surface conditions that determine what frequencies can be recorded.

6.3 Interpretation

The transparent uppermost 0.5 s (c. 1500 m) of crust observed on Stage 1 profiles 1 and 4 is also seen on profile 6. However, further to the south-west the uppermost 0.5 s becomes reflective again along profiles 2, 7 and 10. The reflectivity differs from that observed in the south-east corner of the candidate area along Stage 1 profiles 3 and 5. Here, there are only 3 distinct reflections that can be identified (J1, J2 and K1). Numerous dipping and apparently sub-horizontal reflections interfere with one another. In addition, diffractions from possible mafic lenses are present. The upper 0.5 s also becomes more reflective north of the Singö zone along profile 5b.

There are no clear reflections that can be directly correlated to the major deformation zones (Forsmark Zone, Eckarfjärden Zone and Singö Zone). Two merged profiles across the tectonic lens (Figures 6-1 and 6-2) indicate these zones to be sub-vertical since they appear to disturb or cut-off sub-horizontal reflections. For example, sub-horizontal reflections SW of CDP 75 on profile 2b appear to terminate at approximately the location of the Forsmark Zone (Figure 4-11). Note that even though the J1 reflection migrates across the Eckarfjärden Zone (located at CDP 400 in Figure 5-28) it appears to be disturbed vertically below the surface location of the zone.

Dipping reflections in the merged profiles (Figures 6-1 and 6-2) have distinct south dipping

components. Their projections to the surface appear related to the major sub-vertical deformation zones. Although these dipping zones are locally strong reflectors, they do not appear to extend laterally over more than a few kilometres. This includes the A1 reflector. Its central location within the survey area is one reason that it is observed on most profiles.

The two sub-horizontal reflections or reflection zones (C1 and C2) at about 0.9 s and 1.1 s (Figures 6-1 and 6-2) appear to have a significant lateral extent, on the order of at least several kilometres. They appear to be disturbed when they are below the major deformation zones, however, it is not clear if this is due to signal penetration or to geological factors. They appear to be most distinct within the boundaries of the candidate area. Regardless, their large lateral extent indicate that they are important features of the area.

6.4 Recommendations

For future acquisition the following recommendations are made:

1. Avoid large gaps in the source locations along the profiles. It is better to go around problematic areas than through them without activating sources.
2. When acquiring data in noisy locations, such as close to power plants, a maximum source and receiver spacing of 5 m is recommended.
3. Study how the VIBSIST source can be adapted for use in the terrain with minimal impact to the environment. Use of the VIBSIST source in the terrain would greatly reduce the cost of a 3D survey.

Although the area covered by the current set of profiles is extensive there are a couple of remaining questions on the large scale structure that could be answered by additional seismic surveys. These are:

1. Does the A1 reflector extend to the surface along profile 5 and are the C1 and C2 reflectors continuous below the Singö zone? A limited survey with fixed receiver positions along profile 5 and larger (100-200 g) explosive shots along profile 5b would illuminate both the A1 reflector and the C1 abd C2 reflectors in the gap between profile 5 and 5b and up to CDP 150 on profile 5b, that portion of the profile where the data quality is poorer.
2. Does the J1 reflector cross the Forsmark Zone? Extension of profile 2 to the south by about 2 km would answer this question.
3. Is the A1 reflector limited to the west and what is the southerly extent of the B8 and B9 reflectors? Extension of profile 6 to the north-west, along the road south of the power plant, would answer these questions. Higher quality data should be obtained along this extension than was obtained on profiles 11, 12 and 13 that run right next to the power plant.
4. If the orientations and lateral extent of the J1, J2 and K1 reflectors are of crucial importance to the repository, then a profile running in the NW-SE direction in between profile 6 and profile 7 should be acquired.

In addition to acquiring new data, there are number of processing studies that could be done with the existing data to improve the current sections and interpretations. These include:

1. Process lines 2 and 2b and 5 and 5b as single lines to improve the static corrections where they overlap and increase the fold.
2. Use the data acquired on the Orion stations in Stage 1 to try to map the lateral extent of the A1, C1 and C2 reflectors.
3. Reprocess the most crooked parts of the profiles in an attempt to orient reflections that do not happen to be located where profiles cross one another.

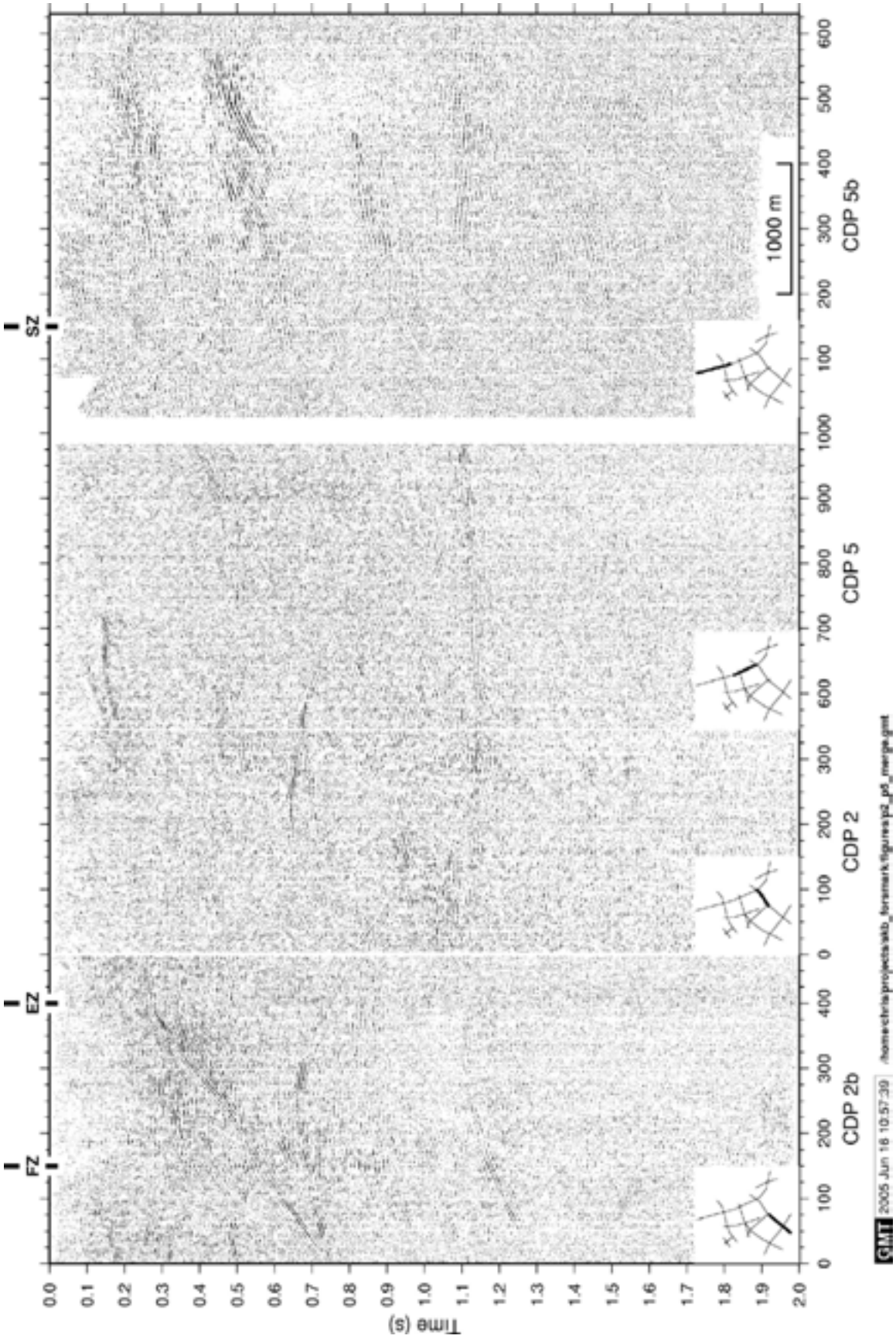

Figure 6-1. Merged stacked section of profiles 2b, 2, 5 and 5b.

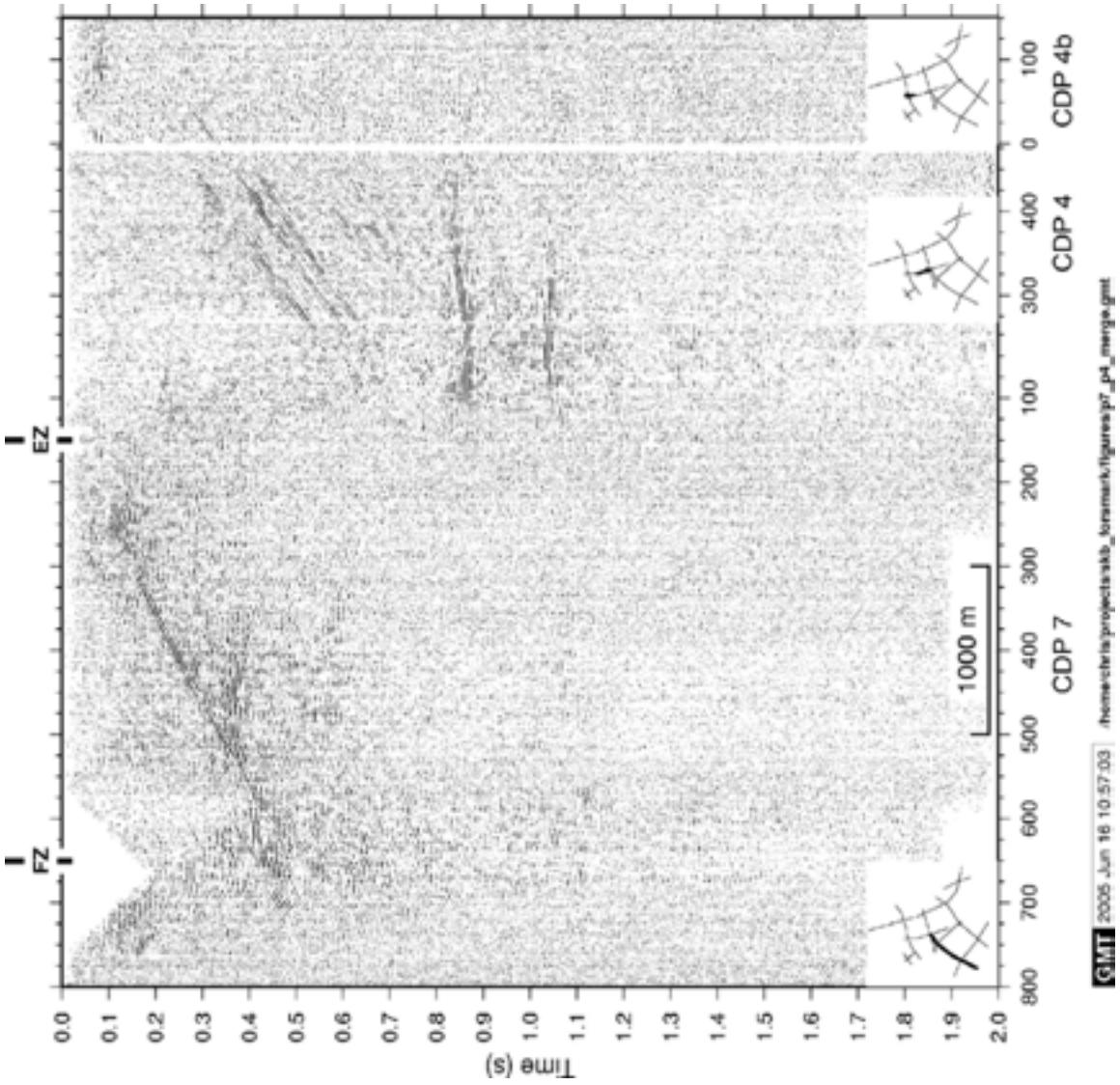

Figure 6-2. Merged stacked section of profiles 7, 4 and 4b.

References

Ayarza P., Juhlin C., Brown D., Beckholmen M., Kimbell G., Pechning, R., Pevzner, L., Pevzner, R., Ayala C., Bliznetsov, M., Glushkov A. and Rybalka A., 2000. Integrated geological and geophysical studies in the SG4 borehole area, Tagil Volcanic Arc, Middle Urals: Location of seismic reflectors and source of the reflectivity, J. Geophys. Res.: 105, 21333-21352.

Cosma, C and Enescu, N., 2001. Characterization of fractured rock in the vicinity of tunnels by the swept impact seismic technique. International Journal of Rock Mechanics and Mining Sciences: 38, 815-821.

Juhlin, C. and Bergman, B., 2004. Reflection seismics in the Forsmark area. Updated interpretation of Stage 1 (previous report R-02-43). Updated estimate of bedrock topography (previous report P-04-99). SKB P-04-158.

Juhlin, C. and Palm, H., 1999. 3D structure below Ävrö island from high resolution reflection seismic studies, southeastern Sweden. Geophysics: 64, 662-667.

Juhlin C., Bergman B. and Palm H., 2002a. Reflection seismic studies in the Forsmark area - stage 1. SKB R-02-43.

Juhlin, C., Bergman, B., Cosma, C., Keskinen, J. and Enescu, N., 2002b. Vertical seismic profiling and integration with reflection seismic studies at Laxemar, 2000: SKB TR-02-04.

Juhlin, C., Bergman, B., Palm, H. and Tryggvason, A., 2004. Oskarshamn site investigation: Reflection seismic studies performed in the Laxemar area during 2004, 2004: SKB P-04-215.

Park, C. B., Miller, R. D., Steeples, D. W. and Black, R. A., 1996. Swept impact seismic technique (SIST): Geophysics: 61, 1789-1803.

Tirén, S. A., Askling, P. and Wänstedt, 1999. Geologic site characterization for deep nuclear waste disposal based on 3D visualization. Engineering Geology: 52, 319-346.

Wu, J., Milkereit, B. and Boerner, D., 1995. Seismic imaging of the enigmatic Sudbury structure. J. Geophys. Res.: 100, 4117-4130.